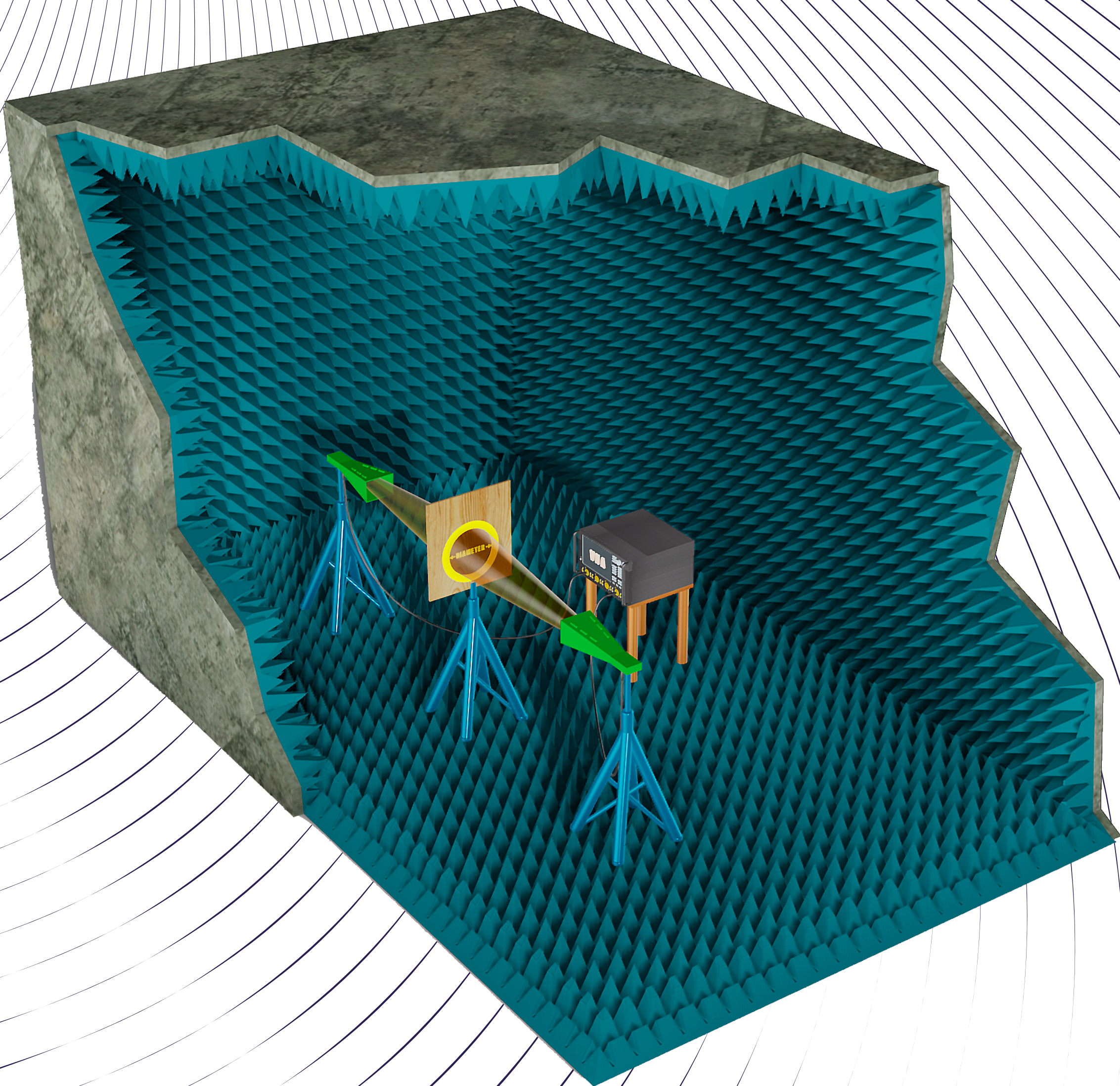

Dielectric properties of building materials for propagation studies at mmWave frequency

Bachelor project, diploma engineering in Electronics and IT at 7. semester

STUDENT REPORT
AALBORG UNIVERSITY

AALBORG UNIVERSITET
STUDENTERRAPPORT

Electronics and IT
Aalborg University
http://www.aau.dk

Title:
Dielectric properties of building materials for propagation studies at mmWave frequency

Theme:
Dielectric properties of materials

Project Period:
Fall semester 2022, 3 months

Project Group:
Group 710

Participants:
Sigurd S. Petersen

Supervisor:
Internal supervisor: Wei Fan
External supervisor: Stanislav Stefanov Zhekov

External censor:
Henrik Kalstrup

Page Numbers:
105

Date of Completion:
The date of completion is 05/01/23

Abstract:

This research project aims to measure the relative complex permittivity of building materials at mmWave. These materials are measured by using the free-space method among different types and NNI (New Non-Iterative) extraction method with the Keysight software. The results of the measurements show the real and imaginary parts of the relative permittivity, and the results are interpreted. Some of the results are similar to another research result with similar material thickness. Since it is impossible to determine that other researchers use the same materials, then it is not that appropriate to compare the results.
The research shows the results of the fourteen selected sample materials for the research and they are of great interest to simulation software, such as ray-tracking and radio communication projection simulation software.
Furthermore, the knowledge of the measurement methods and their advantages and disadvantages are also of great interest for further measuring multiple different materials. Which gives the opportunity to develop data collections for simulation software in the future.

Sigurd Petersen
sp19@student.aau.dk

Preface

The bachelor project explains the theoretical and practical work carried out under the curriculum of *Diploma engineering education in Electronic and IT in 2022*.

The quantities and units in calculations are represented in the International System of Quantities under ISO / IEC 80000 and SI. Other standards and abbreviations will appear introduced in parentheses the first time they are used in a context.

Source references are indicated as a number enclosed in square brackets: "[X]". Each square number will correspond to an index in the bibliography, which can be found in the last part of the report (before the appendices). The number acts in the digital version of the report as a hyperlink giving the possibility to go to the position in the bibliography. Sources are indicated with title, publication/url and possible time of access in the case of online sources. Sources from books are referenced by page numbers "[X, pp. XX-XX]". Material made by the group can be found in the appendix.

Contents

Chapter 1

Introduction

Vast research on the topics of permittivity and permeability throughout the years has piqued the interest of researchers in various avenues of application within the science of engineering [1]. Permittivity is a material characteristic that affects wave propagation. The change of this property is of great importance in various applications: e.g., in medical topics such as detecting cancer by diagnosing tumors [2–10], or in energy, the achievable conversion efficiency of solar panels[11, 12], or within wireless communication, among others. In wireless communication, such as 6G, researchers have researched electromagnetic measurement techniques for measuring permittivity [13, 14], given that the electrical performance of the transmission line also depends on the permittivity. All forms of wireless communication systems have an antenna for transmitting and propagating signals. For example, a patch antenna uses a dielectric material that separates the ground plane from the feed signal element. The antenna design and propagation efficiency depend on the dielectric material permittivity[15]. Therefore, it is also essential to include the permittivity effect on signal propagation contra the desired performance when looking at wireless communication systems. Within the environment of such systems, there can be multiple variables that can affect the transmission line, such as buildings, trees, etc. Particularly construction materials such as bricks, concrete, glass, different types and structures of tiles, facade cladding, plywood, etc.

The dielectric properties of building materials are highly usable for many types of wireless communication simulation, such as full-wave and ray tracing simulations for characteristics of wireless propagation channels in indoor and outdoor environments for wireless communication analysis. Study [16] uses 3D ray tracking simulations at mmWave (28 GHz) in urban environments to show the permittivity effect of various building materials. The study concludes that with an increased frequency band to tens of GHz, the relative permittivity changes and affects the propagation characteristics. Study [17],[18] states that for designing future mmWave (28 GHz) communication, it is important to make an extensive research measurement of various common building materials for practical values and optimization of electromagnetic (EM) performance in the designing stage. In general, the building material does impact the user-experienced data rate and end-to-end latency, which is part of the 5G performance objectives[18], and thereby permittivity of a typical building's materials is important for wireless communication in general. An indoor environment study [19] using EM simulations for investigating signal propagation at mmWave 60 GHz concludes that signal propagation characteristics and penetration level has a direct correlation impact of building material's permittivity, conductivity, and thickness.

Moreover, to understand the basic concept of the parameters used to determine the material properties, chapter one of the report will briefly go through the basic concept of the parameters, material properties, and current measurement achievements. The rest of the report is constructed likewise, where chapter two contains the basic theoretical explanation and the most common measurement methods and setups, where advantages and disadvantages are mentioned for each setup. The following report content show overview and explanation as well as the advantage and disadvantages of the most common conversion techniques. Furthermore, the following content in chapter two contains the free-space setup and its calculations of material size to avoid refraction, diffraction, and reflection, followed by measuring producer and extraction method using s-parameters.
Chapter three explains the associated issues with free-space setup and compares simulations, calculated material size, and validation of the setup, followed by uncertainty analysis of measurements.
Chapter four contains the measurement campaign and the measurement results. Chapter five contains the conclusion of the report.

1.1 Material properties

1.1.1 Permittivity

The dielectric constant, also known as relative permittivity ε_r, describes how a material interacts with an electric field it determines the ability of a given material to store energy, or how an electric field is affected within a medium. In other words, permittivity is the resistance the medium offers to the electric field[20].
The relative permittivity ε_r 1.1 is defined as the ratio of the absolute permittivity ε of the material over permittivity of vacuum $\varepsilon_0 = 8.854 \cdot 10^{-12}[F/m]$, which is often called the free space.

$$\varepsilon_r = \frac{\varepsilon}{\varepsilon_0} \tag{1.1}$$

The absolute permittivity denotes 1.2:

$$\varepsilon = \varepsilon_r \cdot \varepsilon_0 \tag{1.2}$$

Relative permittivity denotes as complex number:

$$\varepsilon_r = \varepsilon_r' - j \cdot \varepsilon_r'' \tag{1.3}$$

Where ε_r' is the real part and measures the amount of energy stored in the material from an external electric field that is applied. The imaginary part ε_r'' is the measured amount of energy lost in the material when an external electrical field is applied, and it is also referred to as the loss factor. For lossless materials, the imaginary part is zero. Further, the ratio between the imaginary part and the real part of the complex permittivity is called the loss tangent and is also referred to as the dissipation factor, which gives the relative lossiness of the material.

$$tan\ \delta = \frac{\varepsilon_r''}{\varepsilon_r'} = \frac{Energy\ lost}{Energy\ stored} = D = \frac{1}{Q} \tag{1.4}$$

The *tan* δ is also described in vector form as in figure 1.1.

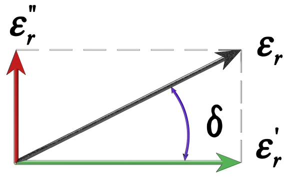

Figure 1.1: Loss tangent is the ratio of the imaginary part to the real part.

The inverse of dissipation factor is called the quality factor:

$$Q = \frac{1}{D} = \frac{1}{tan\ \delta} = \frac{Energy\ stored}{Energy\ lost} \tag{1.5}$$

The quality factor is a dimensionless parameter that describes how underdamped a resonator is and thereby indicates the energy losses relative to the amount of energy stored within the system and is directly linked to the bandwidth of a resonator with respect to its center frequency.

1.1.2 Permeability

The permittivity of a material is related to the electric response. Likewise, there is also a magnetic response parameter for dielectric materials called permeability. Permeability refers to a material's ability to create magnetic flux as it passes through a magnetic field or supports the magnetic field's formation. In other words the permeability is the ability of a material to become magnetized when exposed to a magnetic field. If the material is able to change the direction/orientation of

the dipoles easily when applied a magnetic field, then it is a high-permeability material and easily magnetized.
The relative permeability 1.6 is expressed by the symbol μ_r, and is defined as the permeability of the medium μ over the permeability of free space $\mu_0 = 4 \cdot \pi \cdot 10^-7$ (the permeability constant or the magnetic constant).

$$\mu_r = \frac{\mu}{\mu_0} \tag{1.6}$$

The absolute permeability denotes 1.7.

$$\mu = \mu_r \cdot \mu_0 \tag{1.7}$$

Relative permeability denotes as complex number,1.8:

$$\mu_r = \mu_r' - j \cdot \mu_r'' \tag{1.8}$$

Where the μ_r' is the real part and the μ_r'' is the imaginary part. The equations correlation between permittivity and permeability is shown in figure 1.2.

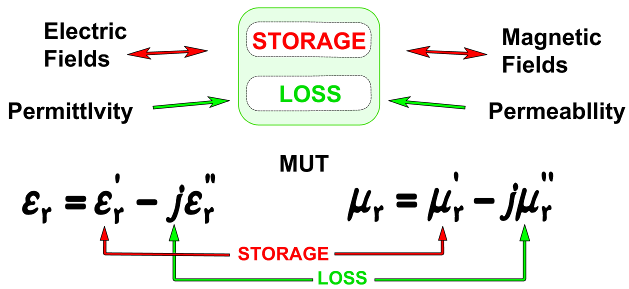

Figure 1.2: The equations correlations in the electric and magnetic field.

On the left-hand figure, 1.2 illustrates the electric field, that can be affected by the material and the other way around as indicated by the arrow in both directions, likewise with the magnetic field on the right-hand side. Furthermore, the permittivity arrow is only in one direction which indicates that the permittivity is a value for a material, and likewise with the permeability. Figure 1.2 also shows that the electric field is correlated with the permittivity and the magnetic field is correlated with the permeability.
The report will focus on permittivity and will not go into further detail about permeability

Wavelength and electromagnetic wave speed

From an antenna engineering perspective, permittivity affects the velocity of wave propagation through a medium and also its wavelength. Equation 1.9 shows the velocity of wave propagation in a given medium:

$$c = \frac{1}{\sqrt{\varepsilon \cdot \mu}} = \frac{1}{\sqrt{\varepsilon_0 \cdot \varepsilon_r \cdot \mu_0 \cdot \mu_r}} = \frac{c_0}{\sqrt{\varepsilon_r \cdot \mu_r}} \tag{1.9}$$

Equation 1.10 shows the wavelength dependency of relative permittivity, if relative permittivity increases then the velocity of the wave propagation in the medium will decrease and the wavelength of a plane wave decreases in size as well, while the frequency remains constant.

$$\lambda = \frac{c}{f} = \frac{c_0}{f \cdot \sqrt{\varepsilon_r}} = \frac{\lambda_0}{\sqrt{\varepsilon_r}} \tag{1.10}$$

For example, antenna miniaturization is often needed in antenna designs, where the wavelength of the antenna is reduced in size. If the permittivity of the surrounding medium is four, then according to 1.9 the wave propagation velocity in that medium would be half of that in free space. The frequency remains constant, but the wavelength according to 1.10 will also decrease two times. Therefore, the size of the antenna can be reduced which means that antenna miniaturization can be achieved just by placing dielectric material with higher than 1 relative permittivity around the printed antenna material.

1.1.3 Classification of material based on their properties

Table 1 shows the classification of materials by the relation between loss tangent and the propagation medium when interacting with materials. Further, the Table gives a quick and basic understanding of the propagation relation of materials.

$\frac{\varepsilon_r''}{\varepsilon_r'}$	**Conductivity types**	**Electromagnetic field propagation**
0	—	Perfect dielectric material, zero-loss environment
$<< 1$	Low conductivity materials, poor conductors	Low-loss environment, good dielectric material
≈ 1	Conductive material, loss	Loss-inducing environment
$>> 1$	High-conductivity materials, good conductors	High-loss environment, poor dielectric medium
∞	Perfect conductor	—

[a] **Table 1, [21, 22]**

The point where the loss tangent is zero, it means that no energy is dissipated, and if all the energy is dissipated, then there is no charging current, and the loss tangent tends to go toward infinity. The loss tangent is also affected by moisture, as well as a combination of temperature, pressure, and frequency. For humid environments, the loss tangent in most cases will increase, and depending on the temperature and frequency, the loss tangents either increase or decrease[23–25].

1.2 Literature on building material property measurement

Multiple researchers have researched the dielectric properties of building materials. Table 2 shows an overview of references of research on the dielectric properties of building materials over multiple frequencies.

[a] Frequency range					
900 MHz [26]	1.1 - 1.7 GHz [27]	1 - 3 GHz [28]	2.4 GHz [29]	0.02 MHz - 5 GHz [30]	2 - 16 GHz [31]
1 - 18 GHz [32]	5.8 GHz [33]	39 GHz [34]	5.8 - 41.5 GHz[35]	4 - 40 GHz [36]	26 - 40 GHz [37]
40 GHz [38]	40 - 50 GHz [39]	57 - 64 GHz [40]	60 GHz [41–43]	5 - 60 GHz [44]	5 - 67 GHz [45]
5.8 - 62.4 GHz [46]	18.7 - 60 GHz [47]	0.2 - 67 GHz [48]	60, 71, 81 GHz [49]	200 - 500 GHz [50, 51]	

[a] **Table 2**

The common factor for almost all measurements in Table 2 is that they only use a few building samples and the applicable frequency range is relatively limited for most. Furthermore, there is no continuous view of the material properties over a large span of frequencies. Therefore, it can also be challenging to use EM simulation tools to simulate real-world ultrawideband signal propagation. If the material properties are not within the whole needed frequency range or simply because the properties are non-existent at that frequency range it can be impossible to simulate properly. Channel frequency dependence is a key research topic, which requires knowledge of material properties at different frequency bands.

1.3 The goal of this report

The main goal of this report is to present an extensive study on the dielectric properties of fourteen building materials, with a frequency range from 17.6 GHz to 58 GHz.
There are multiple measurement approaches and the common ones will be presented in section 2. To accurately measure the material's properties, knowledge of the advantages and disadvantages of the setup and the material's correspondence to the EM wave within the environment is essential. Furthermore, the report will contribute with a clear overview of multiple measurements method, their advantages and disadvantages, and the considerations behind choosing the best-suited measurement method for measuring material or specimen properties.

1.3.1 Metodologi

The approach of the project objectives will be answered or solved with an Electronic and IT point of view. The material that will be used is background knowledge from the Electronic and IT course at 5. semesters within antenna theory and 5. semester project. Additional knowledge from past studies is within Physics, Chemistry, and Electronic knowledge over years. In addition theoretical book materials and knowledge that is explored and obtained from researchers within the field of propagation simulation and dielectric properties of materials, etc.
In reference to the measurement research of dielectric permittivity properties of materials, will consist of quantitative measurements that contain fourteen samples of building materials. The setup for the research design is the same, for every fourteen samples.
The statistical analysis is descriptive [52] where the information from the collected data from each of the samples will be presented in graphs. Software that is used for preprocessing and generating graphs Matlab used, and for measuring and collecting data the Keysight suite software is used. For the simulation of the accuracy of the material size in reference to the Far-field, frequency, and the antenna used for measuring, the software Wireless InSight was used.

Chapter 2

Basic principles and measurement setups

2.1 Basic principles

As mentioned in section 1.1, the parameter of interest is the relativity complex permittivity. Most methods for obtaining this parameter use a one, two, or four-port vector network analyzer (VNA). The port number depends on the measurement setup and what material or specimen is of interest. The VNA characterizes elements/devices by measuring the transmitted and the reflected signals at input and output across frequency bands of interest. The measured quantity is of a complex value with a magnitude and phase, expressed by scattering parameters (S-parameters).
Looking at the basic principle of VNA in figure 2.1, some power will go through the device-under-test (DUT), in this case, material-under-test (MUT) when power is injected, and some will return to the source as a reflection, depending on the impedance mismatch between the input and the load impedance.

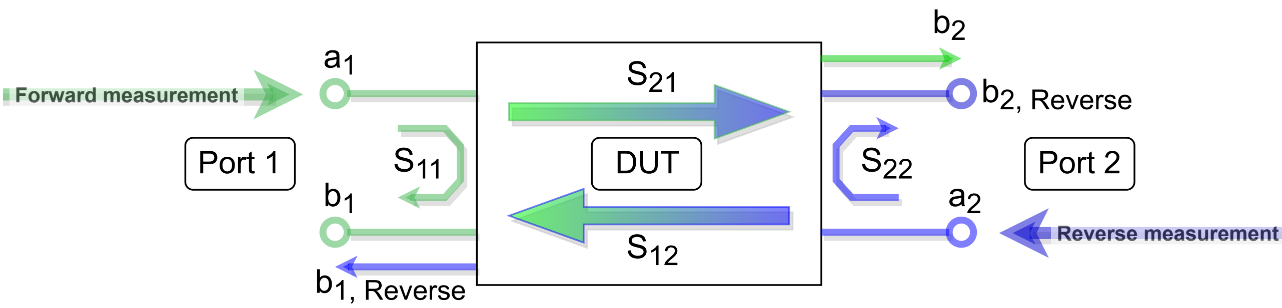

Figure 2.1: S-parameters of VNA

When injecting a signal with a certain amount of power at port 1, parameter S21 reveals through output power (loss or gain) and S11 the reflected power of the injected signal

(input match). Likewise, on the other side (reverse) at port 2, S12 shows the reverse through output power (isolation), and S22 is the reflected part of the reverse injected power (output match). When measuring material, these S-parameters come in complex forms and they are then processed to get the complex permittivity value, which will be explained in details in section 2.4.1.
One of the key parameters is the reflection coefficient [S11] Γ:

$$\Gamma = \frac{V_{reflected}}{V_{incident}} = \frac{Z_L - Z_0}{Z_L + Z_0} \tag{2.1}$$

where:

$$\begin{aligned} \Gamma &= \text{reflection coefficient} \\ V_{reflected} &= \text{voltage of the reflected wave} \\ V_{incident} &= \text{voltage of the forward or incident wave} \\ Z_L &= \text{load impedance} \\ Z_0 &= \text{feeder characteristic impedance} \end{aligned}$$

Another way of expressing the reflection characteristics is by using return loss in (dB):

$$Return_{loss\,(dB)} = -20 \cdot log(|\Gamma|) = -10 \cdot \log\left(\frac{Forward\ Power}{Reflected\ Power}\right) \tag{2.2}$$

Another key parameter is the transmission coefficient [S21] which determines how power passes through the network:

$$T = \frac{V_{transmitted}}{V_{incident}} \tag{2.3}$$

$$T = 1 + \Gamma = 1 + \frac{Z_L - Z_0}{Z_L + Z_0} \tag{2.4}$$

$$T = \frac{2 \cdot Z_L}{Z_L + Z_0} \tag{2.5}$$

The insertion loss in dB:

$$Insertion_{loss\,(dB)} = -20 \cdot \log\left(\frac{V_{transmitted}}{V_{incident}}\right) \tag{2.6}$$

The gain in dB:

$$Gain\ (dB) = 20 \cdot \log\left(\frac{V_{transmitted}}{V_{incident}}\right) \tag{2.7}$$

Using VNA and its scattering parameter makes it possible to characterize a system or network by analyzing above mentioned parameters. These complex S-parameters are used in material measurements to derive complex permittivity values.

The following sections of the report will introduce the overview perspective for the most common setups and enumerate the advantages and disadvantages of these setup configurations. Furthermore, to understand the process of extraction of complex permittivity, the report will introduce an overview of the most common extraction method and demonstrate one of the mentioned.

2.2 Overview of most common measurements methods and setups

There are several ways to measure material permittivity, and the most common and widely used techniques are summarized in Table 3. Each technique has its advantages and disadvantages, as well as each method has its purpose.

[a]

Measurement techniques	Material	S-parameters	Dielectric properties
Open-ended Coaxial	Liquids Semi-solid Biological	S_{11}	ϵ_r
Transmission/Reflection Line	Solid Liquids Anisotropic	S_{11} and S_{21}	ϵ_r and μ_r
Resonant Method (Cavity)	Solid Liquids Rod shaped solid Small samples	Resonance Frequency Q - Factor	ϵ_r and μ_r
Parallel Plate	Thin flat surface	S_{11}	ϵ_r
Plannar transmission	Solid Liquids	S_{11} and S_{11}	ϵ_r
Free space and Arch	Large flat solid High temperature Gas hot liquids	S_{11} and S_{21}	ϵ_r and μ_r

[a] **Table 3**

As seen in Table 3, open-ended coaxial and parallel plate only uses the S11 parameter to extract the permittivity of listed materials, but the remaining methods uses S11 and S21 parameters, just like the free space method.
Furthermore, since the report focuses solely on the free space method, it will just briefly go through each setup listed in Table 3 and state the advantages and disadvantages of the setup, as well as its purpose.

2.2.1 Open-ended coaxial

The open-ended coaxial probe, commonly known as a coaxial probe or coaxial-line probe method, has been used for years as a testing method for measuring lossy materials at broadband with high frequencies i.e. RF and microwave. This is a non-destructive testing method and is best suited for semi-solids and liquids, where the probe is pressed against a specimen or immersed into the liquid, as seen in figure 2.2.

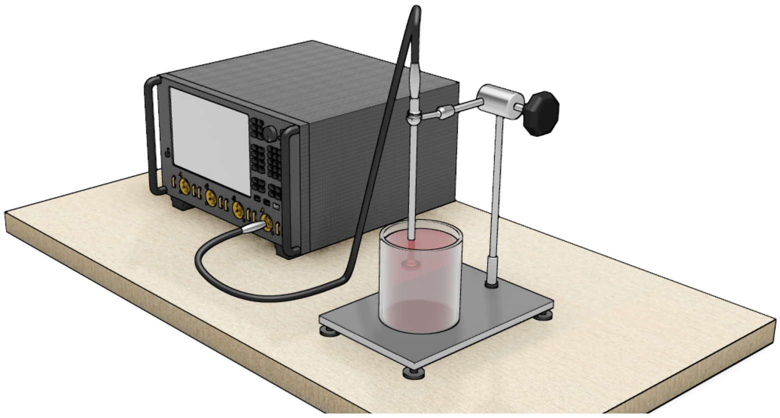

Figure 2.2: Open-ended coaxial method, where a VNA is connected to a probe immersed in the liquid, to measure the S11 parameters for extracting the permittivity.

Furthermore, the open-ended coaxial probe is excellent for measuring the reflection coefficient, where the probe should not make any changes to the sample, and only the sample's surface is accessible without either cutting or access from the other side of the sample. The VNA is connected to the probe via one port, and it will measure the reflection coefficient S11 parameter, which expresses a function of the medium's impedance used for the permittivity extraction. Before measuring, the setup should be calibrated, and for liquids, there are some known liquid characteristics that are used for the calibrations and are described in details in [53, 54].

The advantages of the Open-ended coaxial method:

- The method can be used for broadband frequencies.
- Measuring semi-solid and liquid samples.
- Simple sample preparation.
- Only one port VNA is needed.
- Possible to measure the surface sample, (no need to cut a piece of the sample).
- Method allows for non-destructive testing of the sample.
- Take measurements in a controlled temperature environment.

- When samples are established they can be routinely measured for cross reference in a short time.
- Used for lossy to high-loss materials, where high accuracy is achievable.
- The samples need to be homogeneous and isotropic.
- Can be used under high-temperature [55].

The disadvantages of the Open-ended coaxial method:

- It is not well suited for low-loss or magnetic.
- For solid samples - difficult in preparing the sample as needs to have very smooth surface on both sides to ensure good contact.
- Only has reflection measurements.
- Only measures permittivity 2.2
- When measuring samples, the air gap will affect the measurement accuracy, which is one of the biggest contributions to error, etc.
- Repetitive calibrations.

2.2.2 Transmission / Reflection Line

The transmission line method is another common method, where the material sample is placed in the center section (neon green) of a waveguide (a) or coaxial line (b), as shown in figures 2.3 and 2.4. As before, this setup also requires calibration and sample preparation, so the samples fit tightly into the sample holder. This setup requires a two-port VNA for measuring both reflection and transmission coefficients, where both S11 and S21 parameters are related to extracting the material's complex permittivity and permeability. The waveguide method has higher accuracy and is more sensitive than the coaxial line method but has a relatively narrower frequency range [56].

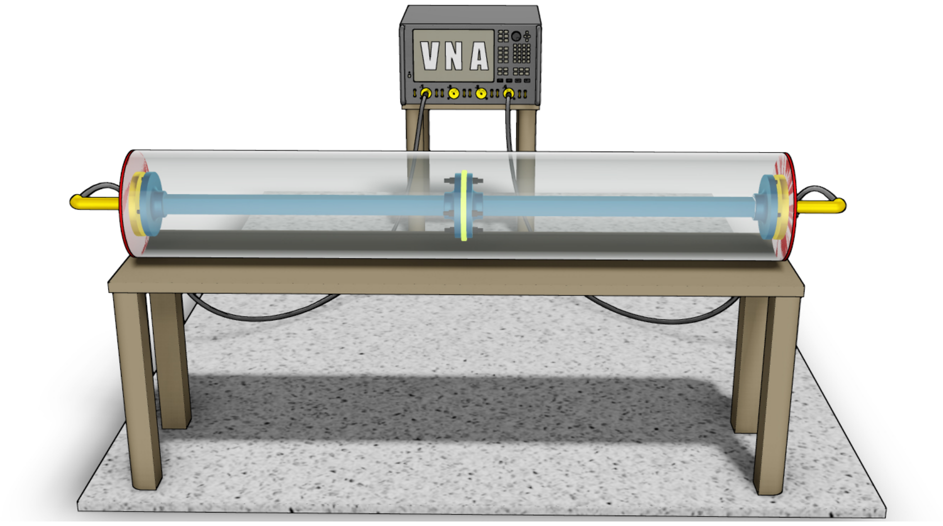

Figure 2.3: Transmission / Reflection Line setup method.

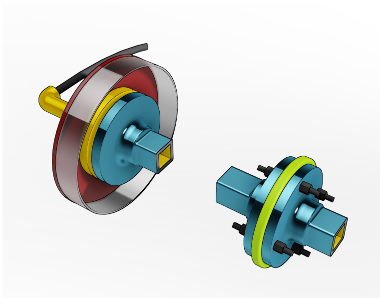

(a) Waveguide method.

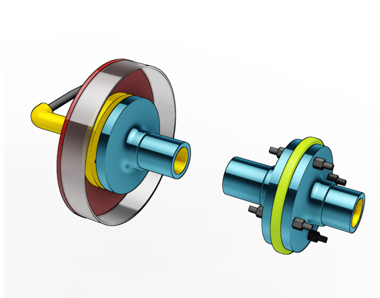

(b) Coaxial line method.

Figure 2.4: Transmission / Reflection Line setup method.

The advantages of the transmission / Reflection line method:

- Waveguide and coaxial lines are used for measuring in broadband for high lossy to lossy material, solids and liquids.
- The method is used for determining the permittivity and the permeability of MUT.
- Can be used for high frequencies.

The disadvantages of the transmission / Reflection line method:

- Because of the air gap that can appear, the measurement accuracy can be affected, thereby limiting the accuracy. The effect worsens as the frequency increases and wavelength decreases, thereby increasing the air gap and relative error.

- Reflections can also appear if the sample placement is not correct. For very high frequencies, correctly positioning a sample gets more complicated, and the positioning error becomes more critical as the wavelength decreases.

- When the sample length is the multiple of one-half wavelength in the material, the accuracy is limited due to resonance. There is a workaround where, as stated, it is possible to eliminate the effect of reflection at fixture interfaces by using a long air line as a fixture and improving gating analysis in the time-domain[57].

2.2.3 Cavity resonant method

Figure 2.5 shows an example of a cavity resonator, but there are many resonant methods, such as split cylinder resonators and Fabry-Perot resonators. The report will only focus on the general concept and its advantages and disadvantages. The general idea is that the resonant cavity is connected to a two-port VNA, where the sample is placed inside the cavity. Since the cavity resonates at a certain frequency and the structure is tuned to a high Q, the inside sample will affect the center frequency and the cavity's quality factor, which is $\frac{1}{\tan\delta}$ as mentioned in 1.5,[58]. With these changes in parameters, it is possible to calculate the complex permittivity or permeability of the sample at a single frequency[55].

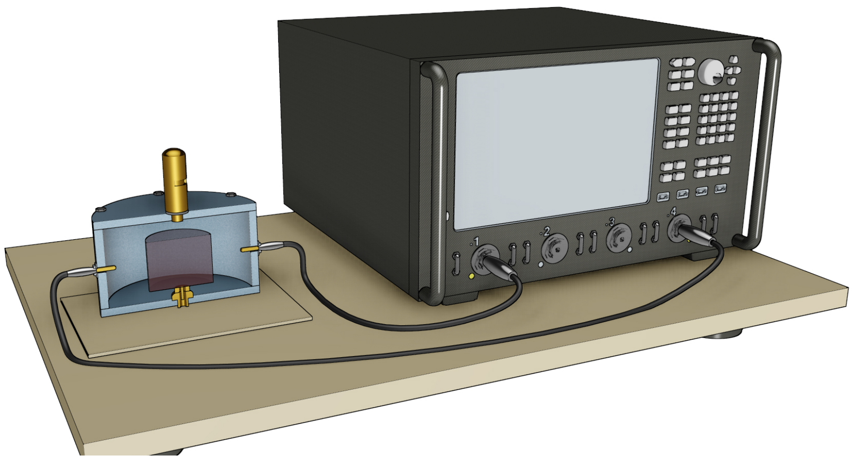

Figure 2.5: Cavity resonant setup method.

This method is limited to a narrow band of frequencies since it uses the resonance frequency of the cavity and its Q factor to determine the dielectric constant. Furthermore, it also needs high-frequency resolutions VNA to detect the changes in center frequency with high accuracy. The cavity resonator sample preparation is easy compared to other methods, and there is also the possibility to make rapid and multiple measurements within the same frequency when the calibration is finished, [58].

The advantages of the cavity resonant method:

- Support for both solids and liquids.
- low-loss material.
- Thin material.
- The measurements can be taken in low and high temperatures $-20°C$ to $140°C$, [59].
- One of the most accurate method.
- Best suitable for low loss materials.
- No repetitive calibration procedure.
- Ability to measure very small samples.

The disadvantages of the cavity resonant method:

- Measurements at only single or at the resonant frequency, (Narrowband).
- Suitable for small size samples.
- This method requires very flat samples, and for some of the thin samples, it is very complicated to achieve a good reading, as samples tend to warp, bend, and cause the tendency of a rough surface as thinner the material sample gets.

2.2.4 Parallel plate

The parallel plate capacitor method is another way of measuring the dielectric constant by placing a thin sample between the electrode plates as a sandwich structure, as seen in figure 2.6. The measurement is conducted by considering the material's dimension and its capacitor capacitance, and using the S11 parameter makes it possible to calculate the permittivity. Three main factors affect the capacitance of a capacitor: the capacitance is proportional to the plate area and inversely proportional to the distance between plates, and the dielectric material's permittivity. However, when the sample is thin, it tends to get flexible and cause an air gap, which leads to a wrong determination of the dielectric constant [60].

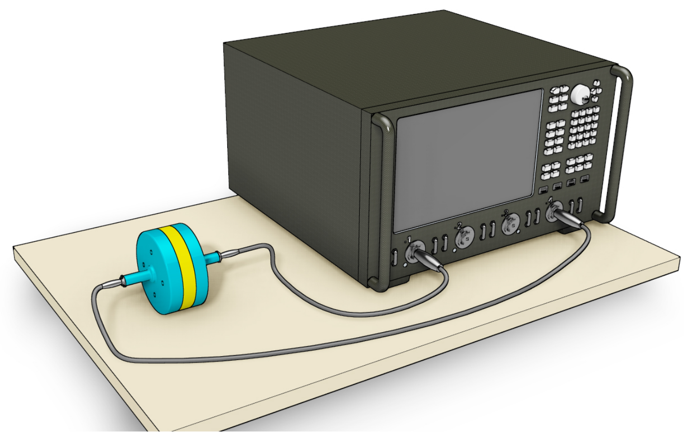

Figure 2.6: Parallel plate setup method.

The advantages of parallel plate method:

- Higher accuracy
- For thin, flat surface samples
- Suitable for high-loss materials
- Measurements are relatively easier

The disadvantages of parallel plate method:

- Support for low frequency
- Electrode polarization effect

2.2.5 Planar transmission

The planar transmission line is a common and widely used method in RF and microwave areas. For example, a patch or PCB antenna has microstrip lines, as seen in figure 2.7, where dielectric characterizing is needed to analyze or see its effect on the antenna's propagation, as mentioned in section 1. The dielectric properties of the substrate are evaluated and then tested where the antenna's characteristics can change. For S11 and S21, the permittivity can be extracted by looking at the parameters when changing the size, thickness, or shape of the antenna[61]. Especially when choosing another PCB permittivity material, the resonant frequency, and the propagation will change, [15, 62–64].

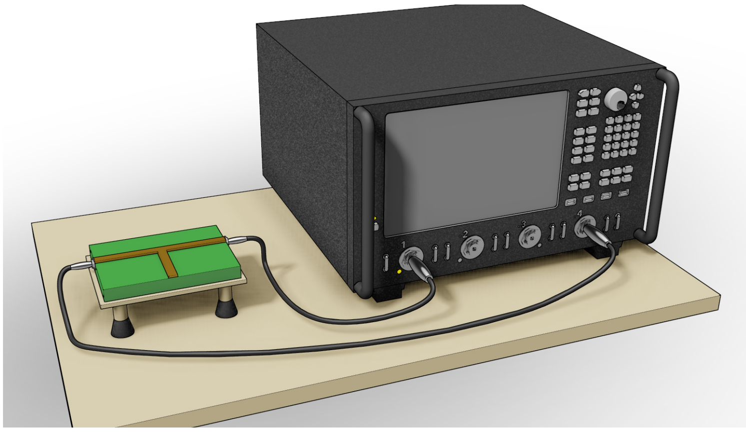

Figure 2.7: Plannar transmission setup method.

The advantages of plannar transmission method:

- Simple, cost-effective and rapid
- No special sample handling
- Can be used for solid or liquid
- High-temperature measurements

The disadvantages of Plannar transmission method:

- Low-quality factor.
- Air gap causes an error.

2.2.6 Free space and Arch

Free space measurement can be categorized into two. First setup, as shown in figure 2.8, where the setup consists of one vector network analyzer (VNA) and two antennas, in this case, two horn antennas and a material-under-test (MUT). The first setup is called the arch method, where the antennas are placed 0° to 180° around the MUT, and the setup looks like an arch seen from above, as seen in figure 2.8. The second setup consists of two antennas aligned across or on the opposite side, with MUT in the middle, as seen in figure 2.9. In this report, the focus will be on the free space setup with different materials and frequency bands.
Both methods use two antennas to focus the em wave on or through the tested material, and both methods are non-contacting and non-destructive.

Arch setup / Free space

Arch is also referred to as NRL arch (Naval Research Laboratory). The principle behind the method and its setup is shown in figure 2.8, where standard horn antennas are connected to a VNA for measuring the S parameter. Usually, this setup is in an anechoic chamber where the antenna is placed on an arch pointing towards the material under test. The advantage of using the method is that while measuring, there is no physical contact with the sample, which make it possible to measure at high temperature. This method is best for relatively thin solid flat materials, which can be tested for a broad band of frequencies.

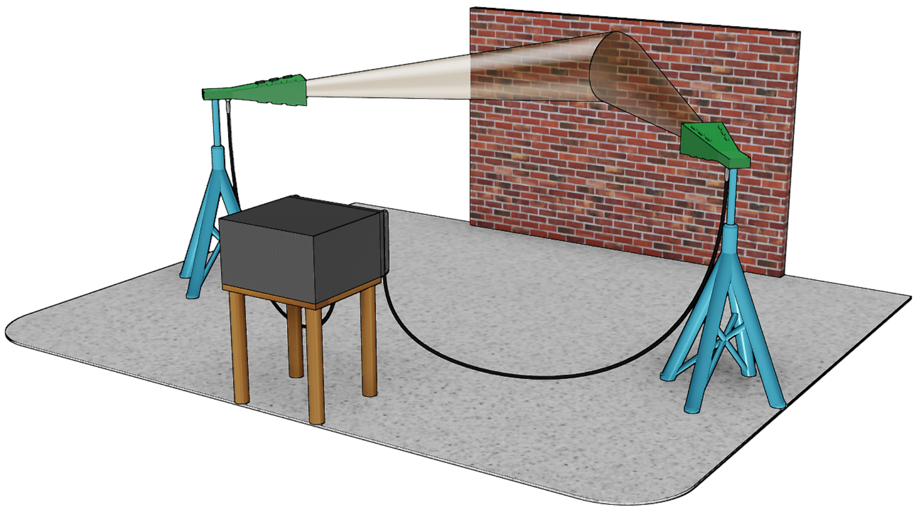

Figure 2.8: Arch setup method.

The procedure of the method is first to calibrate the system by measuring the reflected power using a metal plate as the "perfect" reflection or 0 dB level, and the metal plate needs to be big enough to avoid edge effects. Then the material is placed, and the reflected power from the material is measured S21 parameter. Furthermore, time domain gating is often used to eliminate the antenna cross-talk and reduce environment reflection. When the S-parameter are obtained, the permittivity can be calculated. The idea for this measurement setup is that it is possible to measure the permittivity and permeability for different angles of incidence and see the difference.

Free space setup

The antenna placement is the main difference between the arch and free space setup. In the free space setup, the antenna's placement is aligned across each other, as seen in figure 2.9. This method usually uses the S11 and S21 parameters to determine the complex dielectric values, but there is also the possibility of only using the S11 parameter to determine the complex dielectric value of a material.

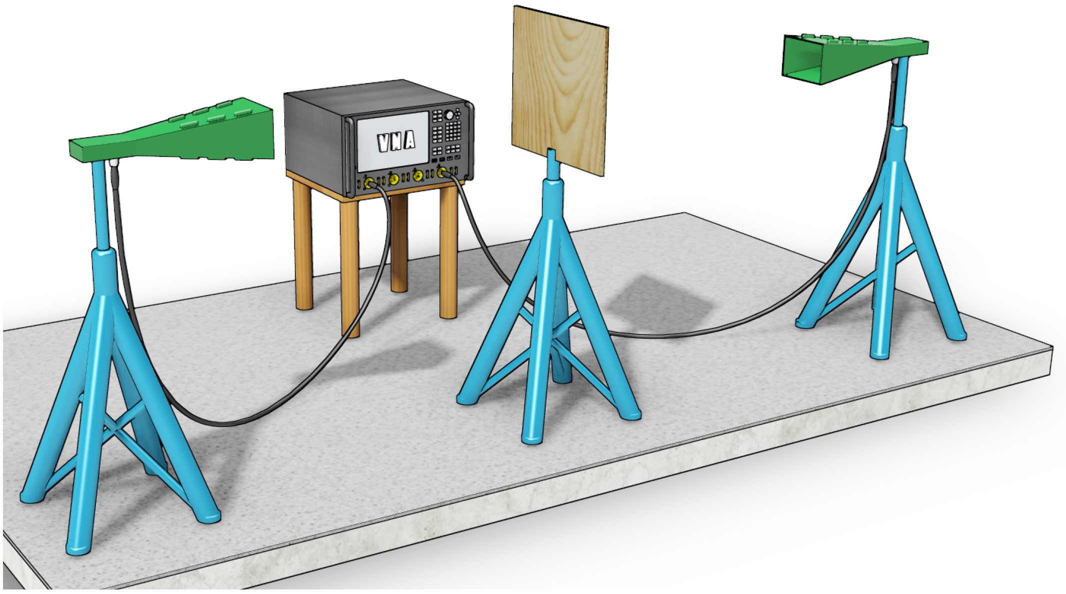

Figure 2.9: Free space setup method.

This method comes with several challenges, such as the material size, which mainly depends on two things: one is the distance between the antenna and the material, and the second is the frequency. Further, there are other difficulties related to the sample size at a lower frequency, such as size limitation and the appearance of reflection, and diffraction in general, which will be elaborated further in section 3.

The advantages of free space and arch methods:

- The method is usually used for broadband frequencies.
- The method allows for non-destructive measurements (without touching the MUT).
- The method allows usage with high temperatures because of the distance to the MUT.
- The method can be used to measure from both sides or only one side of the MUT.
- The method can determine the permittivity and permeability of MUT.
- Fairly easy sample preparation.

- Moderate accuracy for high-loss and low-loss.
- Best for large, flat, and solid materials.

The disadvantages of free space and arch method:

- The MUT size must be large and flat, especially at higher frequencies.
- Reflection and diffraction effects at the edge of the sample can occur if the material relations of frequency, propagation distance, calibration, and size aren't addressed.
- Multiple reflections between the antennas and the MUT surface can occur.
- Alignment issues can occur.

Besides the complications mentioned above in the free space method, there are three other things to consider, namely the calibration, which can be characterized into two parts: the calibration of the VNA with the cables attached, and the surroundings and circumstances. The second thing to consider is which S-parameter will be used for extracting - S11 and S21, or only the S11 parameter. The last thing to consider is the extraction algorithms methods, which are highly dependent on the material and the S-parameter.
The following section will briefly explain the most common extraction algorithms of complex dielectric using S-parameters, and determine what will be used further in this report.

2.3 Overview of conversion techniques

So far, the commonly used setup methods and their advantages and disadvantages are explained in section 2.2. Since the main focus is free space method 2.2.6, the report will focus on the extraction methods related to free space setup. Furthermore, the report will also introduce the advantages and disadvantages of these methods. The overview of the stages involved when testing a material property is as follows and seen in flow charts 2.10 and 2.11.
In general, when measuring the permittivity of materials or specimens, there needs to be some consideration regarding the size and the form or state the sample is in, i.e. liquid, semi-solid or solid, which depends on the setup. However, the measurement's accuracy depends on the appropriate choice of setup and extraction method, as well as the calibration methods throughout the measurement. The flow charts 2.10 shows the general idea of what to consider when making a measurement.

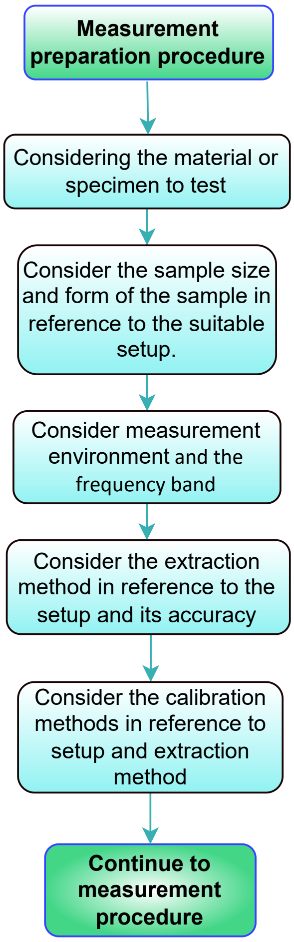

Figure 2.10: General measurement preparation procedure.

When considering methods, calibrations, and the appropriate setup, the next step is the measuring procedure seen in the flow chart 2.11. The first step is to set up the VNA and its option and, if needed to minimize reflection, and diffraction as mentioned 2.2.6, time gating can be used. The next step in some setups is calculating the cutoff frequency, which is used for calculating the extraction of permittivity. The third step is calibrating the VNA with the preset parameters, which only include the attached cables' end. The fourth step for free space is to measure the S-parameters for calibrating the environment without and with a known material blockage between the antennas to get the reference level. Then these reference level recorded S-parameter are then calibrated using an algorithm i.e. TRL, TRM, etc. The setup is calibrated and the unknown material can be placed and measured, which results in another set of S-parameter of the material. Both the S-parameter of the reference level and the measured S-parameter of the material can now be used together for extracting the permittivity by using algorithms like NRW, etc.

Then there is another manual calibration method to the right in the flow chart 2.11, which calibrates the system setup,[65]. The last part is the extraction of the permittivity and permeability, where different algorithms are used depending on the frequency, setup, and the material under test. If the reference point is not correct when measuring a known material or substance, it is possible to calibrate the environment again using algorithms as mentioned and seen in flow chart 2.11.

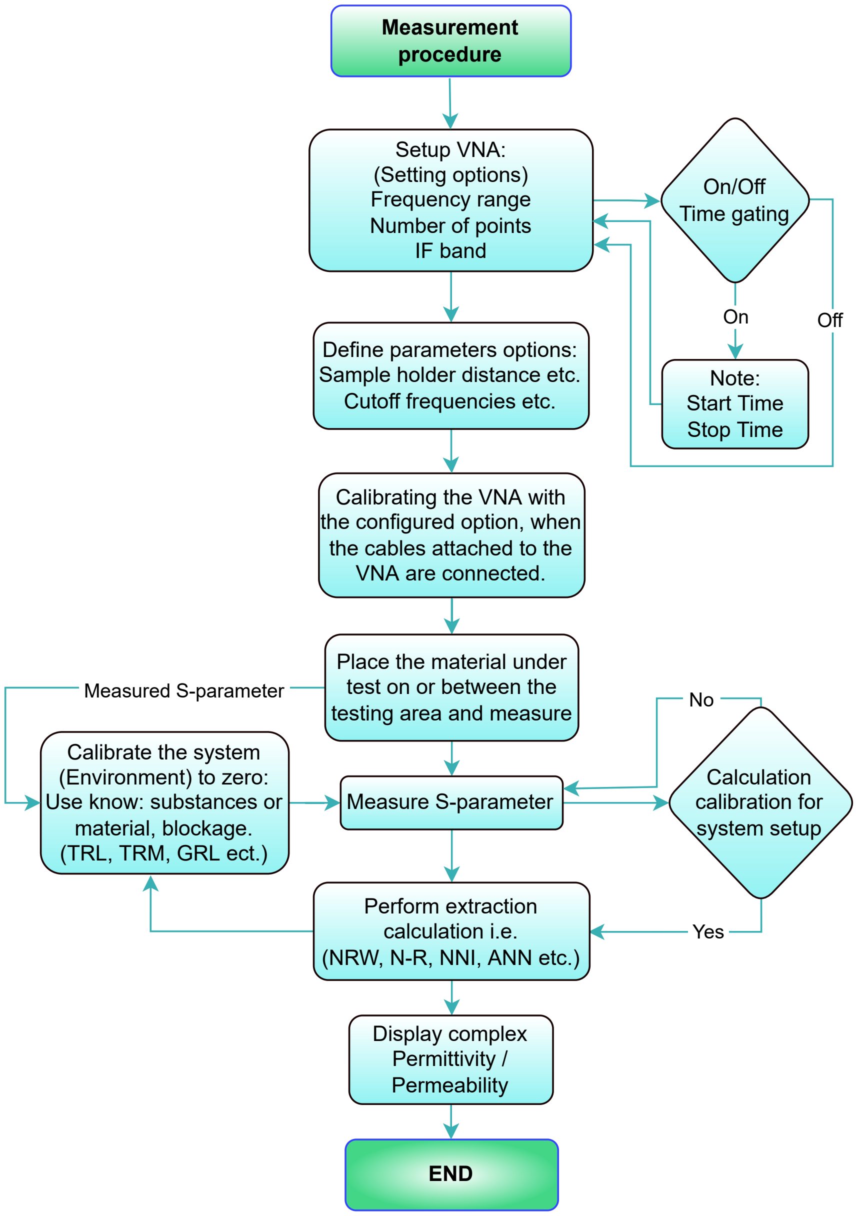

Figure 2.11: General measurement procedure.

Moreover, the extraction method is a centerpiece that affects the outcome and depends on multiple choices, which is why the report will briefly explain the most common extraction method. Chapter three will elaborate on the calibration effect aspect and general issues in the free-space method. Table 4 shows the common extraction method related to free space measurement.

[a] **Conversion techniques**	**S-parameters**	**Dielectric properties**
NRW	S11, S21, S12, S22 or S11, S21	ε_r, μ_r
NIST iterative	S11, S21, S12, S22 or S11, S21	$\varepsilon_r, \mu_r = 1$
NNI	S11, S21, S12, S22 or S11, S21	$\varepsilon_r, \mu_r = 1$

[a] **Table 4**

$$\begin{aligned} \mathit{NRW} &= \text{Nicholson-Ross-Weir} \\ \mathit{NIST\ iterative} &= \text{National Institute of Standards and Technology iterative} \\ \mathit{NNI} &= \text{New non-iterative} \end{aligned}$$

2.3.1 Nicholson-Ross-Weir (NRW)

The NRW method is one of the most commonly used extraction methods using reflection Γ and T transmission coefficients to calculate the permittivity and permeability from the S-parameters.

When the thickness of low-loss materials reaches the point where multiples of the half wavelength, the reflection coefficient S11 amplitude approaches zero, and its phase gets large. These frequencies and thicknesses cause some uncertainty and inaccuracy by using the NRW formula[56]. The mentioned issue can be seen in figure 2.12, where the blue line shows the issue with low-loss material. However, there are several ways to avoid the issue by reducing the sample length or using an approximate method that characterizes the impedance Z near the two frequency resonance regions [66–68]. The red line in figure 2.12 shows a calculated correction of the issue [67].

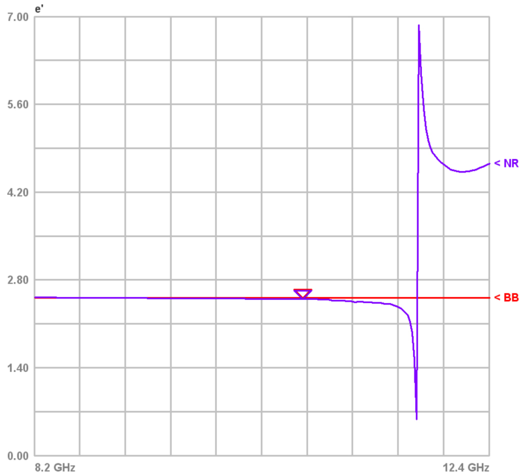

Figure 2.12: NRW $\frac{\lambda}{2}$ issue [67], is due to resonance effects.

The advantages of the NRW method:

- Fast, non-iterative.
- Appropriate for measuring methods like waveguides and coaxial-line.

The disadvantages of the NRW method:

- Divergence at frequencies corresponding to multiples of one-half wavelength.
- Short sample should be used.
- Not suitable for low-loss materials, thickness limitations.
- Instability when $\mu_r = 1$.

The calculation procedure extraction process is shown as a flow chart in figure 2.13.

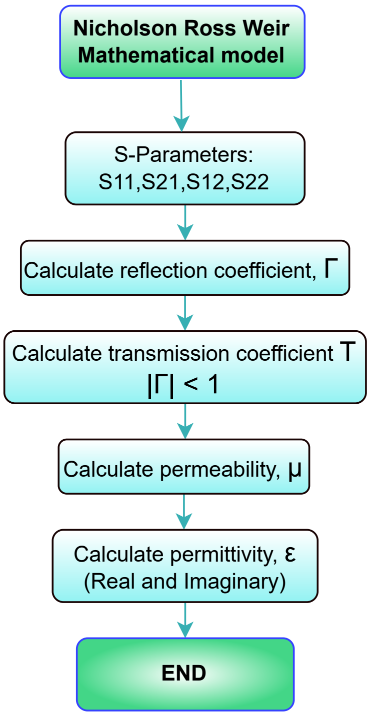

Figure 2.13: NRW measurement procedure.

2.3.2 NIST Iterative

NIST Iterative method uses all four S-parameters of the MUT or a pair of S-parameter, such as S11 and S21, to calculate the reflection and transmission coefficient. However, this method starts by using an initialized guessed value of material permittivity and then uses Newton-Raphson's root finding method to get closer and closer to the true value. Furthermore, this method bypasses the issue in NRW 2.3.1 when the sample thickness is an integer d and is multiplied by one-half wavelength $\frac{d \cdot \lambda}{2}$, which makes it possible to use arbitrary sample length and get a stable permittivity over large frequency spectrum of interest when a good/accurate/close initial guess of the permittivity is made.

The advantages of the NIST Iterative method:

- Stable permittivity, no divergence.
- Stable for low and high loss materials.
- Usage of arbitrary sample length.

- Stable and accurate when the initial guess permittivity value is close to the real value.
- Minimizes the instability by setting $\mu_r = 1$.

The disadvantages of the NIST Iterative method:

- Needs initial guess of permittivity value.
- It can only be used for permittivity measurements, i.e. permeability can't be evaluated.

The calculation procedure extraction process is shown as a flow chart in figure 2.14.

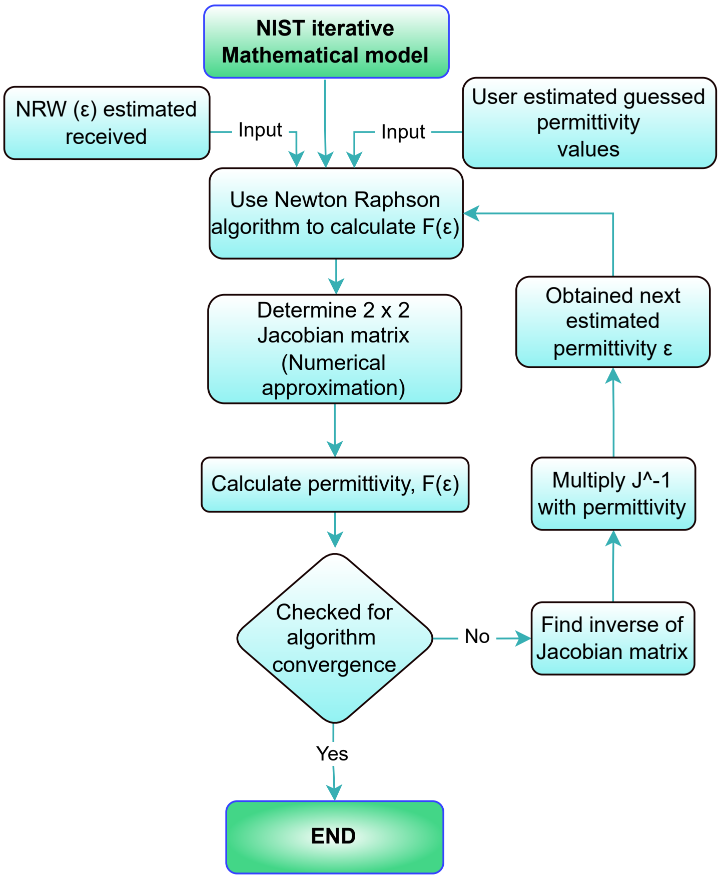

Figure 2.14: NIST Iterative measurement procedure.

2.3.3 New non-iterative

The new non-iterative method is based on a simplified version of the NRW method. All or only a pair of S-parameter, such as S11 and S21, is used to calculate the reflection and transmission coefficient. The method does not show the NRW issue throughout the frequency band, does not use initial permittivity estimation, and performs calculations quickly with accuracy comparable to the iterative method. The advantage of this method is the stability over large frequency ranges for an arbitrary sample length. The limitations are that it can only be used to measure permittivity, and not permeability because it's sat to one by using this method.

The advantages of the New non-iterative method:

- Stable permittivity, no divergence.
- Stable for low and high loss materials.
- Usage of arbitrary samples length.
- Quick, non-iterative.
- Do not use initial guess of permittivity value.
- Accuracy is comparable to the iterative method.

The disadvantages of the New non-iterative method:

- Can only be used for permittivity.

The calculation procedure extraction process is shown as a flow chart in figure 2.15.

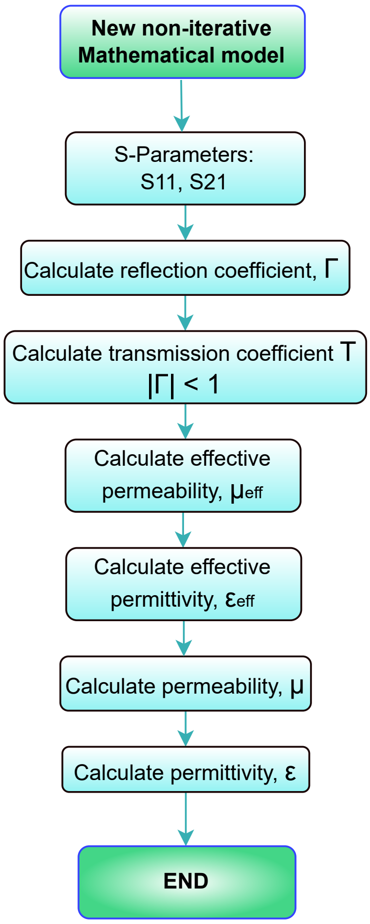

Figure 2.15: New non-iterative measurement procedure.

2.4 Methods used to achieve report measurements objectives

The report's objective is to measure the dielectric properties of fourteen common building materials. The measurement setup method used in this report is the free-space method, as mentioned in the section 2.2.6. The extraction algorithm used to derive the permittivity of the materials is the New non-iterative method, which is implemented into Keysight software [69, 70]. The setup consists of two standard gain horn antennas connected to a VNA, as seen in figure 2.16, one antenna for transmitting, and the other for receiving. There will be a sample holder that can firmly hold the sample without being in the way or reflecting the signal.

Several requirements should be met in order to achieve accurate measurement results using a free-space setup, such as far-field, sample size, and measurement environment.

2.4.0.1 Far-field requirement

The far-field requirement is to ensure that the wave incident onto the material sample can be approximated to plane wave and to be in the far-field, the distance between the antenna and the material must fulfill the requirement 2.8,[71].

$$\mathrm{r} > \frac{2 \cdot D^2}{\lambda} \tag{2.8}$$

where:

r $=$ The distance between the material and the antenna.
$D =$ The maximum antenna aperture dimension or the diameter of minimum sphere that encloses the an
$\lambda =$ The wavelength.

The free-space setup is treated as a uniform transmission line when the far-field requirements are fulfilled [71].

2.4.0.2 Material sample size

One thing is to ensure that the measurements are taken in the far field, but considering propagation projection of the main lobe of the antenna radiation pattern on the material is another important factor when considering the material size. Otherwise, if the material sample is much smaller than the diameter of the propagated electromagnetic wave, the possibility of diffraction and reflection at the edges of the material occurs as illustrated in figure 2.16. The result of a such measurement will contribute to a measurement failure since it is not only the material that is measured upon, [72].

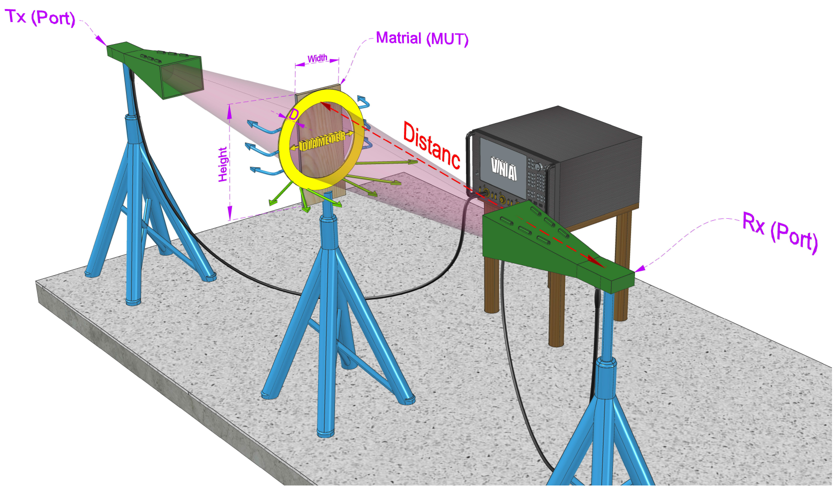

Figure 2.16: Free space error of propagation in reference to reflection, refraction, diffraction on and of the materials edges.

If the material size increases and the antennas were not placed at the far field of each other but placed much closer to the material, the probability of reflection would significantly increase and the result accuracy would degrade and worst case the result would not be usable.
The important thing is to place the material in the far field and calculate the size of the material in reference to the propagated electromagnetic wave on the material.
The size of the material should be at least two wavelengths to minimize the effect of the diffraction from the material, [73]. The propagation beam diameter on the material can be calculated as follows:
First, the standard horn antenna aperture dimension is used to calculate the HPBW, [71, 73].

$$\phi = \frac{70 \cdot \lambda}{D} \tag{2.9}$$

where:

$$\begin{aligned} \phi &= \text{Half-Power beamwidth.} \\ \lambda &= \text{Wavelength} = \frac{c}{f} \\ D &= \text{Antenna aperture dimension.} \end{aligned}$$

The second is to calculate the projection diameter.

$$P_d = 2 \cdot Distance \cdot \tan(\phi) \tag{2.10}$$

where:

$$P_d = \text{Projection diameter.}$$
$$D_{AM} = \text{The distance between the antenna and material.}$$
$$\phi = \text{Half-Power beamwidth.}$$

The calculated projection diameter on the material is illustrated in figure 2.17. To ensure the minimization of diffraction on the edges of the material, the propagation diameter needs to be enlarged a bit further, as illustrated with the yellow ring (G) in figure 2.17,[71, 72].

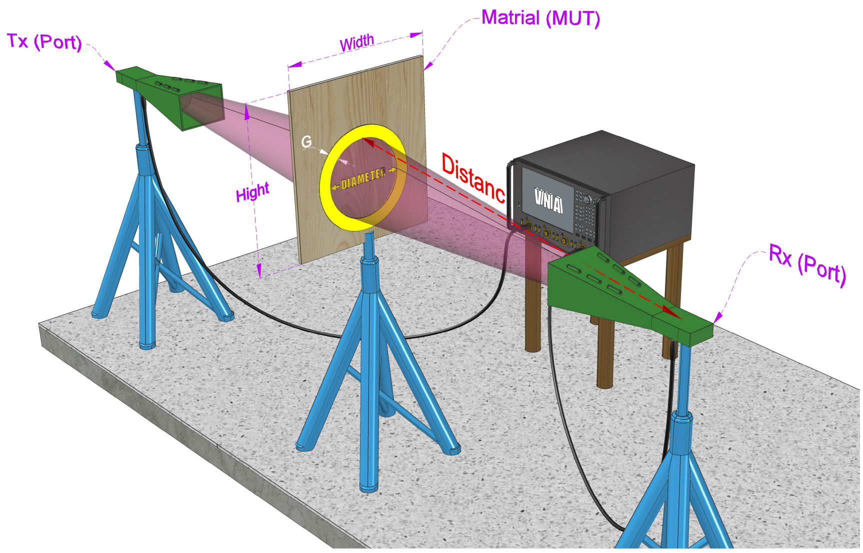

Figure 2.17: Free space error minimization of propagation on material.

The annulus width should be:

$$G = \frac{r}{2} \text{ where } r = \frac{P_d}{2} \tag{2.11}$$

The material size should be:

$$\text{Material size} \gg r + G \tag{2.12}$$

The distance between the antenna and the material should be:

$$D_{AM} > \frac{2 \cdot D^2}{\lambda} \tag{2.13}$$

The sample size can be determined in reference to the frequency and distance between the sample and the antenna.

2.4.0.3 The measurement's environment

When looking at the measurement setup environment in reference to high frequency, the interference is limited to an extent outside an anechoic chamber, given that the propagated beam gets narrower with increased frequencies. However, with lower frequencies, the effects of environments are more important or even a critical factor to consider. The reason for consideration of the measurement environment in reference to the frequency is because of the reflection and multireflection caused by the environment. There are ways to eliminate or minimize the environment's unwanted reflection effect, such as using time gating or conducting the measurement inside an anechoic chamber.
The conducted free-space measurement in this report is conducted inside an anechoic chamber, and the time gating is used to minimize the effect, such as reflection.

The measurement is carried out in the following manner:

1. Select proper antenna and cables.
2. Setup the VNA options, the frequency range, the number of points, and the IF band as instructed in 2.11.
3. Calibrate the VNA with cables by connecting the attached cables and using the correct electronic calibration kit A.
4. Make sure that the antennas are at the same height and facing each other, with the MUT holder in between. (The MUT holder should be of non-reflecting material or as minimal as possible, it could be styrofoam which is about 1.1 in the real part of the permittivity, and practically lossless).
5. Ensure that the distance between the antennas to the material is the same. This step depends on the mathematical extraction equations.
6. Measure all the material sample thickness to micrometer level accuracy. Since the material's overall size is different, the thickness should be measured in micrometers in at least five different spots, at the four edges and in the center of the material, and averaged, and used the variance between the five measurements to estimate the error in the measurement of the thickness. Accuracy is more critical when going to higher frequencies. (This step depends on what mathematical methods are used to extract the material properties)
7. Connect the cables to both horn antenna and check the LOS path without any material between the horn antennas.
8. When LOS is confirmed, check S11 by recording S-parameter and processing it in MatLab or use the VNA directly.

9. Calibrate the environment by recording the S-parameter without any material (This will be used later in MatLab),2.11.
10. Place a metal plate at the reference point where the measured material will be placed and record S-parameters (This will be used later in MatLab).
11. Then place a known material between the antennas, record S-parameters, check for environmental reflection, and note the time gating, start and stop time of the LOS path, and do as in appendix B.
12. Do the calibration of the system environment. (Depends on the extraction method. Using the recorded S-Parameters)
13. Perform the first part of the extraction, the gamma coefficient, and transmission coefficient, as explained in section 2.4.1.
14. Check both coefficients by reverse S-parameters math and check the differences between the measured and reverse calculated S-parameter in MatLab. (Indications of how far off the calibrations are)
15. Suppose the S-parameters are off, then do everything again from step 9. Check where it went wrong.
16. Otherwise, transform the S-parameters into the time domain and use math in MatLab to apply the time gating. And then transfer the S-parameter back to the beginning of the extraction calculation. (If the time gating is set before recording the S-parameters, then it should not be necessary to use time gating at this step)
17. If the time gating is applied one way or another, then extract the material parameter.
18. Check if the result of the known material is off. If so, then do every step again from step 6, and check the thickness used. Otherwise, the result should be obtained.
19. If Keysight material software is used for obtaining the material properties, do it after step 9 and follow the steps in appendix C.

Step 18, the material properties extraction can be done in multiple ways, depending on some criteria, as mentioned in section 2.3. In this free space setup, as mentioned in section 2.4.0.3, the extraction method used to achieve the material properties is described in the next section.

2.4.1 Extraction of material properties using s-parameter

The most popular relative permittivity extraction method is NRW, where complex relative values of permittivity and permeability are simultaneously extracted. The method input requirements are the distance between the material and the antennas and the thickness of the material. Further, the method needs information about if the test material is magnetic or non-magnetic, and if the material is non-magnetic, then μ_r is one.
When transmitting the EM wave, part of the incident wave that hits the material will be reflected back into port one as the reflection coefficient (S11), and some of the EM waves will pass through the material and be received by port two as the transmission coefficient (S21), as seen in figure 2.18.

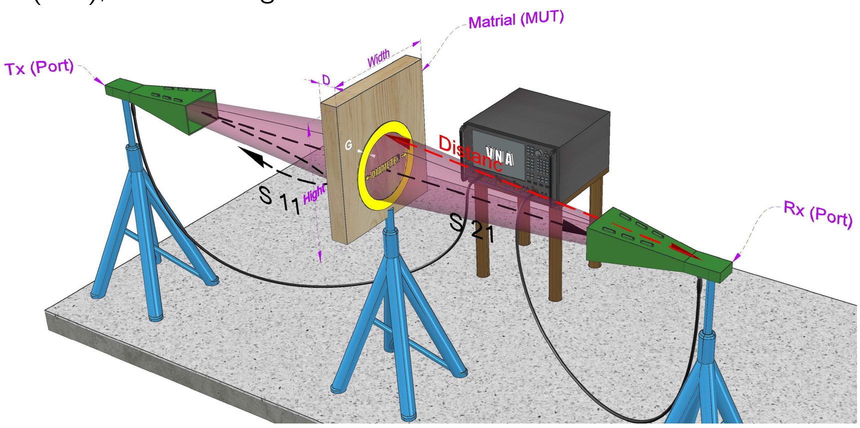

Figure 2.18: Free space error minimization of propagation on material.

However, depending on the environment and the material, one part of the incident EM wave will be reflected within the material, thereby having a delayed throughput which can affect the received transmission coefficient.
The procedure of NRW method to determine the relative permittivity and permeability:

$$S_{11} = \frac{\Gamma \cdot (1 - T^2)}{(1 - \Gamma^2 \cdot T^2)} \qquad S_{21} = \frac{T \cdot (1 - \Gamma^2)}{1 - \Gamma^2 \cdot T^2} \tag{2.14}$$

S_{11} and S_{21} is obtained directly from a VNA. The reflection coefficient can be calculated as:

$$\Gamma = K \pm \sqrt{K^2 - 1} \quad \text{where} \quad |\Gamma| \leq 1 \text{ is required for finding the correct root} \tag{2.15}$$

In terms of the s-parameters:

$$K = \frac{S_{11}^2 - S_{21}^2 + 1}{2 \cdot S_{11}} \tag{2.16}$$

The transmission coefficient can be calculated in terms of s-parameters:

$$T = \frac{S_{11} + S_{21} - \Gamma}{1 - (S_{11} + S_{21}) \cdot \Gamma} \tag{2.17}$$

The permeability can be defined and solved as:

$$\frac{1}{\Lambda} = -\left[\frac{1}{2 \cdot \pi \cdot L} \cdot ln\left(\frac{1}{T}\right)\right]^2 \tag{2.18}$$

$$\mu_r = \frac{1 + \Gamma}{\Lambda \cdot (1 + \Gamma) \cdot \sqrt{\frac{1}{\lambda_0^2} - \frac{1}{\lambda_c^2}}} \tag{2.19}$$

The permittivity can be calculated as:

$$\varepsilon_r = \frac{\lambda_0^2}{\mu_r} \cdot \left(\frac{1}{\lambda_c^2} + \frac{1}{\Lambda}\right) \tag{2.20}$$

$$\varepsilon_r = \frac{\lambda_0^2}{\mu_r} \cdot \left(\frac{1}{\lambda_c^2} - \left[\frac{1}{2 \cdot \pi \cdot L} \cdot ln\left(\frac{1}{T}\right)\right]^2\right) \tag{2.21}$$

It is also possible to calculate non-resonant relative permittivity of non-magnetic material without cutoff frequency by:

$$\varepsilon_r = \left[\left(j \cdot \frac{c}{\omega \cdot L}\right) \cdot ln(T)\right]^2 \tag{2.22}$$

[74],[75],[76] where:

$\mu_r =$ Relative permeability

$\varepsilon_r =$ Relative permittivity

$T =$ Transmission coefficient

$\Gamma =$ Reflection coefficient

$L =$ Length of the material

$\lambda_0 =$ Wavelength in free space

$\varepsilon_0 = 8.85419\ F/m$

$\mu_0 = 4 \cdot \pi \cdot 10^-7\ H/m$

$c =$ Speed of light

$$\lambda_c = \text{Cutoff frequency in (Hz)} \quad = \frac{1}{2 \cdot \pi \cdot \sqrt{\mu_0 \cdot \varepsilon_0}} \cdot \sqrt{\left(\frac{m \cdot \pi}{a}\right)^2 + \left(\frac{n \cdot \pi}{b}\right)^2}$$

$$\lambda_c = \frac{c}{2} \cdot \sqrt{\left(\frac{1}{a}\right)^2 + \left(\frac{1}{b}\right)^2} \quad \text{Or} \quad \frac{c}{2 \cdot g}$$

$a =$ Brood dimension (meters)

$b =$ Short dimension (meters)

$m =$ Number of $1/2$ wavelength across b

$n =$ Number of $1/2$ wavelength across a

$g =$ Antenna largest aperture dimension

Chapter 3

Validation and associated issues with the measurement setup

3.1 The issues associated with the setup

The free-space setup has various challenges, mainly because the method is contactless to the material and therefore has various issues to address. For instance, from the antenna perspective, the antennas should be vertically and horizontally aligned at about 0 degrees at the material. In other words, the antenna's position should be perpendicular to the material's surface to get an optimal result. The antenna alignment assumption comes from treating the waves from the far field as a uniform transmission line, which means the electromagnetic wave dimensions are identical at all planes transverse to the direction of propagation, as mentioned in section 2.4.0.1. However, when the antennas are vertically or horizontally off, the incident wave will propagate on the material at a different angle, which will affect the power received to be inaccurate. The issue implies that the antennas with respect to the material should be static and rugged in the measurement campaign [77].

If the sample does not have the same overall thickness and has a rough surface, it will become an issue for measuring the material. This, at lower frequencies, is negligible due to the larger wavelength not "seeing" the comparatively small roughness of the material. In most cases, the sample size is chosen according to the measurement method and frequency, so it is possible to assume they have the same overall thickness.

A large or semi-flex material tends to bend when the sample is not stretched or fastened to the vertical supporting material holder. If so, the bending of the material will cause inaccurate results because the material is not straight, which will cause the transmission and reflection to be different than with a straight material.

However, creating a rugged sample holder for hard materials is easier than for semi-flexible materials, and the issue that arises with the sample holder is the reflection, which can cause uncertainties in the measurements. Therefore it is essential to choose a material that has minimum reflection, such as styrofoam.

3.2 Critical issues for measurement

One critical issue for the free-space measurement method is the thickness of the material under test and the material holder's stability and ability to be stationary during the whole measurement procedure, as mentioned in the previous section. The same applies to the cables and antennas, which cannot be moved under any circumstances.

However, uncertainty errors can occur when changing the materials onto the sample holder, which can move or change the material's position, and if that happens, then the whole setup needs to be calibrated again to the reference point of the sample. The next critical issue is the calibration part, which needs to be executed in a specific procedure, as described earlier.

Furthermore, when choosing the sample material, it is essential to know how lossy the material is to be able to choose the methods within the free space technique. The methods of measuring are only S11, only 21 [78],[79], or both, and when a material is a high-loss material, the dynamic range of the signal will be too small. When the material is low-loss, it may be useless to measure the S11 if the measured signal power is high and the reflection is very weak. For almost all cases where the loss is within the midrange, both S-parameters are the most appropriate choice, because if the measurement power is lower for one of the S-parameter, then the other is usable.

In most mathematical extraction equations, the distance between antennas and the material is critical for getting an acceptable result [80]. Almost all equations related to the free-space method are based upon a setup where both antennas are equally separated from the sample material to ease the mathematical extraction equation. Otherwise, the equation would be far more complicated.

Environmental reflection is a critical issue at low frequencies, but at higher frequencies, it is less of an issue, and time gating is always available to reduce interference. Further, the setup can be placed into an anechoic chamber to improve the environmental conditions.

3.3 Calibration issues

The calibration procedure is completed in three stages, the VNA, the system environment, and the system setup calibration. When calibrating the VNA, it is necessary to check the cables and connector's capability within the frequency range before calibrating and setting all the parameters for the VNA. When the VNA calibration is complete, the reference point for measuring is at the connectors attached to the antennas, also referred to as the calibration to the port, as seen in figure 3.1.

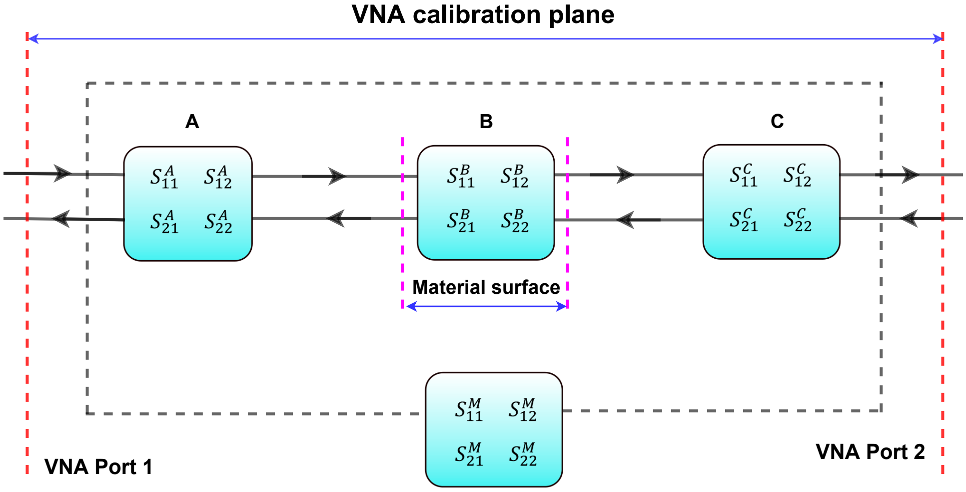

Figure 3.1: VNA calibration plane.

When calibrating the free-space setup environment, the calibration or measuring plane is moved from the end of the connectors that are attached to the antennas to the material surface. This procedure can be done in several different ways depending on which S-parameter is used to measure the material properties. One way is if only the S11 parameter is used, then it is possible to calibrate the material plane by measuring the material thickness and placing a metal plate first at the front and then back of where the samples should be and get the S-parameter reference to calibrate for each position of the sample plane. Another method is by using two different known thicknesses of the same material. The method used in this report is Gated-Reflect-Line (GRL) which only needs one known material thickness that will block the signal, in this case, a metal plate. Further, the method needs also a free-space measurement without a material placed in between the antennas.

The general issue in all methods is the measurement precision of the material thickness and precision of the sample placement. In [70], the author states that the calibration errors of permittivity percentage-wise between Thru-Reflect-Line (TRL)[20], Thru-Reflect-Match (TRM), and GRL[81] are respectively 2.9%, 2.4%, and 0.02%. When the free-space setup environment is calibrated, the reference plane includes the antenna and the environment and should be at the sample surface, as shown with the red dashed line in figure 3.1,[77].

One of the uncertainty errors is the temperature at the material's surface and the humidity. Both have a factor error, but the temperature is negligible [82]. The remaining source of error, such as reflection, diffraction, and load mismatch errors due to some flaws in the calibration, can be minimized by using time gating. The VNA calibration is done as in appendix A, and when the calibration of the VNA is done, then the calibration of the environment can be done as seen in B, and the calibration of the Keysight software can be configured to free-space measurement and configure the material specified, as seen in C.

The first thing after the calibration is done, is to check if it is correct by first connecting the cables together and looking at the S11 and S21 to confirm the cables.
Figure 3.2 shows S21 when the cables are connected to each other, and confirms that all power that is transmitted also is received, and thereby the cables from the VNA and connectors are intact and calibrated correctly.

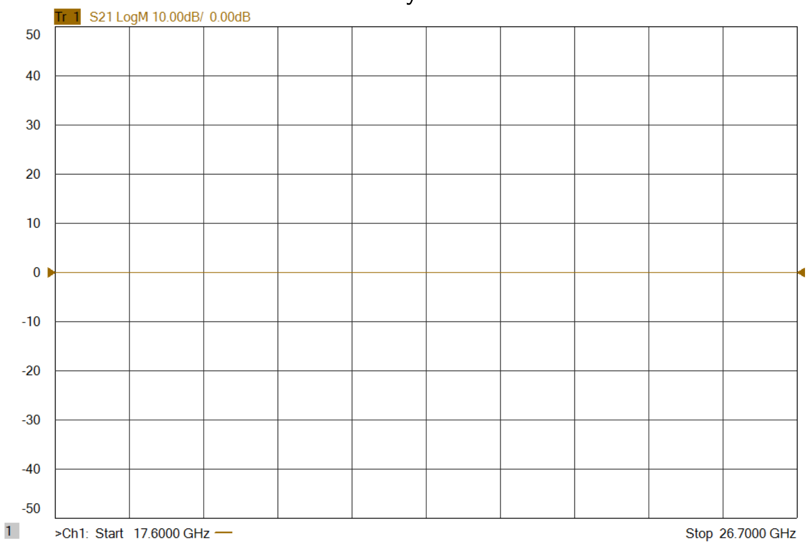

Figure 3.2: S21 in dB

The second thing is to connect the cables to the antennas and look at VSWR, S11, and S21.
The VSWR can be measured by connecting a coaxial cable to the antennas with a preset frequency band of interest, in order to see the impedance mismatch. The VSWR is the ratio between an RF system's incident and reflected wave. It determines the power transmission efficiency from a source to the load through a transmission line. The minimum value of VSWR is 1, an ideal condition where the load absorbs 100% of power from the source, but in the real world, it never gets to 1. Generally, the rule of thumb is if the VSWR is less than 2, it is considered acceptable, but it depends on the requirements it

will be used for. Figure 3.3 shows the VSWR for the free-space setup, where the coax cables are attached to the antenna.

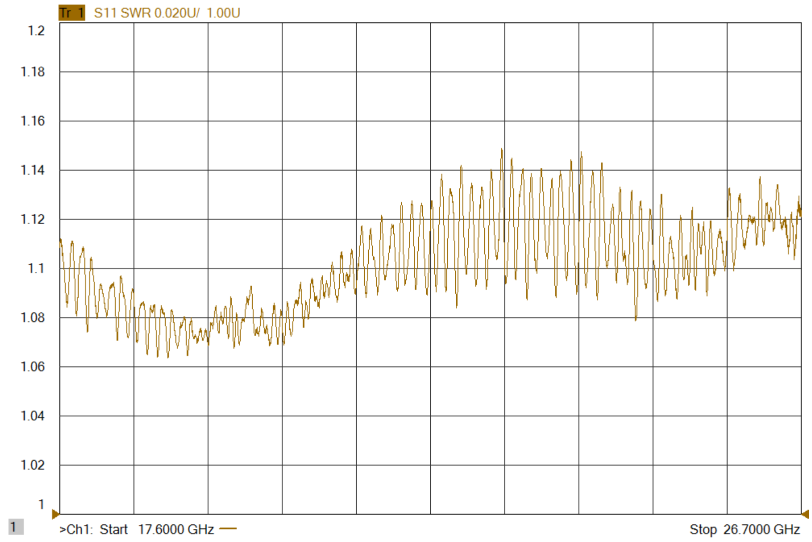

Figure 3.3: The VSWR

Figure 3.3 shows a VSWR lower than 1.16 which means that almost all of the power is transmitted and is not returned. S11 parameter can be seen in the dB scale in figure 3.4.

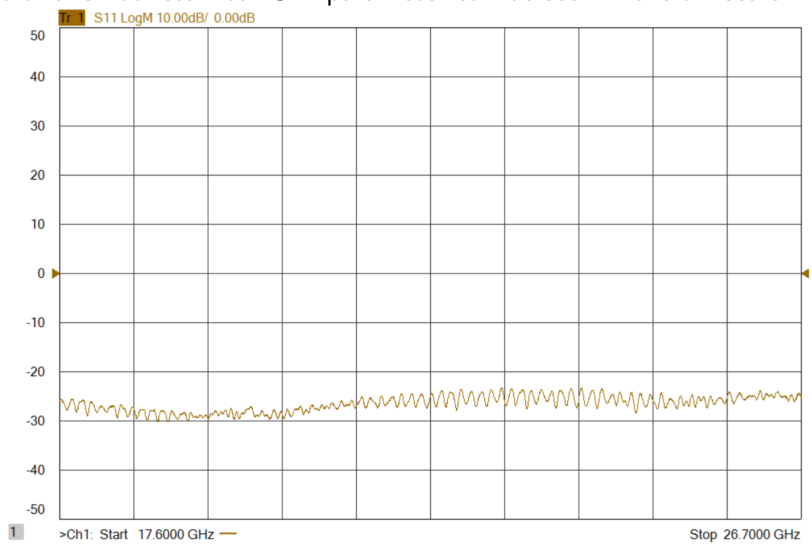

Figure 3.4: S11 in dB

Figure 3.4 shows also that the returned signal is lower than -20 dB over the frequency band, which is a good performance, and thereby most of the power is transmitted.
S11 and S21 in dB scale in the frequency domain show how good the "probe" or system is to measure materials at the frequency range.

3.4 Validation of the setup and the principles

This section contains the validation of the setup and its principles and shows elements to support and confirm the measurement setup validity.
The free space system validation is performed in three different stages, and the first stage is the calibration of the VNA and the setup. The second stage is the setup placement in reference to elements within the setup, and the third validation is the surrounding environment and its uncertainty.
The calibration of the VNA is done by an Ecal kit, as shown in appendix A. The report does not go into detail about verifying if the Ecal kit is of acceptable accuracy.
Verifying the alignment of antennas perpendicular to the material under test and to each other. The height of the antennas is ensured by measuring the distance from the same ground reference with a laser measurement tool that has an accuracy of $\pm 2\%$. The laser was also used for correcting the perpendicular alignment, and measuring the distance from the antenna to the material. When the laser dot is at the center of the antenna, the waves are anticipated to be plane waves because the antenna's position is in the far field.
As mentioned before, the ruggedness of the setup is critical. The antennas, material holder, and cables should not be moved under any circumstances. The material holder is made out of styrofoam for some material in order to minimize possible reflection from it. Furthermore, it is possible when measuring flexible material to build like a sandwich and hold the material under test as flat as possible without radically affecting the measurement. This is possible because styrofoam only has a permittivity of about 1.05.
The next step is to verify that the measured LOS path is the correct one, which is done by blocking the signal and confirming that the time delay is the same and that the signal power is decreased, which confirms the LOS path. The signal path propagation is confirmed, and by looking at the S11 and S21 it is possible to see how the system itself without any material performs in the frequency range.
Furthermore, the free-space setup was placed in an anechoic chamber at the antenna lab facility at Aalborg university to eliminate reflection. Time gating was used for further improvement of removing the interference or clearing unwanted signal from the sides, as seen in figure 3.5.

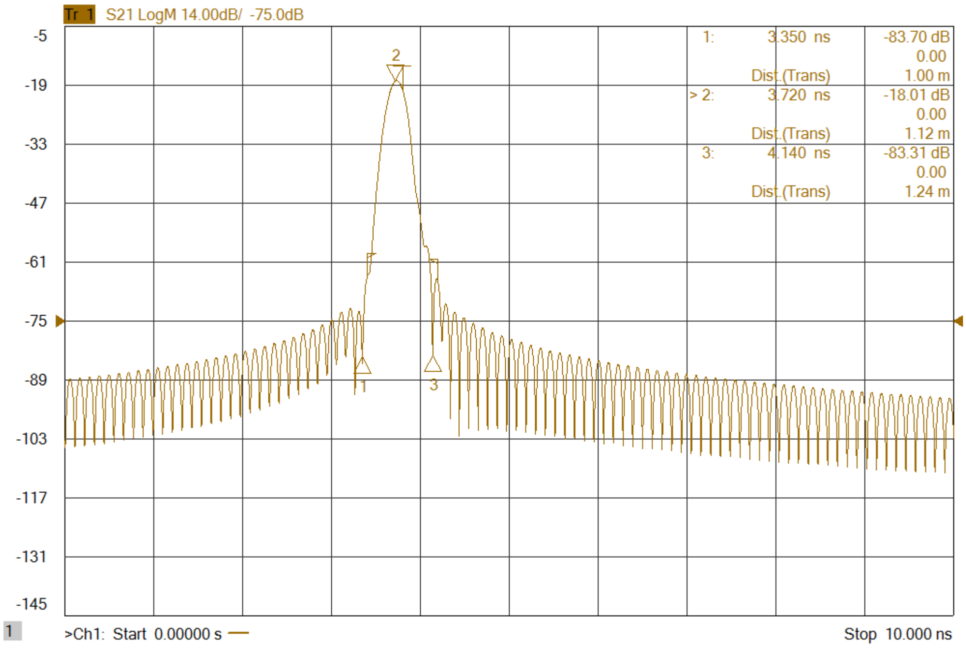

Figure 3.5: S21 with time gating, for removing unwanted interference signal.

The last thing before taking a test measurement of a known material is to ensure that the antennas are at the far field and that the propagated beam diameter on the material is within the material margins. Table 5 shows the calculated and simulated differences. The calculation is done as mentioned in section 2.8, and the simulation are made in software called Wireless InSight. The calculation is done calculate the antenna far fields requirements as mentioned in section 2.4, and second is the material size and the HPBW. Then the HPBW, the antenna aperture dimension, and a fixed distance between the material and the antenna are used to simulate the diameter of the propagated signal onto the material by using "Wireless InSight" software. Figure 3.6 shows the simulated setup with the transmitter antenna and a simulated material, which contain a lot of small antennas that will show the distributions of the propagated signal, as shown in figure 3.7.

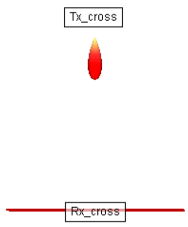

Figure 3.6: Simulation of the setup of an transmitter and reciver as the material

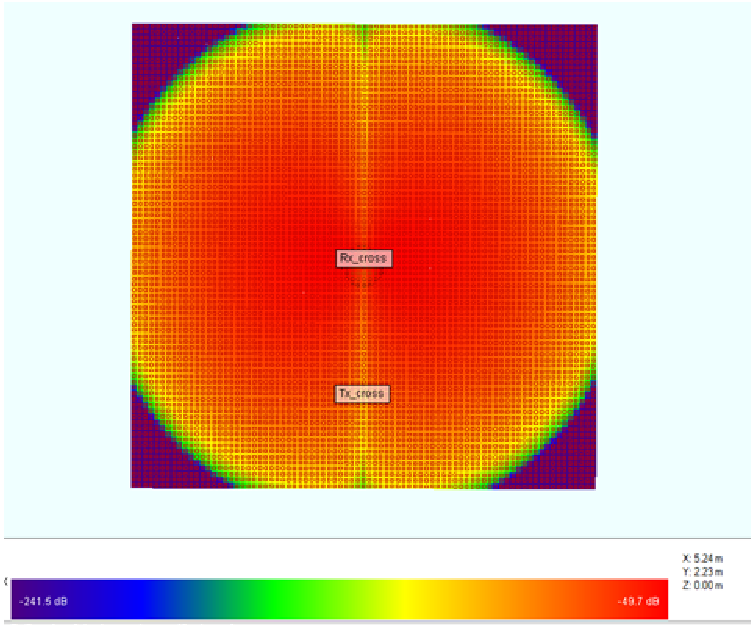

Figure 3.7: S21 in dB

Then by using the antenna's received power, it is possible to see where it degrades in both horizontal and vertical positions.
Table 5 shows a deviation under 1 cm accuracy, but looking closer at each received point then, there is a small gap between some of the received power, implying that there could have been more receivers to get a more accurate result. Generally, it is acceptable because if the repetition of the simulation had increased the number of receivers, then it would give a propagated diameter with a deviation of less than 3 mm at the same distance.

Projection diameter calculated	**Projection diameter simulated [83]**	**The deviation in (cm)**
16.64	17.00	0.36
10.91	11.00	0.09
11.16	11.50	0.34
7.33	8.00	0.67
7.41	8.00	0.59
4.87	5.00	0.13

[a] **Table 5**

The last validation is to see how accurate the system is. This is done by taking two measurements, one without any material, which should give a permittivity very close to one, and the second measurement is done with a known material permittivity.

3.5 Uncertainty analysis of measurements

The software calibration stability and measurements are analyzed, concluding that both parameters are drifting over time, as seen in appendix E.
The calibration uncertainty of the system is 0.02% – 2.4% in reference to Keysight [70]. Furthermore, even though the software supports IFband changes, it doesn't measure appropriately under 2 KHz, and the program freezes if IFband is below 1 KHz. The distance between the TX antenna and the material is highly sensitive when the material is of high density, and the thickness is either less than 2 mm or thicker than 20 mm. If the material isn't perpendicular to the antennas, then low-density material will have a minor effect on the readings compared to high-density material. The software sometimes gets stuck on a particular value level if the exact measurements are repeated several times when the material is bending, or the material orientation is slightly changed. When the material has a rough surface, it is hard to get a usable reading of the permittivity, and even worse for the imaginary part, which often goes below 0.
The material variation thickness and the measuring precision method of the thickness create another uncertainty. First, the material itself and the thickness are inhomogeneous; second, a digital caliper is not the most precise measuring tool when measuring the thickness of the material, as seen in figure 4.8.
Taking everything into consideration, such as:

- The drifting of calibration and material measurement 0.5%
- The calibration of 2.4%
- The slab position change of 0.3%
- The uncertainty of the correct thickness can vary a lot from material to material, especially with high-density material.
- If the material is 20 degrees off from being perpendicular to the antennas, it will introduce an uncertainty of about 0.2% - 0.6%
- The alignment of the antennas 0.1%

The total uncertainty of material measurements is 3.5% and plus the material density uncertainty effect.

Chapter 4

Measurement campaign setup and results

This section explains the measurement content, the tools, and the setup of the experiment. The objective of the measurement campaign is to measure the permittivity of common building materials from 18 GHz - 58 GHz, which is divided into three different frequency bands. The frequency bands are from 18 GHz - 58 GHz, which is divided into three frequency bands, namely 17.6 GHz - 26.7 GHz, 26.4 GHz – 40.1 GHz, and 39.3 GHz – 58 GHz.

4.1 Setup for the experiment

The experiment was conducted in an anechoic chamber at Aalborg University's antenna laboratory. The setup is shown in figure 4.1, and the equipment used for the experiment is the following:

- (1) Antenna reflection absorbers for both antennas.
- (2),(4) Two standard gain horn antennas for each frequency band, (20240-20,22240-20,24240-20).
- (3) Camera PTZ 310H.
- (5) Turntable (HRT I 6498) that is able to control the material, so it is perpendicular to the antenna.
- (6) Vector network analyzer N5227B (VNA).
- (7) Distance laser measurement tool.

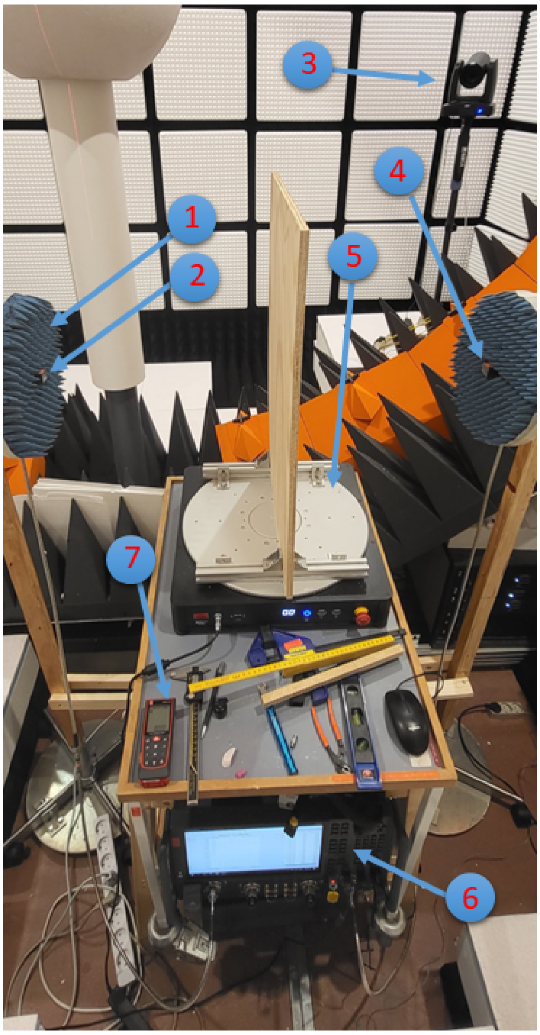

Figure 4.1: Free space setup for the material measurement.

The setup was built to be rugged and stable enough to be able to carry heavy elements. First, the height of the antenna was measured from the turntable, as seen in figure 4.2 to ensure that the propagated beam would not get a reflection from the surface of the turntable plate. The minimum height distance required is the radius of the calculated projection beam, as discussed in section 2.4.0.2.

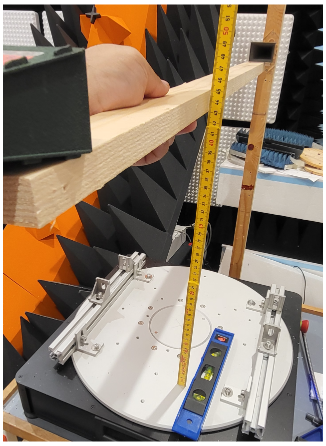

Figure 4.2: Ensuring the height of the antennas is sufficient in reference to 2.4, so the aluminum plate would not have an effect on the measurements.

Furthermore, the antennas were leveled in horizontal/vertical axis 3.1 to minimize any polarization effect, as seen in figure 4.3. By leveling both antennas at the same time with respect to each other, then the height level is the same for both antennas as seen in figure 4.4.

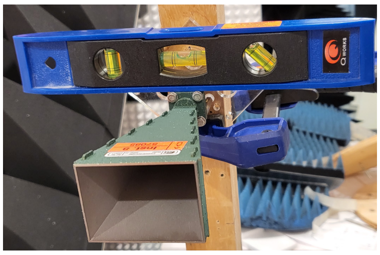

Figure 4.3: Ensuring the antenna's horizontal position.

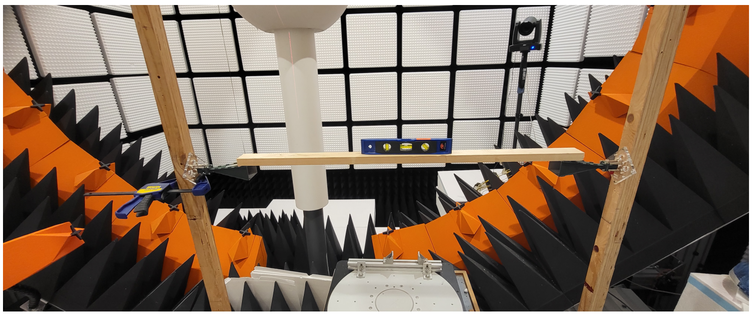

Figure 4.4: Ensuring that the height of both antennas is the same.

The alignment of the antennas was done using a laser as shown in figure 4.5. The alignment is to ensure that the propagated beam from the antennas is directed at each other and the material can be perpendicular to the antennas 3.1.

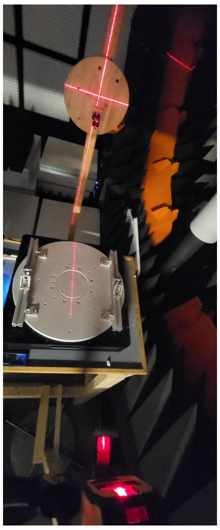

Figure 4.5: Aligning the antennas from both sides and the material holder.

The setup was constructed so the distance between the antenna and the material was the same on each side of the material, and this was done by using a laser to measure the distance, as seen in figure 4.6.

Figure 4.6: Measuring the distance from both antennas onto the surface of the material.

Moreover, to ensure that the distance from the antenna to the material is not shorter on the top than the bottom then each material got measured as seen in figure 4.7. The measurement for the vertical position of the material ensures that the material position vertically is the same to some extent from both sides 3.1.

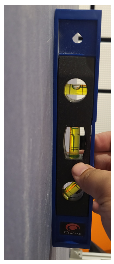

Figure 4.7: Ensuring the vertical material position.

The material is not homogenous and thereby the thickness variate over the material surface as seen in figure 4.8.

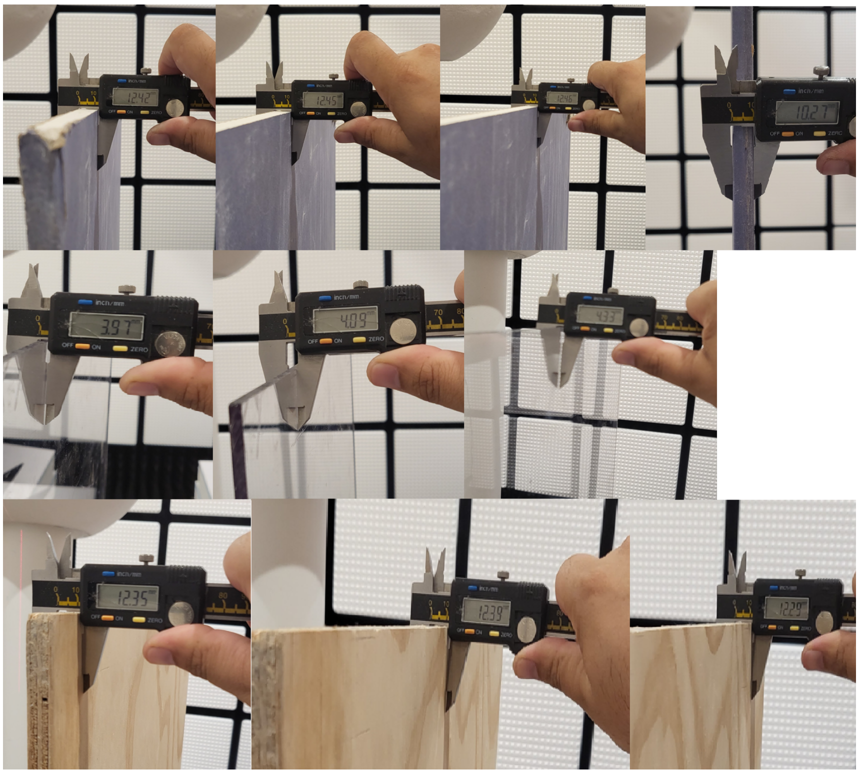

Figure 4.8: Material thickness variation.

Furthermore, to ensure to some extent that the incident wave is perpendicular to the material 3.1, then it is possible to turn the turntable until both planes of the material and the horn antenna is perpendicular, as seen in figure 4.9.

Figure 4.9: Ensuring the material is perpendicular to the antenna's beam.

The setup is built in reference to the issues that were discussed in section 3, in order to avoid measurement faults. The setup is complete and needs to be calibrated as mentioned step by step in appendix A, B, C. The common building material that is used for the measurement are as follows:

Material sample	Thickness of the material (mm)
[1] Plexiglass	4.10
[2] Plywood	12.20
[3] Plywood	12.38
[4] Masonite	3.16
[5] PP material	1.95
[6] Plastic material	1.40
[7] Laminate floor	8.00
[8] Gypsum board	12.42
[9] Moisture-shielded gypsum board	12.42
[10] Acoustic troldtekt board	21.66
[11] Acoustic rockfon board	19.48
[12] Outdoor tile	20.41
[13] Facade cladding panel	9.56
[14] Outdoor concrete tile	50.50

[a] **Table 6, D**

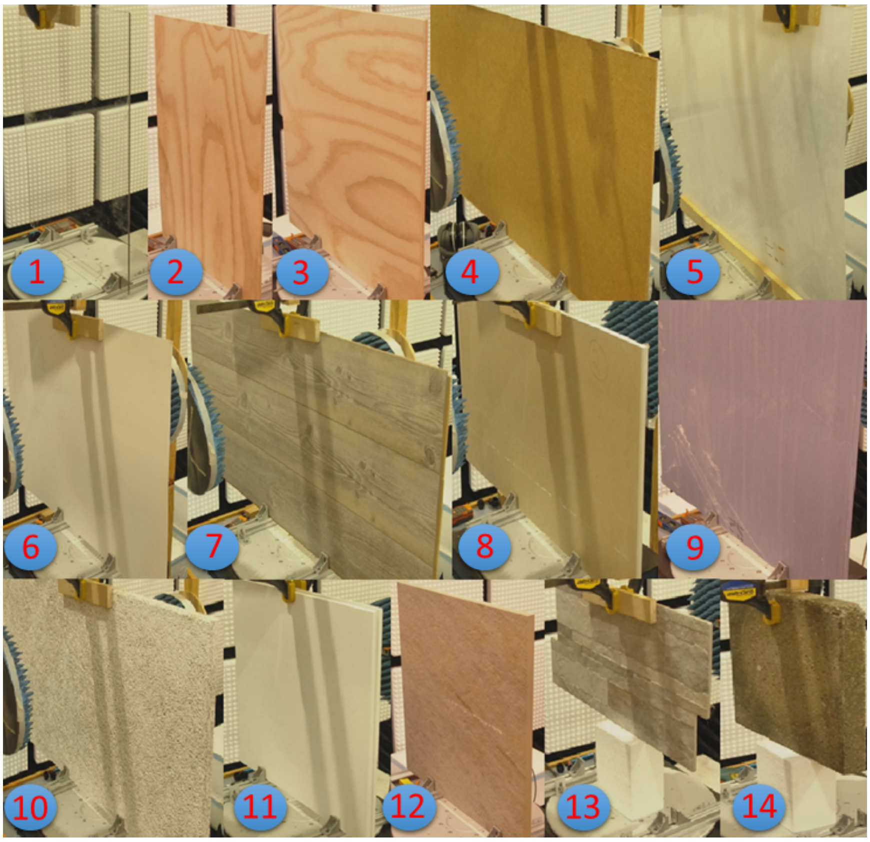

Figure 4.10: Material sample.

4.2 Measurement results

This section will introduce the results of fourteen common building materials pt. used in Denmark, and they are grouped into four groups with the y-axis as real ε_r' and imaginary ε_r'' parts of the complex relative permittivity, respectively, and the x-axis as the frequency. Just keep in mind that dielectric is an insulating material, such as used for insulation cables, capacitors, printed circuit boards, etc, and it is a complex number with a real and imaginary parts.

The real permittivity component measures the material's ability to store or quantify the stored energy, and remit energy from an external electric field that is applied. The real permittivity component is directly proportional to the field amplitude and it also indicates the degree to which a material can be polarized [84, 85]. The greater the degree of polarization, the greater the value of the real permittivity component ε_r'.

The imaginary part ε_r'' is always positive and it measured the amount of energy lost or absorbed in the material when an external electrical field is applied, and it is also referred to as the loss factor, as mentioned in section 1.1. A material with a high imaginary part absorbs more electromagnetic energy than a material with a lower imaginary part, and when the imaginary part is higher the radio waves can't travel as fast as the speed of light and can not travel far through the material.

Figure 4.11 shows four materials, plexiglass, two different plywood materials with different thicknesses, and masonite. The plexiglass is around 2.6 real part of the complex relative permittivity, plywood 12.20 mm is around 1.87, plywood 12.38 mm is around 1.8, and masonite 3.16 mm is around 2.4. The Plexiglas's result is similar to others, such as [86–88] they all are around 2.6 in the real part of the complex permittivity.

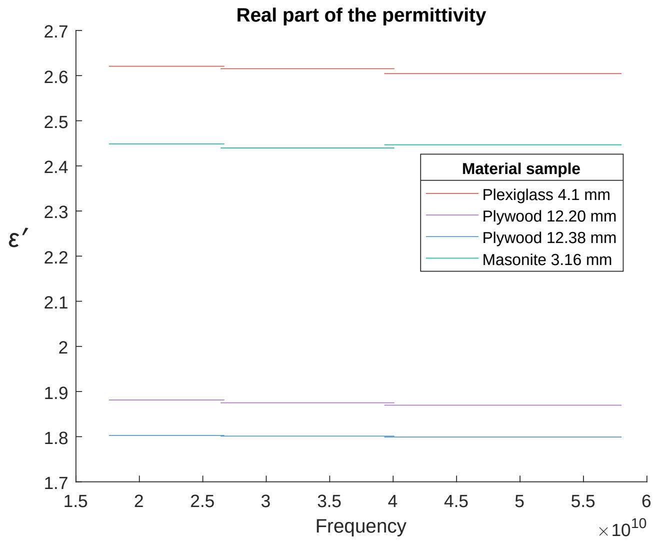

Figure 4.11: The real part of the permittivity measuring results for Plexiglas, two plywood, and Masonite.

Furthermore, figure 4.11 shows Plexiglas has the highest permittivity among the four material, which indicate that Plexiglas has a higher insulation ability and polarizes more in response to the applied electric field than the other materials, thereby storing more energy. The Plexiglas polarizes more, does not mean it is easy to polarize, just the opposite.

Both Plywood materials have a lower real part permittivity than Plexiglas and Masonite, which shows that both Plywood materials have a lower ability to store energy and thereby lower and easier polarization [84, 85].

All materials are taken in three different frequency ranges as shown in figure 4.11 and the others figures, and it is possible to see overlapping or very close permittivity between the frequency ranges.

Figure 4.13 shows the imaginary part of the complex relative permittivity, which tells how lossy the material is. The loss tangent is zero for a lossless material, and increases with increasing loss, as seen in figure 4.13 the plexiglass material is lossless material in reference to Masonite. In other words, the wave has it easier to penetrate Plexiglas than Masonite and plywood material. The plywood material structure is a bit different in the layers, as seen in figure 4.12, and almost the same thickness and loss, as seen in figure 4.13.

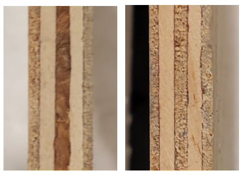

Figure 4.12: Plywood materials, the left one is Plywood 12.20 mm, and the right one is Plywood 12.38 mm.

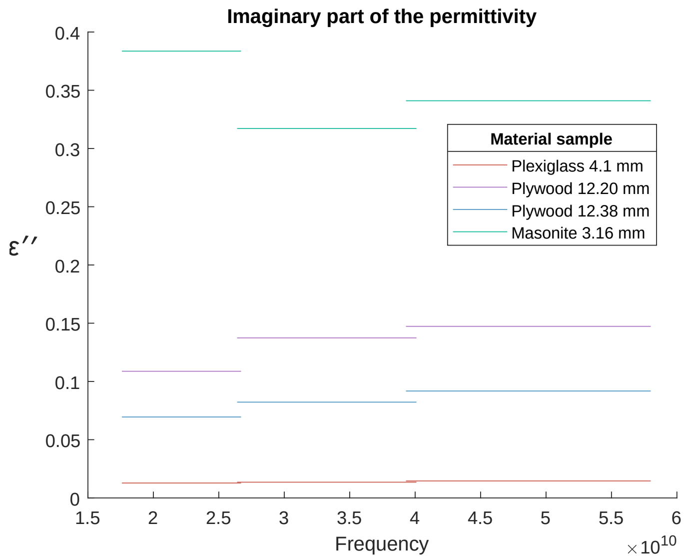

Figure 4.13: The imaginary part of the permittivity measuring results for the same materials as in 4.11.

Figure 4.14 shows the real permittivity component of a PP material about 2.23, Plastic material about 2.27, Laminate floor material about 2.63, and Gypsum board material about 2.43. The highest real permittivity component is the Laminate floor material which is about the same energy storage ability as Plexiglas.

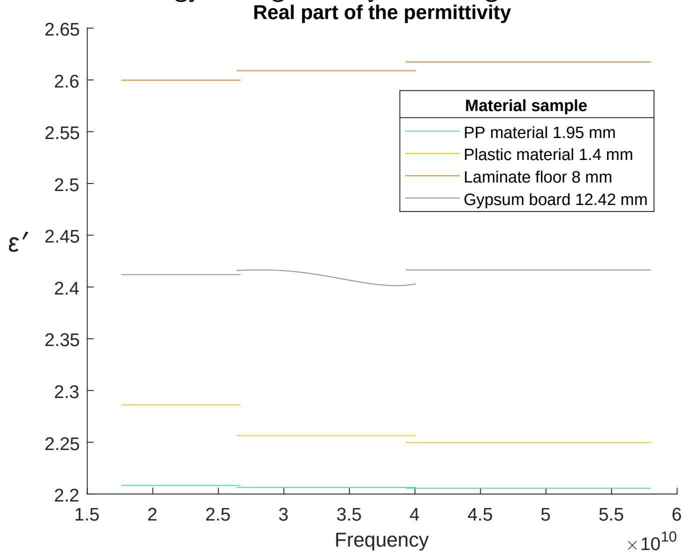

Figure 4.14: The real part of the permittivity measuring results for PP material, Plastic material, Laminate, Gypsum board.

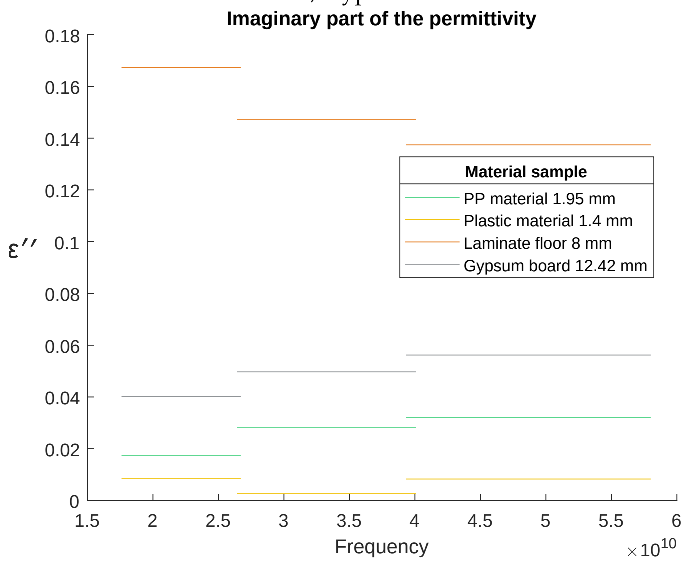

Figure 4.15: The imaginary part of the permittivity measuring results for the same materials as in 4.14.

Even though Plastic material, PP material, and Gypsum board have a real permittivity higher than two, the materials do not absorb much of the signal, as the loss factor shows in figure 4.14. Figure 4.16 shows four other materials, and the Moisture-shielded Gypsum board is about 0.3 higher than Gypsum board that is used inside houses and the loss factor is very low and both are about the same level, as seen in figure 4.17.

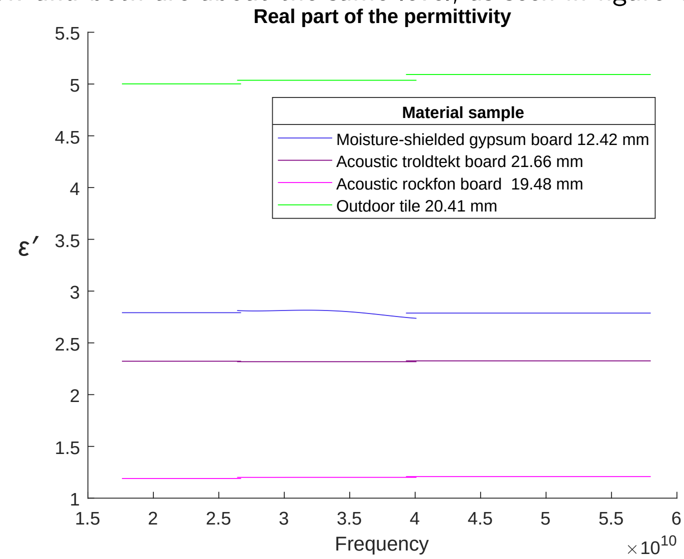

Figure 4.16: The real part of the permittivity measuring results for moisture-shielded gypsum board, acoustic troldtekt board, acoustic rockfon board, outdoor tile.

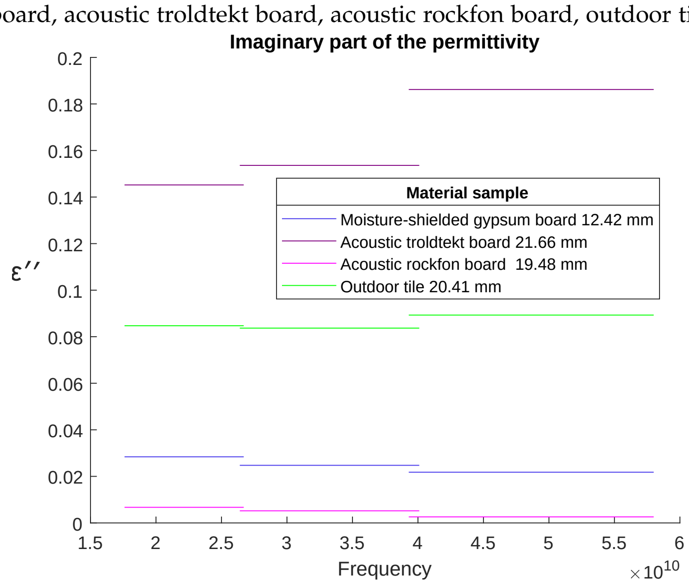

Figure 4.17: The imaginary part of the permittivity measuring results for the same materials as in 4.16.

The Acoustic troldtekt (real part permittivity 2.4) and Acoustic rockfon (real part permittivity 1.2) material are almost the same in thickness, and the real part of the permittivity differ about 1.2, and the panel is used as absorbs panels. The Acoustic troldtekt imaginary part is higher and thereby the loss is higher the waves that hit the material gets more resistance and the power is absorbed in the material and the wave will not travel

far into the material compared to the Acoustic rockfon material.
Figure 4.16 also shows a measurement of an outdoor tile with a real part permittivity of about 5, and that is expected since the outdoor tile is of a hard and compact density material and thereby also hard for the waves to pass thru compared to plywoods material, which is of a softer and loser density material [24, 25].
Figure 4.18 shows the real permittivity part of Facade cladding panel at about 4.45 and Outdoor concrete tile at about 5.42. The Outdoor tile and the Outdoor concrete tile have½ similar permittivity and looking at the imaginary part then it is higher than compared to other materials, and the material has a high absorption of the energy of the wave.

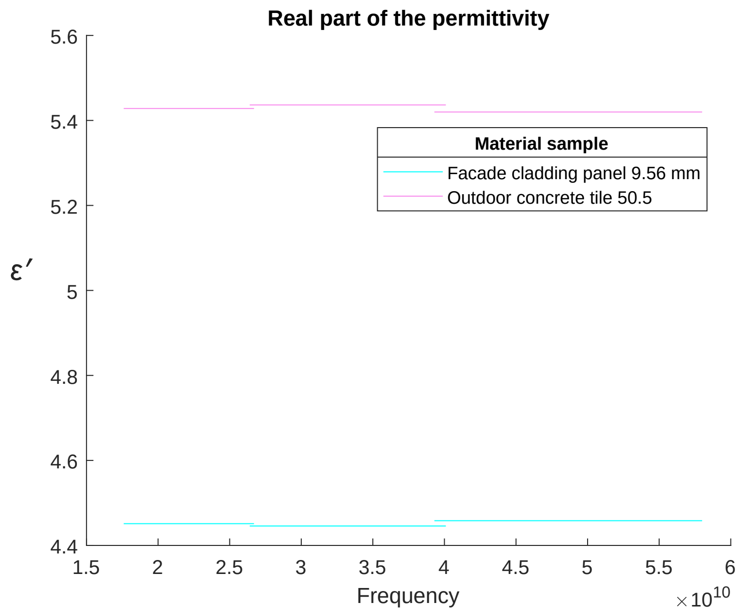

Figure 4.18: The real part of the permittivity measuring results for facade cladding panel, outdoor concrete tile.

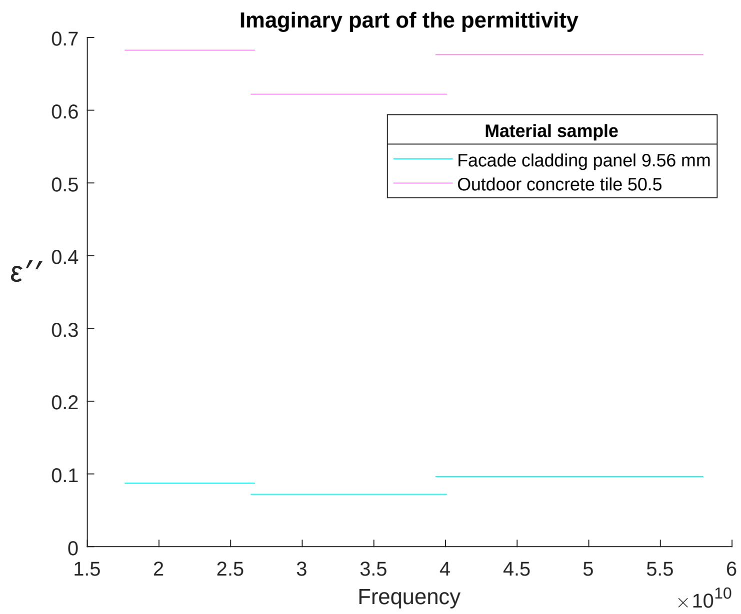

Figure 4.19: The imaginary part of the permittivity measuring results for the same materials as in 4.18.

Facade cladding panel has also a high real permittivity part in reference to other materials that are measured except the tiles. Figure 4.19 shows also the imaginary part of the Facade cladding panel material and the imaginary part is very low and thereby the material has a very low ability to absorb the waves.

Summarize

The result of the measurement shows values of the relative complex permittivity both real and imaginary parts, which is of great interest to see the differences from material to material. These values can be interpreted and used for ray-tracing simulation software, etc. Furthermore, this setup and the method that is used are of great interest since it is possible to measure multiple different materials, and thereby when using simulation, the simulated radio propagation environment would be more realistic and accurate in reference to the real-world scenario.
Moreover, the permittivity depends on the material's humidity, [24, 25], the structure of combined atoms, and its ability to be polarized, [84, 85]. In some cases, the permittivity can differ from other researchers' results. Furthermore, the same materials can be produced by different manufacturers, where the percentage of the combined material element can be different, and thereby also give different permittivity results. If the material consists of fewer elements or is pure of one element then the result should be similar.

Chapter 5

Conclusion

This report is about measuring the dielectric properties of common building materials for propagation studies at mmWave frequency range from 17.6 GHz to 58 GHz.
The report includes an overview of multiple measurement methods and approaches, which depends upon the frequency and the size of the test material. The method's advantages and disadvantages are explained, and the common permittivity extraction method using s-parameters and their procedure is presented, 2.3,2.4.0.3,2.4.1.
Within the multiple measurement methods, the free-space method is chosen for this research report. One of the advantages of the free-space method is that it allows for non-destructive measurement and the method is good for broadband frequencies measurements, as mentioned in section 2.2.6.
When measuring permittivity, there are certain requirements, such as the Far-field and the material size, etc. which are calculated and explained in chapter 2.4.
The report further includes the mathematics behind the extraction method that is used for prepossessing the data. In the report, the validation and associated issues with the measurement setup are examined, processed, and tested, E. Moreover, critical issues for measurement and calibration issues are also explained in section 3. Lastly on chapter 3 is the validation and simulation of the setup and its principle and uncertainty analysis of the system.
The measurement setup was built with the uncertainty analysis and the setup issues in mind, to get the best possible setup for the measurement. In the theory part, calculations were made, such as the Far-field and material size, etc. The setup was built in reference to the material size, weight of the material, and setup functionality, such as the ability to turn the material for alignment. The antenna's level and alignment to each other and to the material perpendicularly both horizontally and vertically needed to be done. The distances needed to be the same between the material and the antennas, and then the material holder position was measured using the VNA. For every measurement, several thickness measurements were taken since the material did not have the same thickness overall and the measurement procedure was followed as shown in section 2.4.0.3.

The result of the measurement shows the relative complex permittivity both real and imaginary parts, which is of great interest to see and interpret the differences from material to material. Looking at one result, such as the Outdoor tile, has a real part permittivity of around five as expected, as seen in figure 4.18. Since the mass density of Outdoor tile is higher compared to Plexiglas or PP material [24, 25, 84, 85]. The Outdoor tile absorbs the energy and the material is more but harder to polarize because of the molecule structure. The imaginary part is shown in figure 4.19.

The results of those fourteen common building material permittivities are essential for prototyping of antennas and simulating communication propagation. The knowledge of the permittivity can be added to the simulation for buildings, streets, etc. in order to get a more accurate picture of the real-world communication interaction of the environment. These results can show, how much a signal with a specific frequency will be attenuated with materials, and which of the materials would be better or worse in a given scenario. In some situations, you would like the transmitted signal to be reflected and scattered as much as possible in order to cover a valley or urban area. Then it would be possible to simulate a similar scenario with permittivity values of buildings material, then design, and tune the antenna to the best-suited environment. Such simulation software could be any RF communication and design tool for antenna or ray-tracing simulation software to easier estimate the real-world scenario when the systems are deployed. Furthermore, the knowledge of the setups and methods, as well as the advantages and disadvantages is of great interest and usable, since it is possible to measure multiple different materials and build a big data collection for simulation for the future.

Bibliography

[1] *complex permittivity permeability: Topics by Science.gov*. https://www.science.gov/topicpages/c/complex+permittivity+permeability.html. (Accessed on 09/16/2022).

[2] B. Greenebaum and F. S. Barnes. *Bioengineering and Biophysical Aspects of Electromagnetic Fields*. Boca Raton, FL, USA: CRC Press, Oct. 2018. ISBN: 978-1-42000947-7. URL: https://books.google.dk/books/about/Bioengineering_and_Biophysical_Aspects_o.html?id=1NfLBQAAQBAJ_&redir_esc=y.

[3] E. C. Fear et al. "Confocal microwave imaging for breast cancer detection: localization of tumors in three dimensions". In: *IEEE Transactions on Biomedical Engineering* 49.8 (Aug. 2002), pp. 812–822. ISSN: 1558-2531. DOI: 10.1109/TBME.2002.800759. URL: https://doi.org/10.1109/TBME.2002.800759.

[4] C. Gabriel, S. Gabriel, and E. Corthout. "The dielectric properties of biological tissues: I. Literature survey". In: *Physics in Medicine & Biology* 41.11 (Nov. 1996), pp. 2231–2249. ISSN: 0031-9155. DOI: 10.1088/0031-9155/41/11/001. URL: https://doi.org/10.1088/0031-9155/41/11/001.

[5] S. Gabriel, R. W. Lau, and C. Gabriel. "The dielectric properties of biological tissues: II. Measurements in the frequency range 10 Hz to 20 GHz". In: *Physics in Medicine & Biology* 41.11 (Nov. 1996), pp. 2251–2269. ISSN: 0031-9155. DOI: 10.1088/0031-9155/41/11/002. URL: https://doi.org/10.1088/0031-9155/41/11/002.

[6] S. Gabriel, R. W. Lau, and C. Gabriel. "The dielectric properties of biological tissues: III. Parametric models for the dielectric spectrum of tissues". In: *Physics in Medicine & Biology* 41.11 (Nov. 1996), pp. 2271–2293. ISSN: 0031-9155. DOI: 10.1088/0031-9155/41/11/003. URL: https://doi.org/10.1088/0031-9155/41/11/003.

[7] Mariya Lazebnik et al. "A large-scale study of the ultrawideband microwave dielectric properties of normal, benign and malignant breast tissues obtained from cancer surgeries". In: *Physics in Medicine & Biology* 52.20 (Oct. 2007), pp. 6093–6115. ISSN: 0031-9155. DOI: 10.1088/0031-9155/52/20/002. URL: https://doi.org/10.1088/0031-9155/52/20/002.

[8] A. J. Surowiec et al. "Dielectric properties of breast carcinoma and the surrounding tissues". In: *IEEE Transactions on Biomedical Engineering* 35.4 (Apr. 1988), pp. 257–263. ISSN: 1558-2531. DOI: 10.1109/10.1374. URL: https://doi.org/10.1109/10.1374.

[9] William T. Joines et al. "The measured electrical properties of normal and malignant human tissues from 50 to 900 MHz". In: *Medical Physics* 21.4 (Apr. 1994), pp. 547–550. ISSN: 0094-2405. DOI: 10.1118/1.597312. URL: https://doi.org/10.1118/1.597312.

[10] Susan Rae Smith, Kenneth R. Foster, and Gerald L. Wolf. "Dielectric Properties of VX-2 Carcinoma Versus Normal Liver Tissue". In: *IEEE Transactions on Biomedical Engineering* BME-33.5 (May 1986), pp. 522–524. ISSN: 1558-2531. DOI: 10.1109/TBME.1986.325740. URL: https://doi.org/10.1109/TBME.1986.325740.

[11] Jie Qiu et al. "Preparation and applinrcation of dielectric polymers with high permittivity and low energy loss: A mini review". In: *Journal of Applied Polymer Science* 139.24 (June 2022), p. 52367. ISSN: 0021-8995. DOI: 10.1002/app.52367. URL: https://doi.org/10.1002/app.52367.

[12] [Online; accessed 17. Sep. 2022]. Sept. 2022. URL: https://backend.orbit.dtu.dk/ws/portalfiles/portal/131993749/Untitled.pdf.

[13] Masahiro Horibe, Yuto Kato, and Ryo Sakamaki. "Electromagnetic Measurement Techniques for Materials and Device Used in 6G Wireless Communications". In: *2020 2nd 6G Wireless Summit (6G SUMMIT)*. IEEE, Mar. 2020, pp. 1–5. DOI: 10.1109/6GSUMMIT49458.2020.9083897. URL: https://doi.org/10.1109/6GSUMMIT49458.2020.9083897.

[14] [Online; accessed 17. Sep. 2022]. July 2022. URL: https://www.keysight.com/us/en/assets/7121-1085/article-reprints/RF-Enabling-6G-Opportunities-and-Challenges-from-Technology-to-Spectrum.pdf.

[15] *IEEE Xplore Full-Text PDF:* [Online; accessed 4. Oct. 2022]. Oct. 2022. URL: https://ieeexplore-ieee-org.zorac.aub.aau.dk/stamp/stamp.jsp?tp=&arnumber=7220116.

[16] *IEEE Xplore Full-Text PDF:* [Online; accessed 4. Dec. 2022]. Dec. 2022. URL: https://ieeexplore-ieee-org.zorac.aub.aau.dk/stamp/stamp.jsp?tp=&arnumber=8254893&tag=1.

[17] *IEEE Xplore Full-Text PDF:* [Online; accessed 4. Dec. 2022]. Dec. 2022. URL: https://ieeexplore-ieee-org.zorac.aub.aau.dk/stamp/stamp.jsp?tp=&arnumber=6655403.

[18] [Online; accessed 4. Dec. 2022]. Aug. 2022. URL: https://www.repository.cam.ac.uk/bitstream/handle/1810/338459/mia2.12274.pdf?sequence=3.

[19] [Online; accessed 4. Dec. 2022]. May 2021. URL: https://www.bibliomed.org/mnsfulltext/218/218-1618601309.pdf?1663512681.

[20] L. F. Chen et al. *Microwave Electronics: Measurement and Materials Characterization*. Hoboken, NJ, USA: Wiley, Apr. 2004, pp. 192–199. ISBN: 978-0-470-84492-2. URL: https://www.wiley.com/en-us/Microwave+Electronics:+Measurement+and+Materials+Characterization-p-9780470844922.

[21] Pavel Koštial et al. "Utilization of ceramic materials in the process of electromagnetic wave conversion to heat usable for space heating of residential facilities". In: *MATEC Web of Conferences* 292 (Sept. 2019), p. 01014. ISSN: 2261-236X. DOI: 10.1051/matecconf/201929201014. URL: https://doi.org/10.1051/matecconf/201929201014.

[22] Contributors to Wikimedia projects. *Permittivity - Wikipedia*. [Online; accessed 2. Jan. 2023]. Dec. 2022. URL: https://en.wikipedia.org/w/index.php?title=Permittivity&oldid=1128557252.

[23] J. Ilic. "Wood: Electrical Properties". In: *Encyclopedia of Materials: Science and Technology*. Walthm, MA, USA: Elsevier, Jan. 2001, pp. 9629–9633. ISBN: 978-0-08-043152-9. DOI: 10.1016/B0-08-043152-6/01744-7. URL: https://doi.org/10.1016/B0-08-043152-6/01744-7.

[24] *PII: B0080431526017447 _vert Elsevier Enhanced Reader*. [Online; accessed 4. Jan. 2023]. Jan. 2023. DOI: 10.1016/B0-08-043152-6/01744-7. URL: https://doi.org/10.1016/B0-08-043152-6/01744-7.

[25] *Dielectric Constant - an overview _vert ScienceDirect Topics*. [Online; accessed 4. Jan. 2023]. Jan. 2023. DOI: 10.1016/B978-0-12-387738-3.00001-9. URL: https://doi.org/10.1016/B978-0-12-387738-3.00001-9.

[26] Daniel Peña et al. "Measurement and modeling of propagation losses in brick and concrete walls for the 900-MHz band". In: *Antennas and Propagation, IEEE Transactions on* 51.1 (Jan. 2003), pp. 31–39. ISSN: 0018-926X. DOI: 10.1109/TAP.2003.808539. URL: https://doi.org/10.1109/TAP.2003.808539.

[27] *IEEE Xplore Full-Text PDF:* [Online; accessed 25. Oct. 2022]. Oct. 2022. URL: https://ieeexplore-ieee-org.zorac.aub.aau.dk/stamp/stamp.jsp?tp=&_arnumber=1356062&tag=1.

[28] Christopher Thajudeen et al. "Measured complex permittivity of walls with different hydration levels and the effect on power estimation of TWRI target returns". In: *Progress in Electromagnetic Research B* 30.30 (Jan. 2011), pp. 177–199. ISSN: 1937-6472. DOI: 10.2528/PIERB10091004. URL: https://doi.org/10.2528/PIERB10091004.

[29] *IEEE Xplore Full-Text PDF:* [Online; accessed 25. Oct. 2022]. Oct. 2022. URL: https://ieeexplore-ieee-org.zorac.aub.aau.dk/stamp/stamp.jsp?tp=&arnumber=1651504.

[30] *IEEE Xplore Full-Text PDF:* [Online; accessed 25. Oct. 2022]. Oct. 2022. URL: https://ieeexplore-ieee-org.zorac.aub.aau.dk/stamp/stamp.jsp?tp=&arnumber=8442321.

[31] Guillaume Tesserault, Nadine Malhouroux, and Patrice Pajusco. "Determination of Material Characteristics for Optimizing WLAN Radio". In: *2007 European Conference on Wireless Technologies*. IEEE, Oct. 2007, pp. 225–228. ISBN: 978-2-87487-003-3. DOI: 10.1109/ECWT.2007.4403987. URL: https://doi.org/10.1109/ECWT.2007.4403987.

[32] [Online; accessed 25. Oct. 2022]. Sept. 2018. URL: https://www.arpapress.com/Volumes/Vol25Issue3/IJRRAS_25_3_05.pdf.

[33] *Building material characterization from complex transmissivity measurements at 5.8 GHz*. [Online; accessed 25. Oct. 2022]. Oct. 2022. URL: https://ieeexplore-ieee-org.zorac.aub.aau.dk/document/884501.

[34] *IEEE Xplore Full-Text PDF:* [Online; accessed 25. Oct. 2022]. Oct. 2022. URL: https://ieeexplore-ieee-org.zorac.aub.aau.dk/stamp/stamp.jsp?tp=&arnumber=9411366.

[35] Iñigo Cuiñas and Manuel García Sánchez. "Permittivity and Conductivity Measurements of Building Materials at 5.8 GHz and 41.5 GHz". In: *Wireless Personal Communications* 20.1 (Jan. 2002), pp. 93–100. ISSN: 1572-834X. DOI: 10.1023/A:1013886209664. URL: https://doi.org/10.1023/A:1013886209664.

[36] *IEEE Xplore Full-Text PDF:* [Online; accessed 25. Oct. 2022]. Oct. 2022. URL: https://ieeexplore-ieee-org.zorac.aub.aau.dk/stamp/stamp.jsp?tp=&arnumber=8888911.

[37] *IEEE Xplore Full-Text PDF:* [Online; accessed 25. Oct. 2022]. Oct. 2022. URL: https://ieeexplore-ieee-org.zorac.aub.aau.dk/stamp/stamp.jsp?tp=&arnumber=8325753.

[38] Ana VÁzquez Alejos, Manuel GarcÍa Sanchez, and IÑigo Cuinas. "Measurement and Analysis of Propagation Mechanisms at 40 GHz: Viability of Site Shielding Forced by Obstacles". In: *IEEE Transactions on Vehicular Technology* 57.6 (Mar. 2008), pp. 3369–3380. ISSN: 1939-9359. DOI: 10.1109/TVT.2008.920052. URL: https://doi.org/10.1109/TVT.2008.920052.

[39] *Complex Permittivity of Typical Construction Materials over 40–50 GHz*. [Online; accessed 25. Oct. 2022]. Oct. 2022. URL: https://ieeexplore-ieee-org.zorac.aub.aau.dk/document/8608541.

[40] *IEEE Xplore Full-Text PDF:* [Online; accessed 25. Oct. 2022]. Oct. 2022. URL: https://ieeexplore-ieee-org.zorac.aub.aau.dk/stamp/stamp.jsp?tp=&arnumber=5425497.

[41] L. M. Correia and P. O. Frances. "Transmission and isolation of signals in buildings at 60 GHz". In: *Proceedings of 6th International Symposium on Personal, Indoor and Mobile Radio Communications*. Vol. 3. IEEE, Sept. 1995, p. 1031. ISBN: 978-0-7803-3002. DOI: 10.1109/PIMRC.1995.477305. URL: https://doi.org/10.1109/PIMRC.1995.477305.

[42] *IEEE Xplore Full-Text PDF:* [Online; accessed 25. Oct. 2022]. Oct. 2022. URL: https://ieeexplore-ieee-org.zorac.aub.aau.dk/stamp/stamp.jsp?tp=&arnumber=6901885&tag=1.

[43] *Reflection and transmission behaviour of building materials at 60 GHz*. [Online; accessed 25. Oct. 2022]. Oct. 2022. URL: https://ieeexplore-ieee-org.zorac.aub.aau.dk/document/529141.

[44] Yosef Pinhasi, Asher Yahalom, and Sergey Petnev. *Propagation of ultra wideband signals in lossy dispersive media*. June 2008. ISBN: 978-1-4244-2097-1. DOI: 10.1109/COMCAS.2008.4562803. URL: https://doi.org/10.1109/COMCAS.2008.4562803.

[45] *IEEE Xplore Full-Text PDF:* [Online; accessed 25. Oct. 2022]. Oct. 2022. URL: https://ieeexplore-ieee-org.zorac.aub.aau.dk/stamp/stamp.jsp?tp=&arnumber=8911653.

[46] I. Cuinas et al. "Comparison of the electromagnetic properties of building materials at 5.8 GHz and 62.4 GHz". In: *Vehicular Technology Conference Fall 2000. IEEE VTS Fall VTC2000. 52nd Vehicular Technology Conference (Cat. No.00CH37152)*. Vol. 2. IEEE, Sept. 2000, 780–785vol.2. ISBN: 978-0-7803-6507. DOI: 10.1109/VETECF.2000.887111. URL: https://doi.org/10.1109/VETECF.2000.887111.

[47] Bruno Feitor et al. "Estimation of dielectric concrete properties from power measurements at 18.7 and 60 GHz". In: *2011 Loughborough Antennas & Propagation Conference*. IEEE, Nov. 2011, pp. 1–5. DOI: 10.1109/LAPC.2011.6114146. URL: https://doi.org/10.1109/LAPC.2011.6114146.

[48] *IEEE Xplore Full-Text PDF:* [Online; accessed 25. Oct. 2022]. Oct. 2022. URL: https://ieeexplore-ieee-org.zorac.aub.aau.dk/stamp/stamp.jsp?tp=&arnumber=8982230.

[49] *IEEE Xplore Full-Text PDF:* [Online; accessed 25. Oct. 2022]. Oct. 2022. URL: https://ieeexplore-ieee-org.zorac.aub.aau.dk/stamp/stamp.jsp?tp=&arnumber=9539540.

[50] *IEEE Xplore Full-Text PDF:* [Online; accessed 25. Oct. 2022]. Oct. 2022. URL: https://ieeexplore-ieee-org.zorac.aub.aau.dk/stamp/stamp.jsp?tp=&arnumber=9391155.

[51] *Complex Permittivity Evaluation of Building Materials at 200-500 GHz Using THz-TDS*. [Online; accessed 25. Oct. 2022]. Oct. 2022. URL: https://ieeexplore-ieee-org.zorac.aub.aau.dk/document/9391390.

[52] Alan Agresti. *Statistical Methods for the Social Sciences, Global Edition*. London, England, UK: Pearson Education Limited, Apr. 2018. ISBN: 978-1-29222031-4. URL: https://www.saxo.com/dk/statistical-methods-for-the-social-sciences-global-edition_alan-agresti_paperback_9781292220314.

[53] Alessandra La Gioia et al. "Open-Ended Coaxial Probe Technique for Dielectric Measurement of Biological Tissues: Challenges and Common Practices". In: *Diagnostics* 8.2 (June 2018). DOI: 10.3390/diagnostics8020040. URL: https://doi.org/10.3390/diagnostics8020040.

[54] Turgut Ozturk. "Characterization of Liquids Using Electrical Properties in Microwave and Millimeter Wave Frequency Bands". In: *Journal of Nondestructive Evaluation* 38.1 (Mar. 2019), pp. 1–9. ISSN: 1573-4862. DOI: 10.1007/s10921-018-0553-6. URL: https://doi.org/10.1007/s10921-018-0553-6.

[55] [Online; accessed 4. Oct. 2022]. Sept. 2022. URL: https://academy.cba.mit.edu/classes/input_devices/meas.pdf.

[56] [Online; accessed 4. Oct. 2022]. Apr. 2022. URL: https://cdn.rohde-schwarz.com/pws/dl_downloads/dl_application/00aps_undefined/RAC-0607-0019_1_5E.pdf.

[57] *IEEE Xplore Full-Text PDF:* [Online; accessed 3. Oct. 2022]. Oct. 2022. URL: https://ieeexplore-ieee-org.zorac.aub.aau.dk/stamp/stamp.jsp?tp=&arnumber=7839223.

[58] [Online; accessed 4. Oct. 2022]. Jan. 2013. URL: https://library.csbe-scgab.ca/docs/journal/47/c0231.pdf.

[59] Shyam Narayan Jha et al. "Measurement techniques and application of electrical properties for nondestructive quality evaluation of foods—a review". In: *Journal of food science and technology* 48.4 (Aug. 2011), p. 387. DOI: 10.1007/s13197-011-0263-x. URL: https://doi.org/10.1007/s13197-011-0263-x.

[60] T. T. Grove, M. F. Masters, and R. E. Miers. "Determining dielectric constants using a parallel plate capacitor". In: *American Journal of Physics* 73.1 (2005), pp. 52–56. ISSN: 0002-9505. URL: https://www.academia.edu/21081206/Determining_dielectric_constants_using_a_parallel_plate_capacitor.

[61] Tanveerul Haq et al. "Extremely Sensitive Microwave Sensor for Evaluation of Dielectric Characteristics of Low-Permittivity Materials". In: *Sensors* 20.7 (Mar. 2020), p. 1916. ISSN: 1424-8220. DOI: 10.3390/s20071916. URL: https://doi.org/10.3390/s20071916.

[62] Hector-Noel Morales-Lovera et al. "Microstrip sensor and methodology for the determination of complex anisotropic permittivity using perturbation techniques". In: *Scientific Reports* 12.2205 (Feb. 2022), pp. 1–8. ISSN: 2045-2322. DOI: 10.1038/s41598-022-06259-8. URL: https://doi.org/10.1038/s41598-022-06259-8.

[63] *IEEE Xplore Full-Text PDF:* [Online; accessed 4. Oct. 2022]. Oct. 2022. URL: https://ieeexplore-ieee-org.zorac.aub.aau.dk/stamp/stamp.jsp?tp=&arnumber=7220116.

[64] *IEEE Xplore Full-Text PDF:* [Online; accessed 4. Oct. 2022]. Oct. 2022. URL: https://ieeexplore-ieee-org.zorac.aub.aau.dk/stamp/stamp.jsp?tp=&arnumber=9614543.

[65] Fábio Júlio F. Gonçalves et al. "Free-Space Materials Characterization by Reflection and Transmission Measurements using Frequency-by-Frequency and Multi-Frequency Algorithms". In: *Electronics* 7.10 (Oct. 2018), p. 260. ISSN: 2079-9292. DOI: 10.3390/electronics7100260. URL: https://doi.org/10.3390/electronics7100260.

[66] [Online; accessed 9. Oct. 2022]. Jan. 2018. URL: https://www.jpier.org/PIERB/pierb58/08.13121308.pdf.

[67] *IEEE Xplore Full-Text PDF:* [Online; accessed 9. Oct. 2022]. Oct. 2022. URL: https://ieeexplore-ieee-org.zorac.aub.aau.dk/stamp/stamp.jsp?tp=&arnumber=5488184.

[68] Adriano Luiz de Paula, Mirabel Cerqueira Rezende, and Joaquim José Barroso. "Modified Nicolson-Ross-Weir (NRW) method to retrieve the constitutive parameters of low-loss materials". In: *2011 SBMO/IEEE MTT-S International Microwave and Optoelectronics Conference (IMOC 2011)*. IEEE, Oct. 2011, pp. 488–492. DOI: 10.1109/IMOC.2011.6169293. URL: https://doi.org/10.1109/IMOC.2011.6169293.

[69] *Opt.001 Measure Menu*. [Online; accessed 5. Dec. 2022]. June 2022. URL: https://rfmw.em.keysight.com/wireless/helpfiles/N1500A/Opt.001_Measure_Menu.htm#DefineMeas.

[70] P. G. Bartley and S. B. Begley. "Improved Free-Space S-Parameter Calibration". In: *2005 IEEE Instrumentationand Measurement Technology Conference Proceedings*. Vol. 1. IEEE, May 2005, pp. 372–375. ISBN: 978-0-7803-8879. DOI: 10.1109/IMTC.2005.1604138. URL: https://doi.org/10.1109/IMTC.2005.1604138.

[71] Constantine A. Balanis. *Antenna Theory: Analysis and Design, 4th Edition*. Hoboken, NJ, USA: Wiley, Feb. 2016. ISBN: 978-1-118-64206-1. URL: https://www.wiley.com/en-us/Antenna+Theory:+Analysis+and+Design,+4th+Edition-p-9781118642061.

[72] Nozhan Hosseini et al. “Attenuation of Several Common Building Materials: Millimeter-Wave Frequency Bands 28, 73, and 91 GHz”. In: *IEEE Antennas and Propagation Magazine* 63.6 (Jan. 2021), pp. 40–50. ISSN: 1558-4143. DOI: 10.1109/MAP.2020.3043445. URL: https://doi.org/10.1109/MAP.2020.3043445.

[73] Nozhan Hosseini et al. “Attenuation of Several Common Building Materials in Millimeter-Wave Frequency Bands: 28, 73 and 91 GHz”. In: *ArXiv e-prints* (Apr. 2020). DOI: 10.1109/MAP.2020.3043445. eprint: 2004.12568. URL: https://doi.org/10.1109/MAP.2020.3043445.

[74] Sergio L. S. Severo et al. “Non-resonant Permittivity Measurement Methods”. In: *Journal of Microwaves, Optoelectronics and Electromagnetic Applications* 16 (Jan. 2017), pp. 297–311. ISSN: 2179-1074. DOI: 10.1590/2179-10742017v16i1890. URL: https://doi.org/10.1590/2179-10742017v16i1890.

[75] [Online; accessed 22. Oct. 2022]. June 2014. URL: https://nvlpubs.nist.gov/nistpubs/Legacy/TN/nbstechnicalnote1341.pdf.

[76] [Online; accessed 22. Oct. 2022]. Aug. 2013. URL: https://nvlpubs.nist.gov/nistpubs/Legacy/TN/nbstechnicalnote1355r.pdf.

[77] Fábio Júlio F. Gonçalves et al. “Free-Space Materials Characterization by Reflection and Transmission Measurements using Frequency-by-Frequency and Multi-Frequency Algorithms”. In: *Electronics* 7.10 (Oct. 2018), p. 260. ISSN: 2079-9292. DOI: 10.3390/electronics7100260. URL: https://doi.org/10.3390/electronics7100260.

[78] *Development of Measurement and Extraction - ProQuest*. [Online; accessed 21. Oct. 2022]. Oct. 2022. URL: https://www.proquest.com/docview/2259776578?fromopenview=true&pq-origsite=gscholar.

[79] Chuang Yang, Jian Wang, and Cheng Yang. “Estimation methods to extract complex permittivity from transmission coefficient in the terahertz band”. In: *Optical and Quantum Electronics* 53.8 (Aug. 2021), pp. 1–10. ISSN: 1572-817X. DOI: 10.1007/s11082-021-03087-4. URL: https://doi.org/10.1007/s11082-021-03087-4.

[80] *IEEE Xplore Full-Text PDF:* [Online; accessed 21. Oct. 2022]. Oct. 2022. URL: https://ieeexplore-ieee-org.zorac.aub.aau.dk/stamp/stamp.jsp?tp=&arnumber=8293139.

[81] Philip G. Bartley and Shelley B. Begley. “A new free-space calibration technique for materials measurement”. In: *2012 IEEE International Instrumentation and Measurement Technology Conference Proceedings*. IEEE, pp. 13–16. DOI: 10.1109/I2MTC.2012.6229351. URL: https://doi.org/10.1109/I2MTC.2012.6229351.

[82] B. Riddle, J. Baker-Jarvis, and J. Krupka. "Complex permittivity measurements of common plastics over variable temperatures". In: *IEEE Transactions on Microwave Theory and Techniques* 51.3 (Mar. 2003), pp. 727–733. ISSN: 1557-9670. DOI: 10.1109/TMTT.2003.808730. URL: https://doi.org/10.1109/TMTT.2003.808730.

[83] *Remcom*. [Online; accessed 24. Oct. 2022]. Oct. 2022. URL: https://www.remcom.com/wireless-insite-em-propagation-software.

[84] Ole Vesterlund Nielsen. *Basiskemi A*. [Online; accessed 4. Jan. 2023]. Jan. 2023. URL: https://www.williamdam.dk/basiskemi-a__41203.

[85] H. Mygind. *Basiskemi B*. [Online; accessed 4. Jan. 2023]. Jan. 2023. URL: https://www.williamdam.dk/basiskemi-b__2483965.

[86] Stanislav Stefanov Zhekov, Ondrej Franek, and Gert Frolund Pedersen. "Dielectric Properties of Common Building Materials for Ultrawideband Propagation Studies [Measurements Corner]". In: *IEEE Antennas and Propagation Magazine* 62.1 (Feb. 2020), pp. 72–81. ISSN: 1558-4143. DOI: 10.1109/MAP.2019.2955680. URL: https://doi.org/10.1109/MAP.2019.2955680.

[87] Xinyi Wang et al. "Research on Penetration Loss of D-Band Millimeter Wave for Typical Materials". In: *Sensors* 22.19 (Oct. 2022), p. 7666. ISSN: 1424-8220. DOI: 10.3390/s22197666. URL: https://doi.org/10.3390/s22197666.

[88] A. K. Verma, Nasimuddin, and A. S. Omar. "Microstrip resonator sensors for determination of complex permittivity of materials in sheet, liquid and paste forms". In: *Microwaves, Antennas and Propagation, IEE Proceedings -* 151.1 (Mar. 2005), pp. 47–54. ISSN: 1350-2417. DOI: 10.1049/ip-map:20041155. URL: https://doi.org/10.1049/ip-map:20041155.

Appendix A

Calibrating the VNA

Calibrating PNA Network Analyzer

1. Connect the test cables used under measurements, as shown in figure 1.

Figure 1

2. Untangle the attached cables and connect each end to the N4692A 10Mhz - 40GHz Electronic Calibration Module from Keysight, as shown in figure 2.

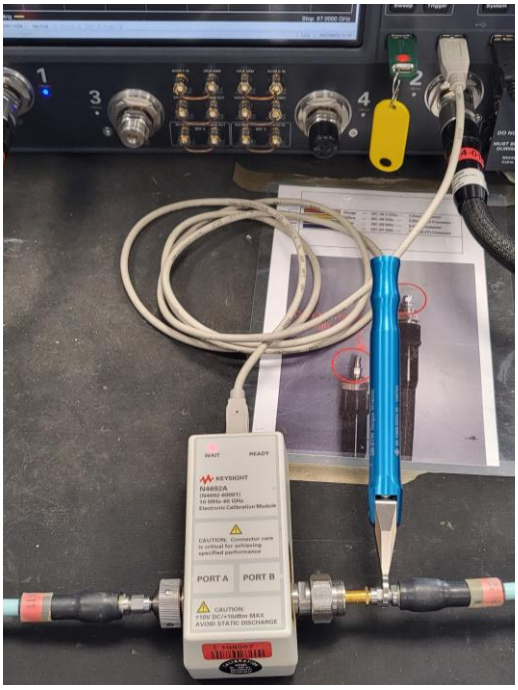

Figure 2

Then the VNA needs to be setup:

3. Click on ”Preset”. Then go the frequency and change to desired frequency, as example seen in figure 4.

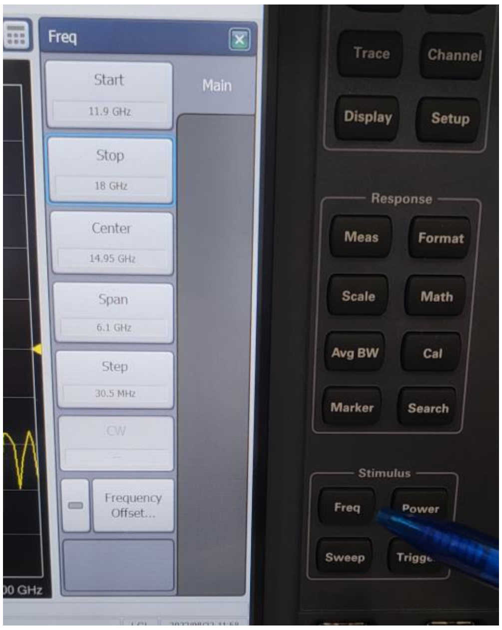

Figure 3

4. Set the number of points by pushing ”Sweep”, as seen in figure 5.

Figure 4

5. The pres ”Power” to set the transmission power, as seen in figure 6.

Figure 5

6. Then click on ”Avg BW” to change the IF Bandwidth, as seen in figure 7.

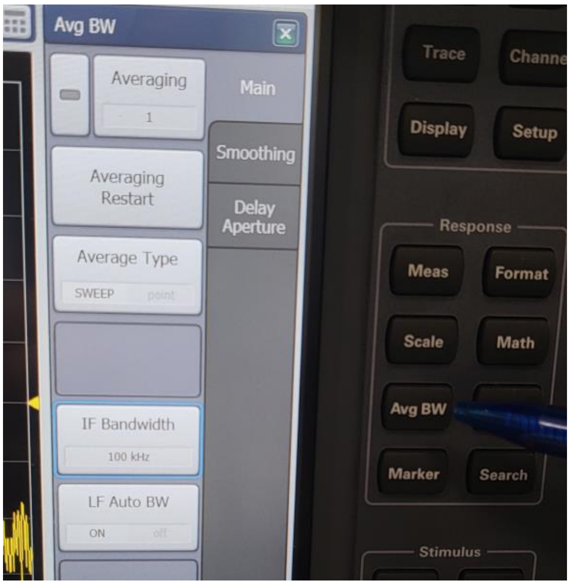

Figure 6

7. Click ”Meas” to change the measured S parameter, as seen in figure 8.

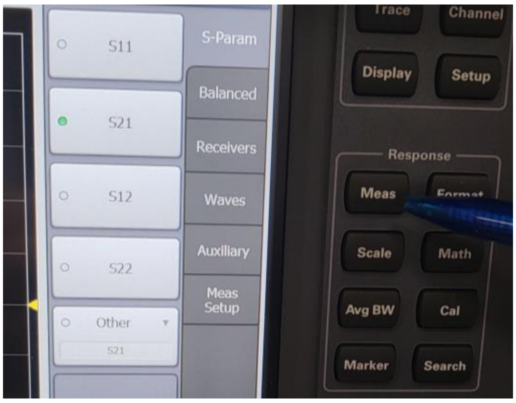

Figure 7

8. Click on ”Math,” then turn on the ”Transform” mode and set the start and stop time.

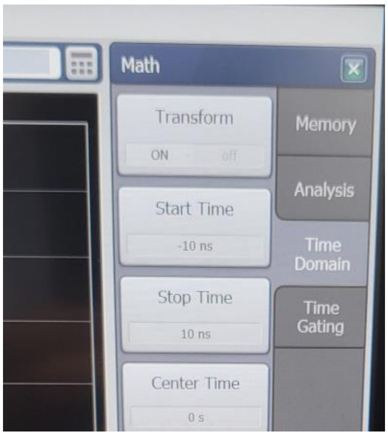

Figure 8

9. Then Wait until the red light on the kit gets green, as seen in figure 3.

Figure 9

10. Now click on “Cal” and select Ecal, as seen in figure 10.

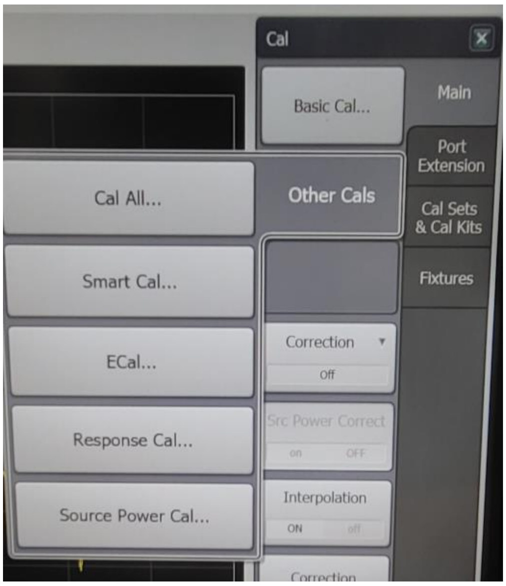

Figure 10

11. Now select the connection ports on the VNA, this case is nr.1 and nr.2 in use, and there are two ports in use, then click on “2 Port ECal” and click “next,” as seen in figure 11.

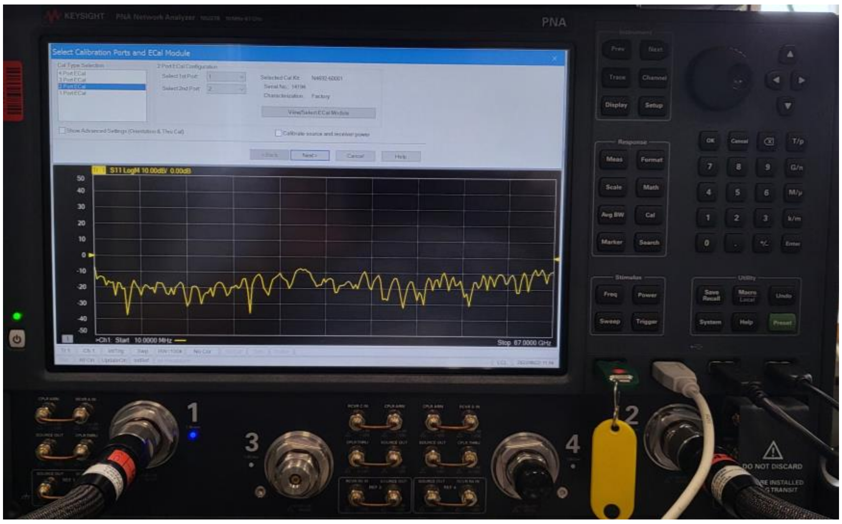

Figure 11

12. Then click on “Measure.”

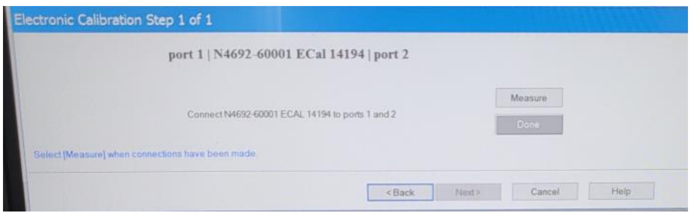

Figure 12

13. Then click on “Save As User CalSet.”

Figure 13

14. Then name it something that you remember and click “OK.”

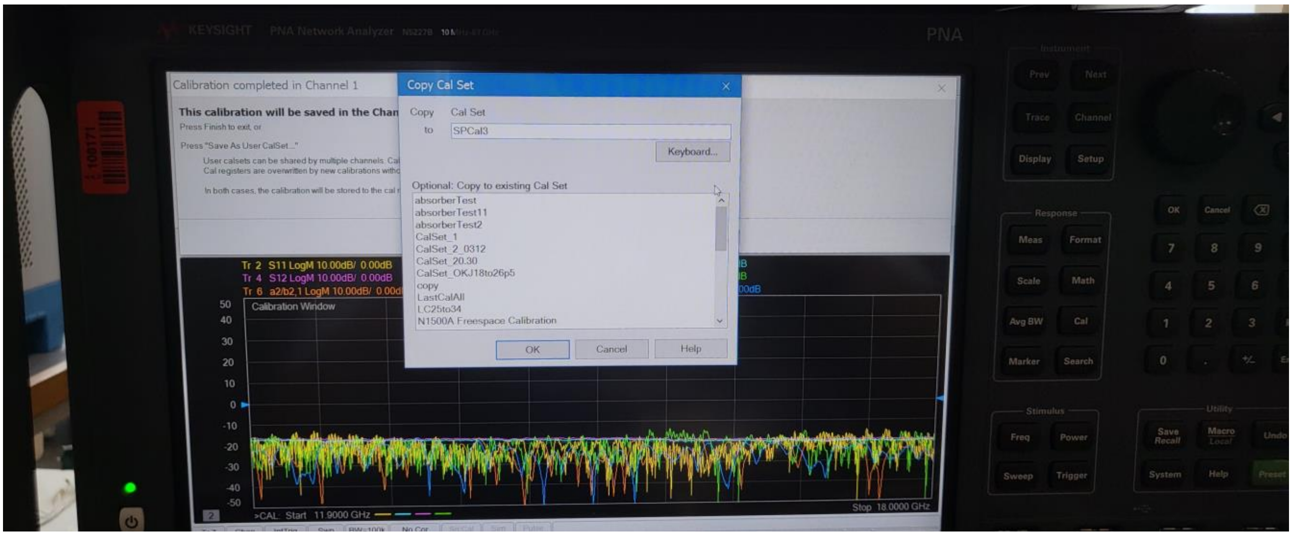

Figure 14

Appendix B

Measuring the LOS and using time gating

Measuring the LOS and using time gating.

Then disconnect the Calkit (N4692A), connect the cables to the antennas, and you should see the signal below in figure 1. If not, find the signal using ”Scale” and ”Math,” wherein the time domain can be set.

(Important, Note the ”Start and Stop time” of the signal and the ”Gate Span”)

An example LOS signal can be seen in figure 1. which can be confirmed by blocking the signal path.

1. Use ”Marker” to find the start of the signal, her it is 3.47nS

Figure 1

2. Find the end of the LOS signal, as shown in figure 2. (About 6 nS)

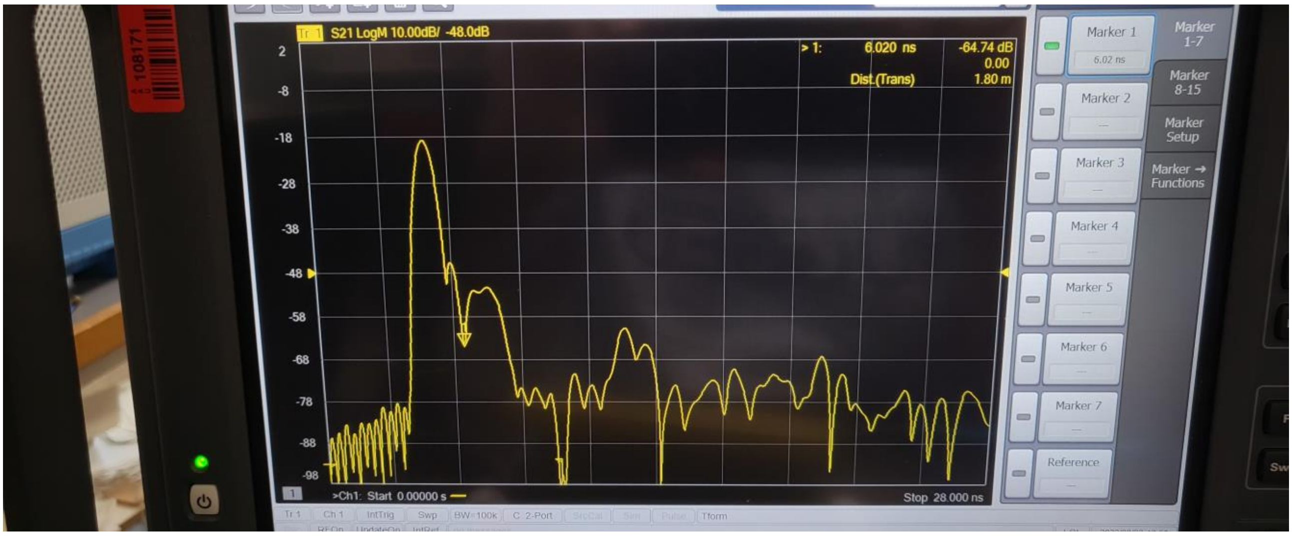

Figure 2

3. Then go to ”Math” and select ”Time Gating,” and set the ”Gate start” to 0.

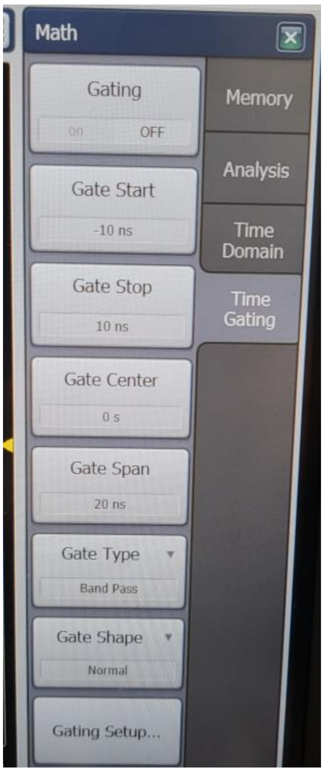

Figure 3

4. Then looking in figure 4, the Gate is a ”filter/window” to file out, as seen in figures 4 and 5. Just set the ”Gate Stop” close to the LOS, as seen in figure 6.

Figure 4

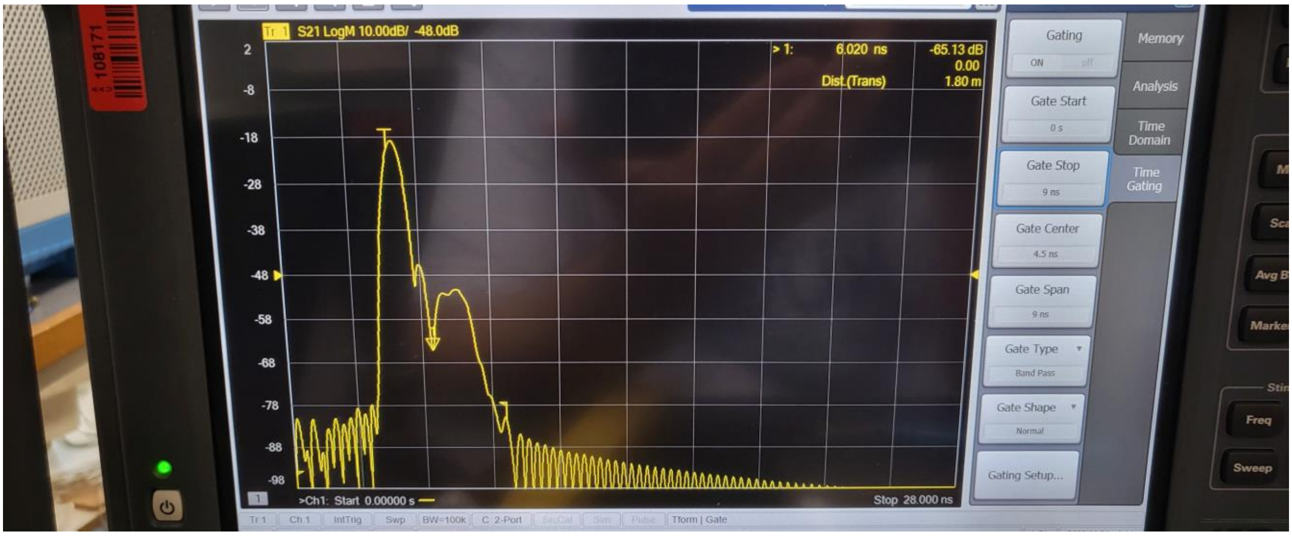

Figure 5

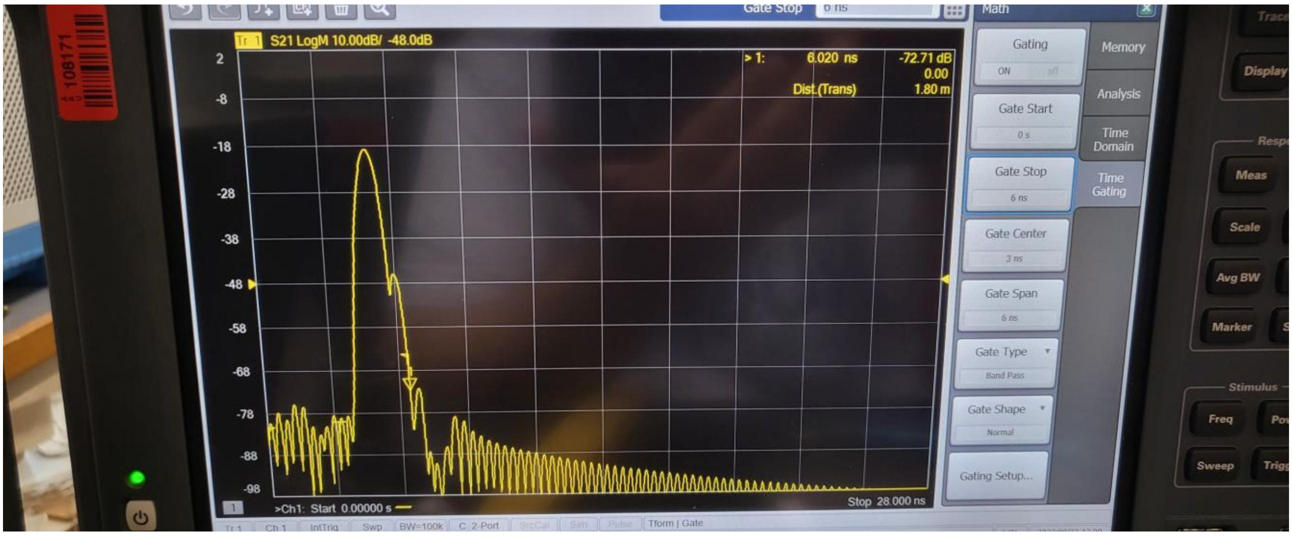

Figure 6

5. Note the "Gate Span"

Appendix C

Keysight Materials Measurement Suite Configuration

Keysight Materials Measurement Suite Configuration

1. Insert the USB dongle into the VNA, then open the software, as seen in figure 1.

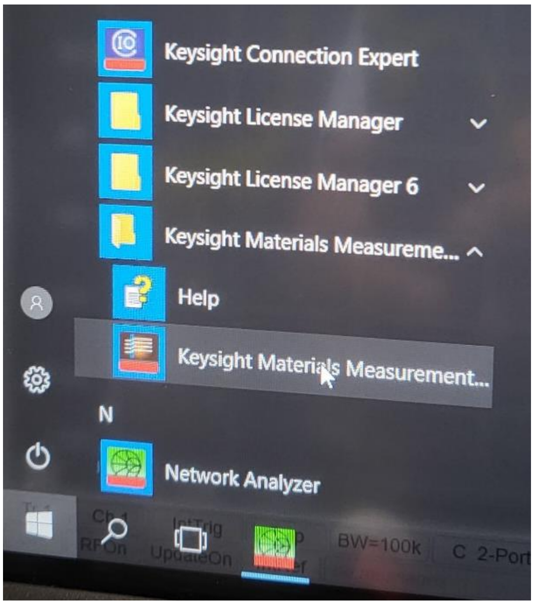

Figure 1

2. Then Choose the" Transmission Line And Free Space Method"

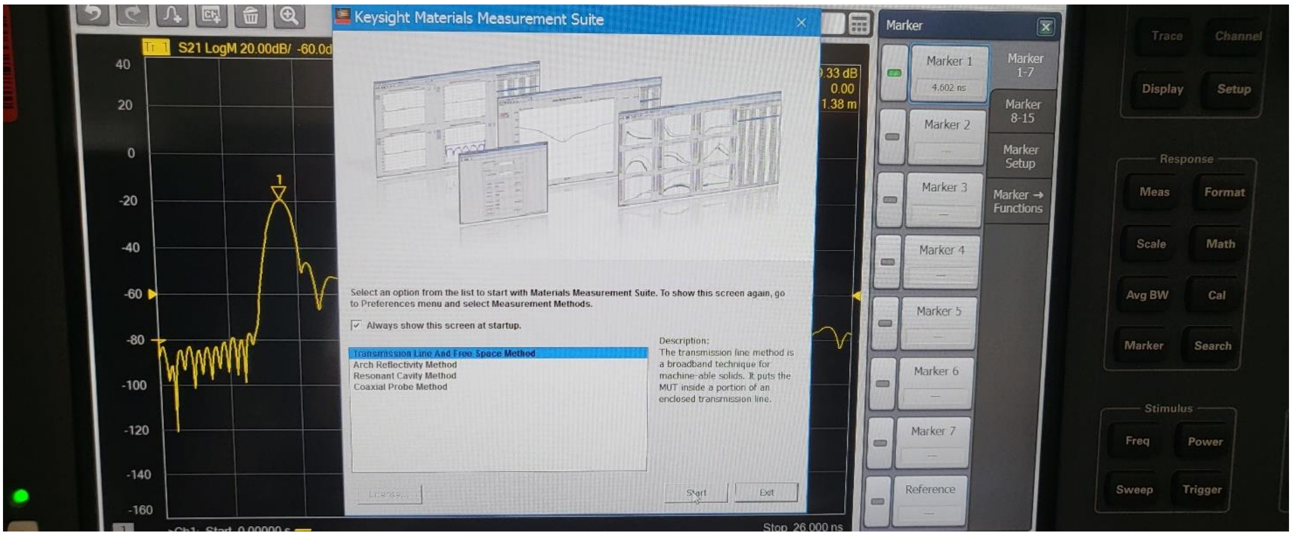

Figure 2

3. Then click on" Define Measurement," as seen in figure 3.

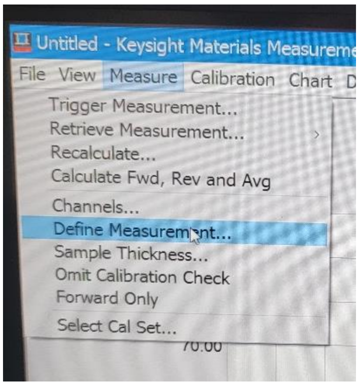

Figure 3

4. Then change all the parameters to the exact same as was set on the VNA calibrations.

(Example is shown in figure 4 of another Calibration setting where 2,5 and 5,5 GHz are of interest)

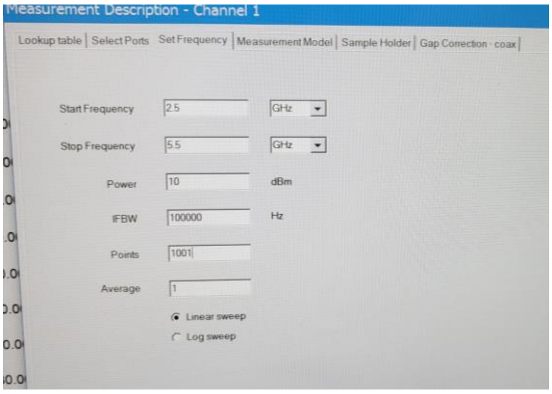

Figure 4

5. Then make sure that the setting in the next fan is as shown in figure 5.

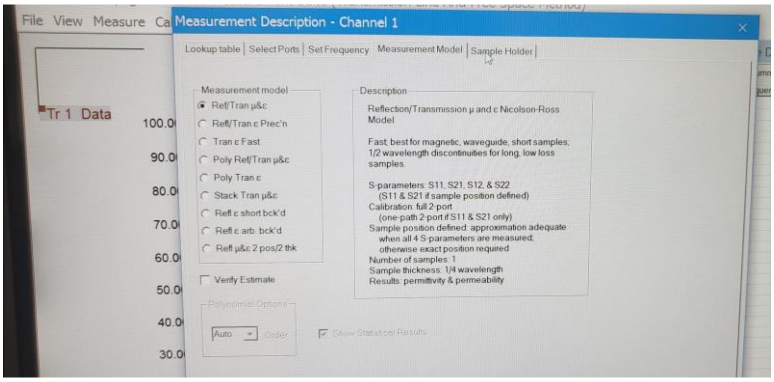

Figure 5

6. Then on the next fan, under" Sample Holder," set the parameters, and remember to choose" Freespace" under the sample holder. Then press" Apply" and" OK". (Metal plate, in my case, is 1,96 mm)

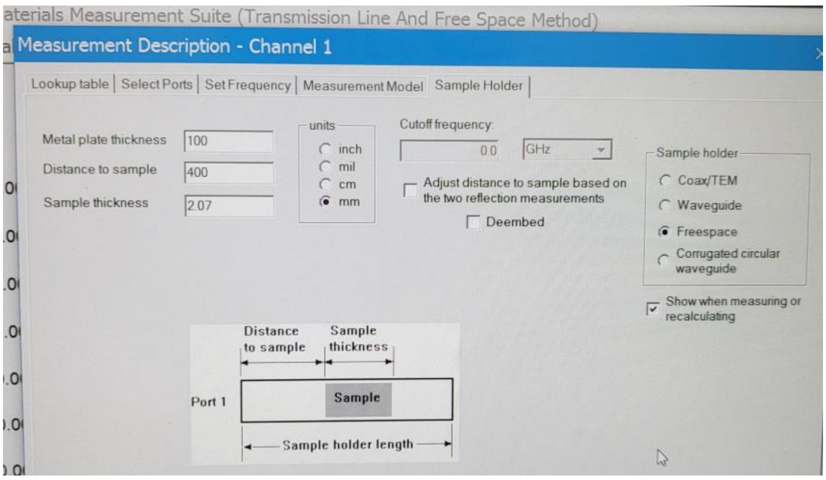

Figure 6

7. Then go to "Calibration" under "Forespace Calibration "and choose the first one, as seen in figure 7.

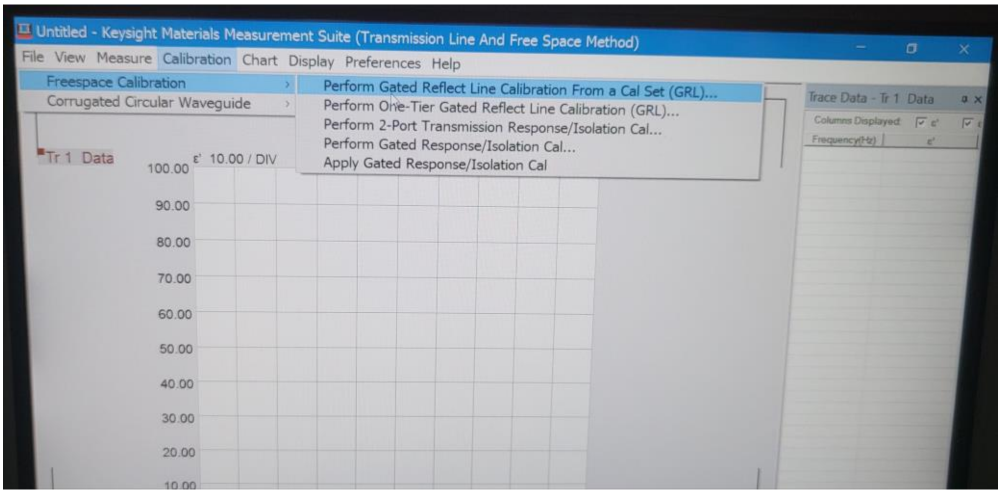

Figure 7

8. Select the calibration that was saved earlier when calibrating the VNA, as shown in figure 9.

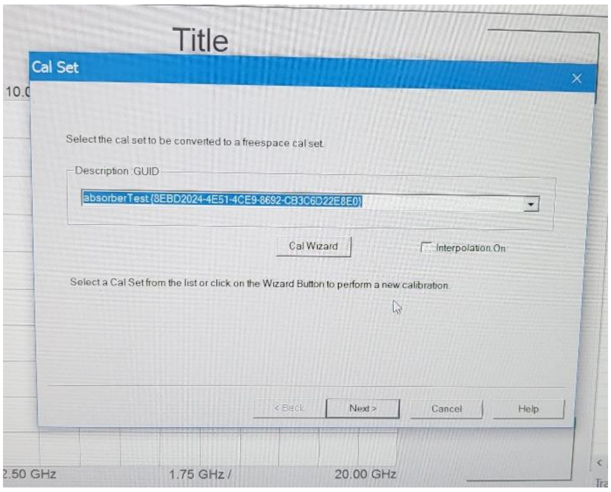

Figure 8

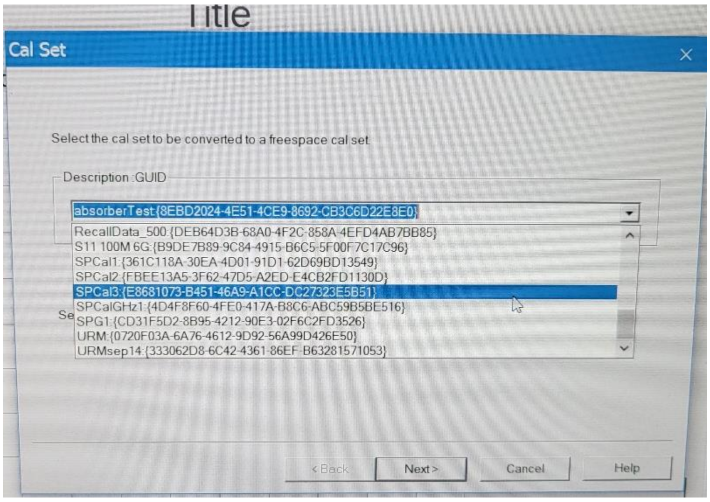

Figure 9

9. Then set the start and stop time of the LOS path or (signal of interest), then set the Gate Span the same as in the VNA, and click on next, as shown in figure 10.

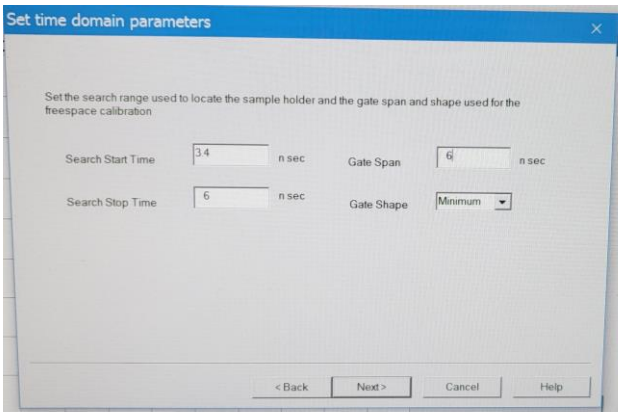

Figure 10

10. Now set the metal plate in. The distance between the metal plate and the middle of the antenna on both sides is about 400 mm, as shown in figure 11.

Figure 11

11. Then measure the metal plate's thickness and click "Measure."

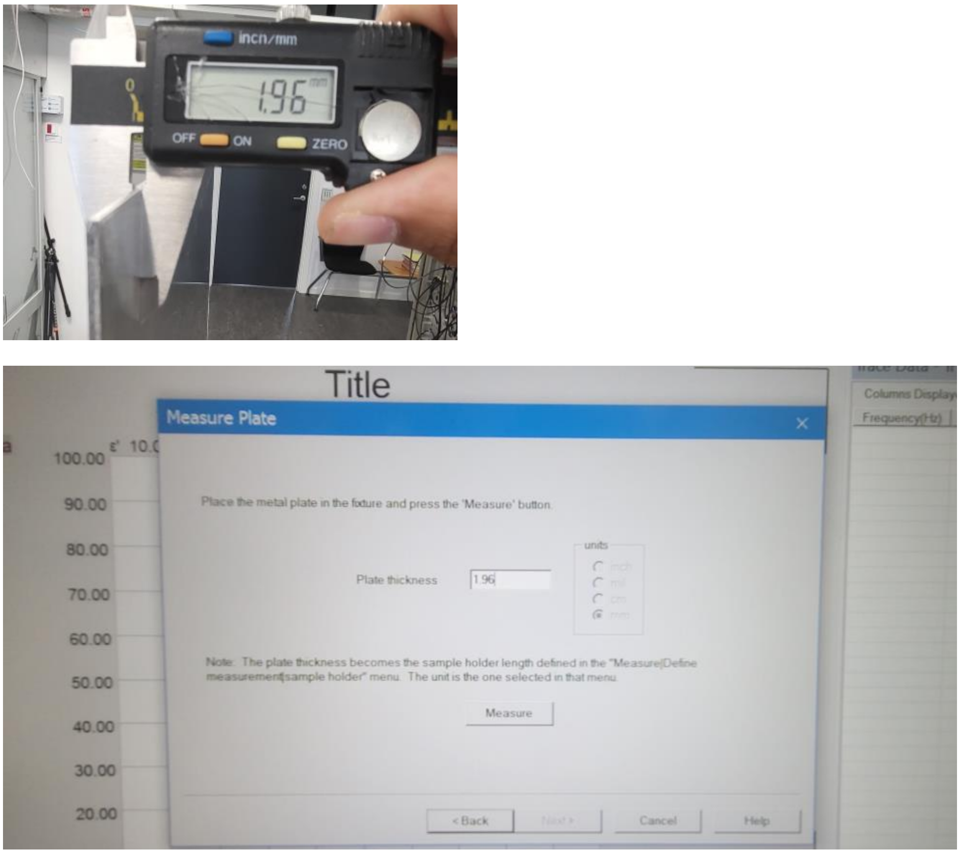

Figure 12

12. Then remove the metal plate, press "Measure, " and press "Finish" without changing the name.

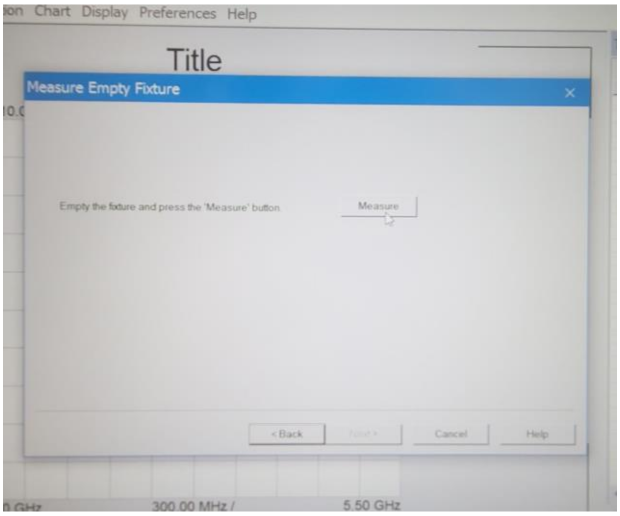

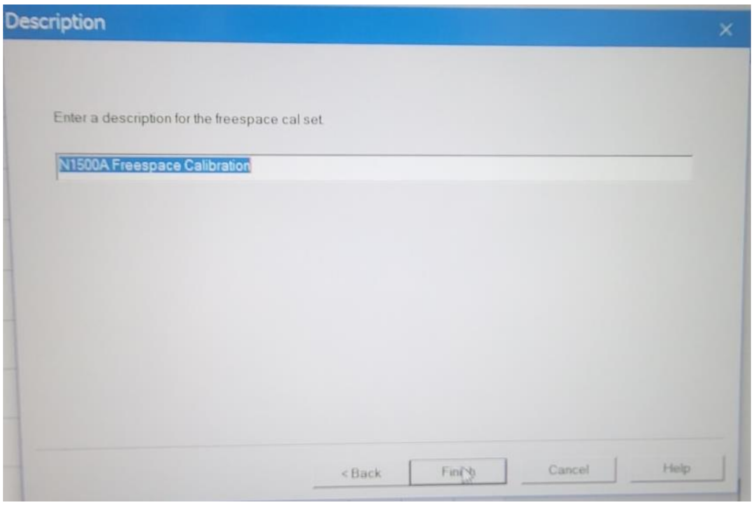

13. Then a popup window will show as in figure x. Press "Yes."

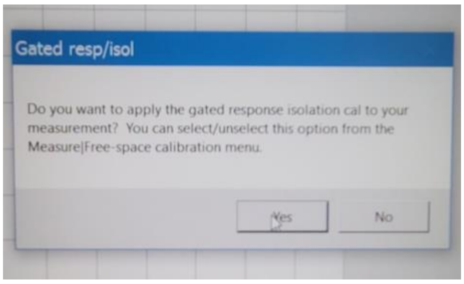

14. Then press "Trigger Measurement" and press "Yes" for the popup.

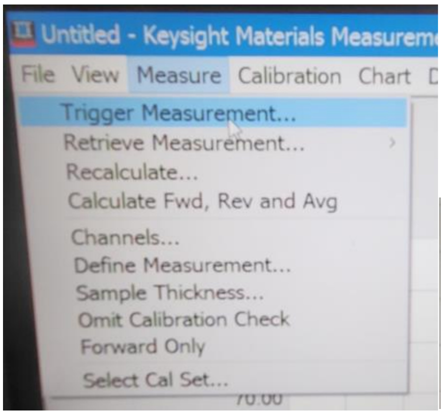

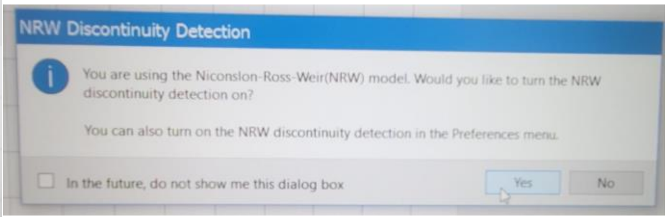

15. Then you will get a graph that looks similar to the below figure, which is not the figure of interest.

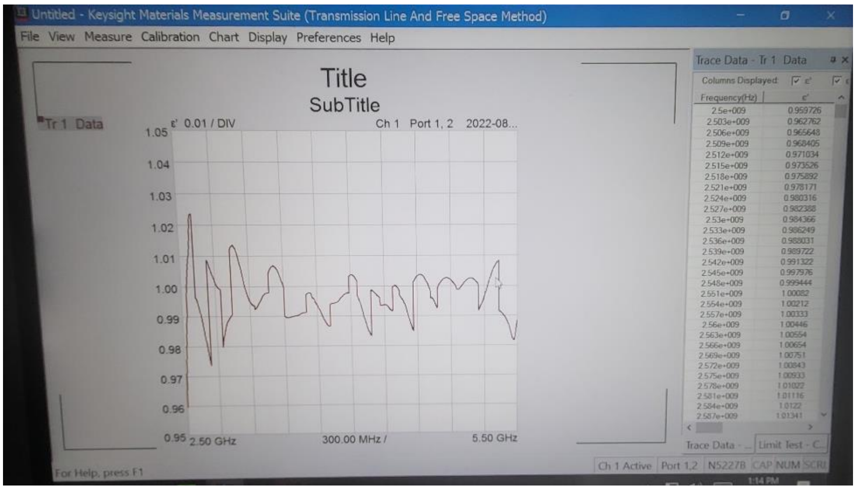

16. Then go back to "Define Measurement."

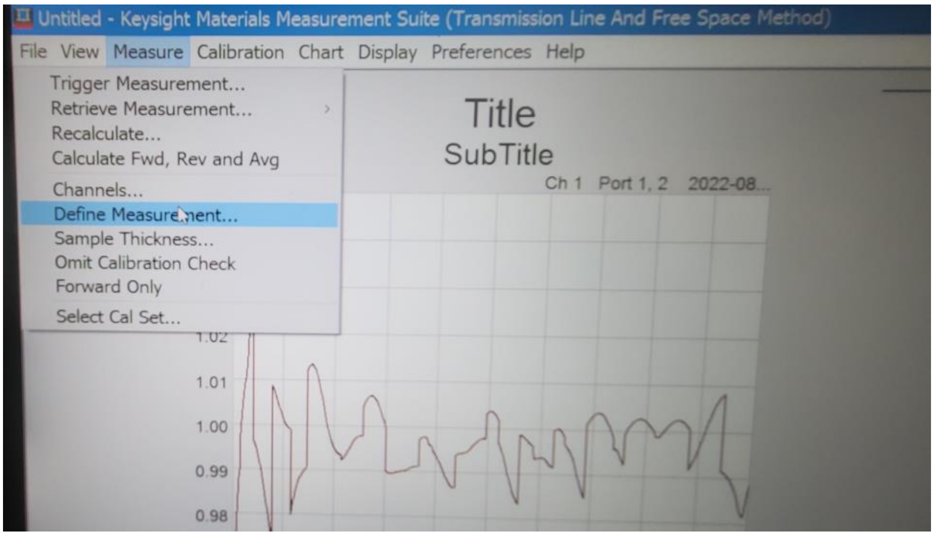

17. Then select "Poly Tran c" and click on "Apply" and "OK."

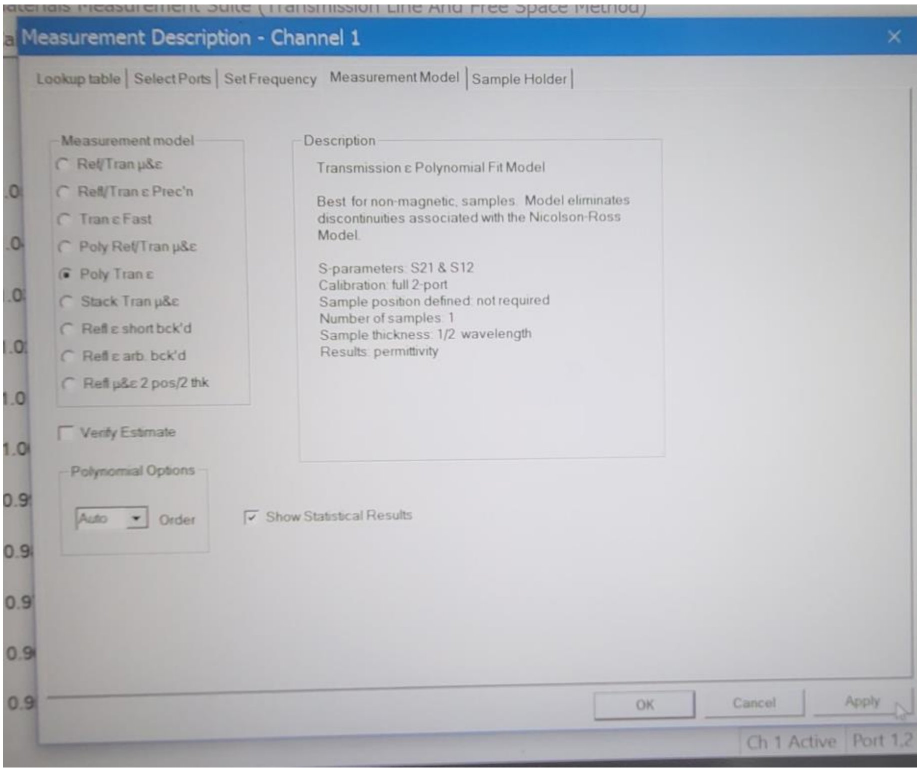

18. Then click on "Trigger Measurement."

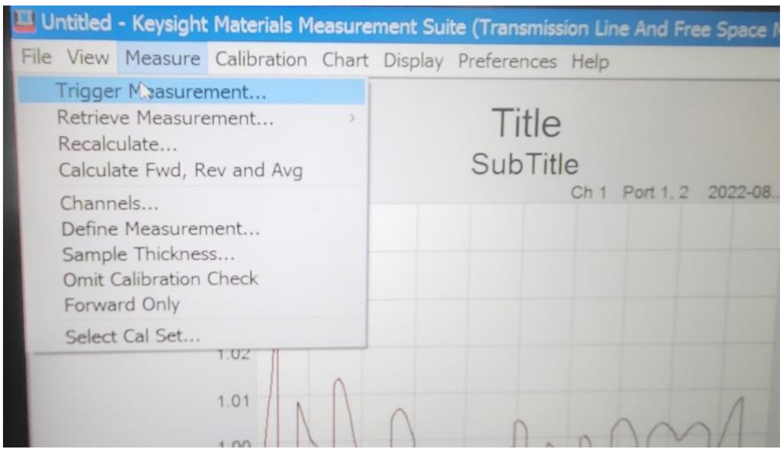

19. Now you should have a similar to a straight line which is the graph we are interested in. This measurement is where nothing is between the antennas and only air, so the permittivity should be close to 1, as shown in the figures below.

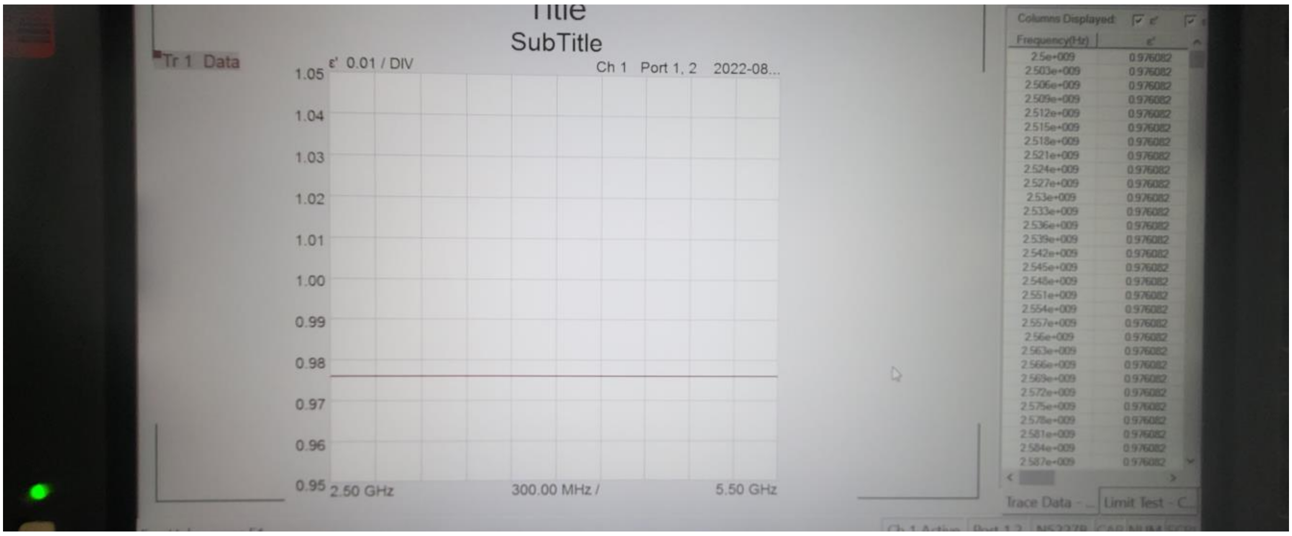

Appendix D

Material used in measurements

Plexiglass 4.1 mm

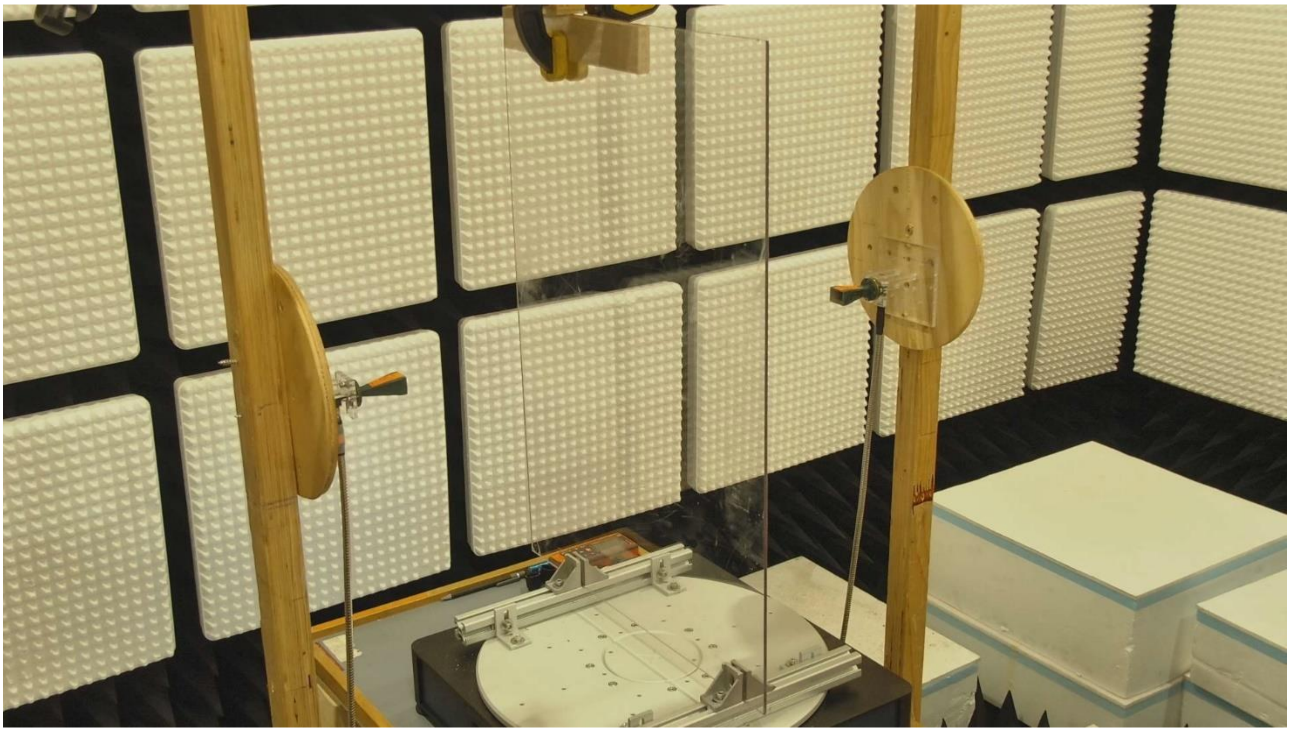

Plywood 12.20 mm

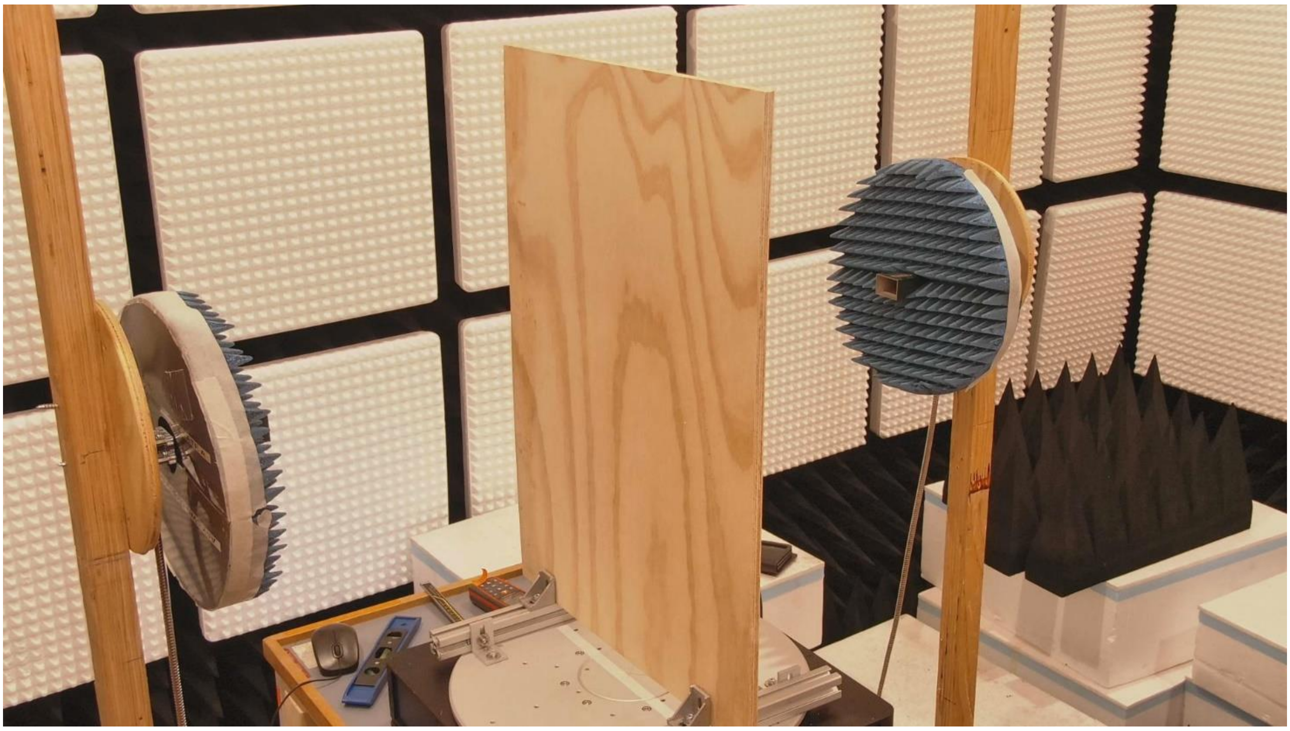

Plywood 12.38 mm

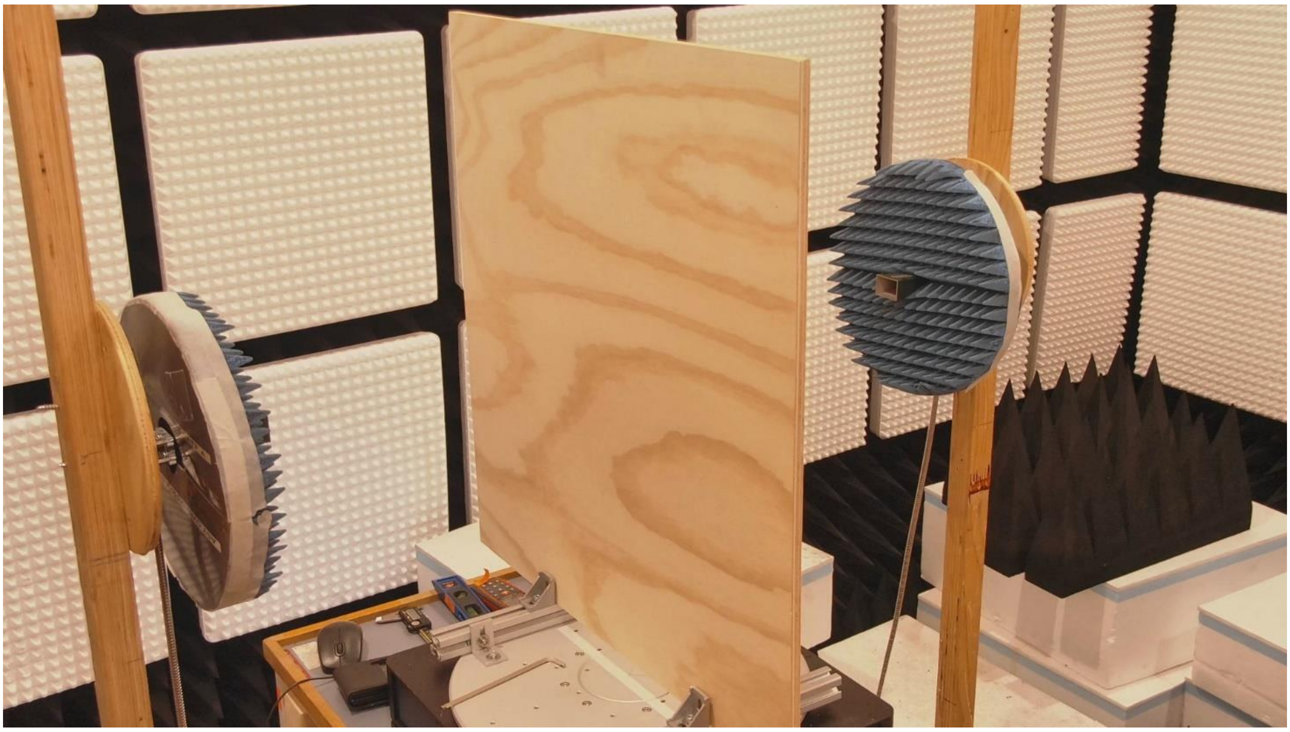

Masonite 3.16 mm

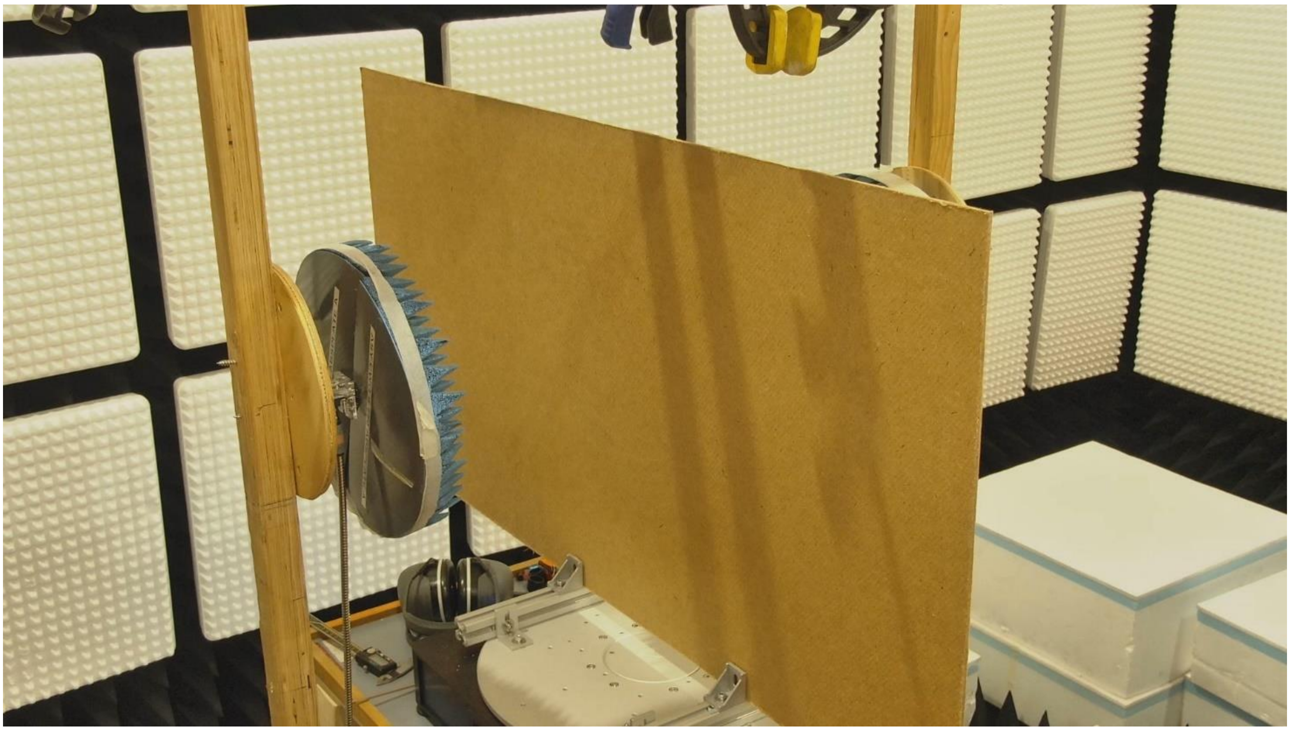

PP material 1.95 mm

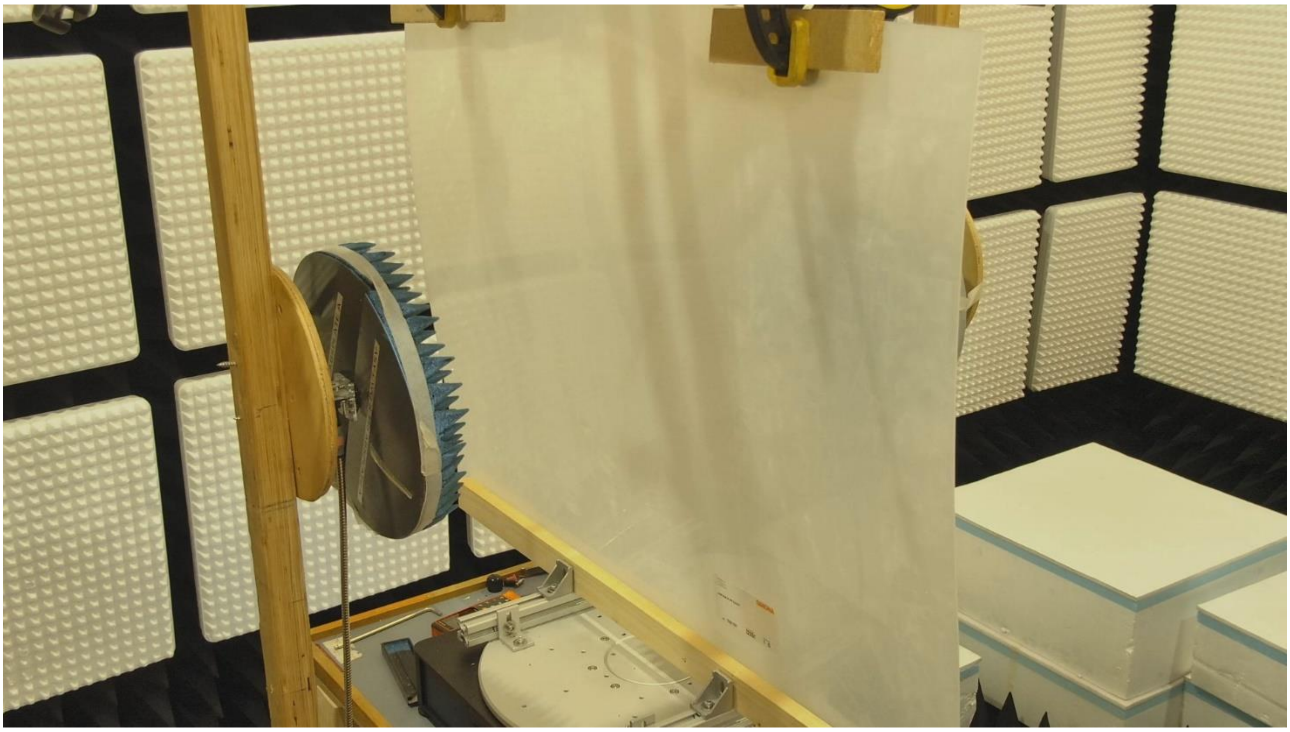

Plastic material material 1.4 mm

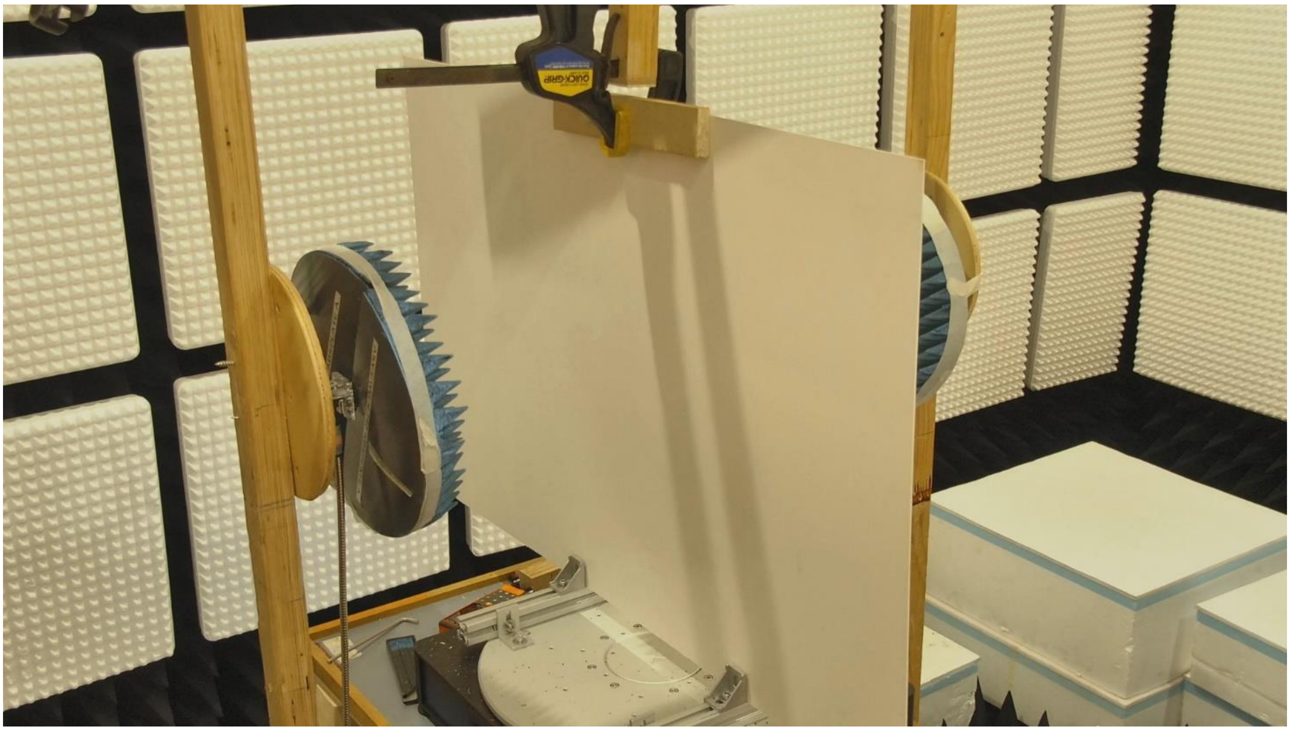

Laminate floor 8 mm

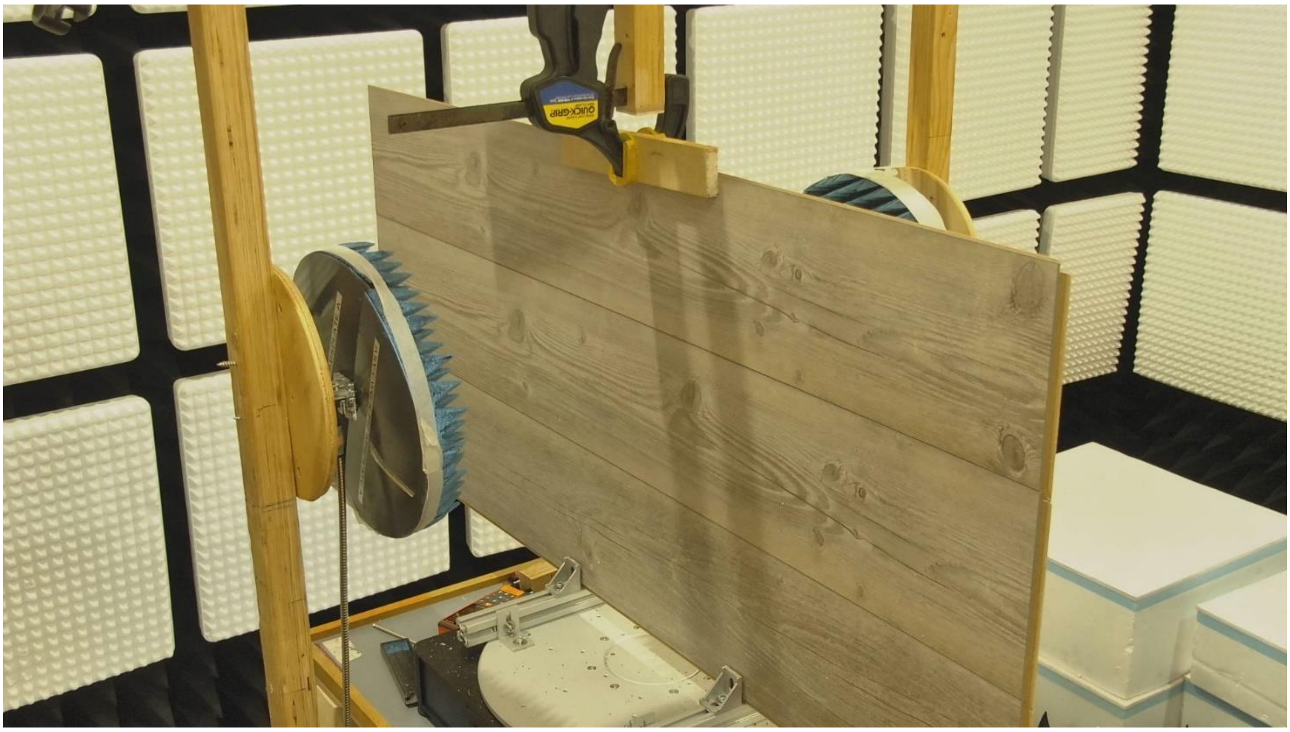

Gypsum board 12.42 mm

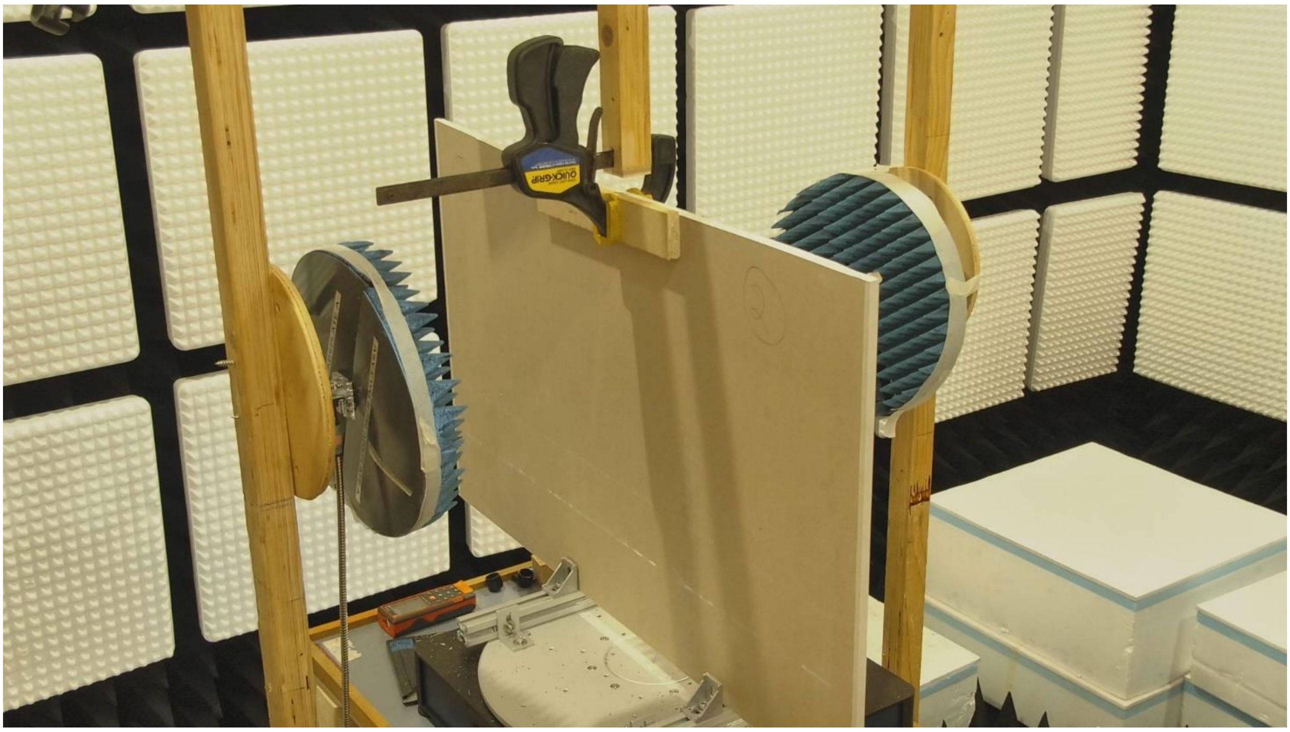

Moisture-shielded gypsum board 12.42 mm

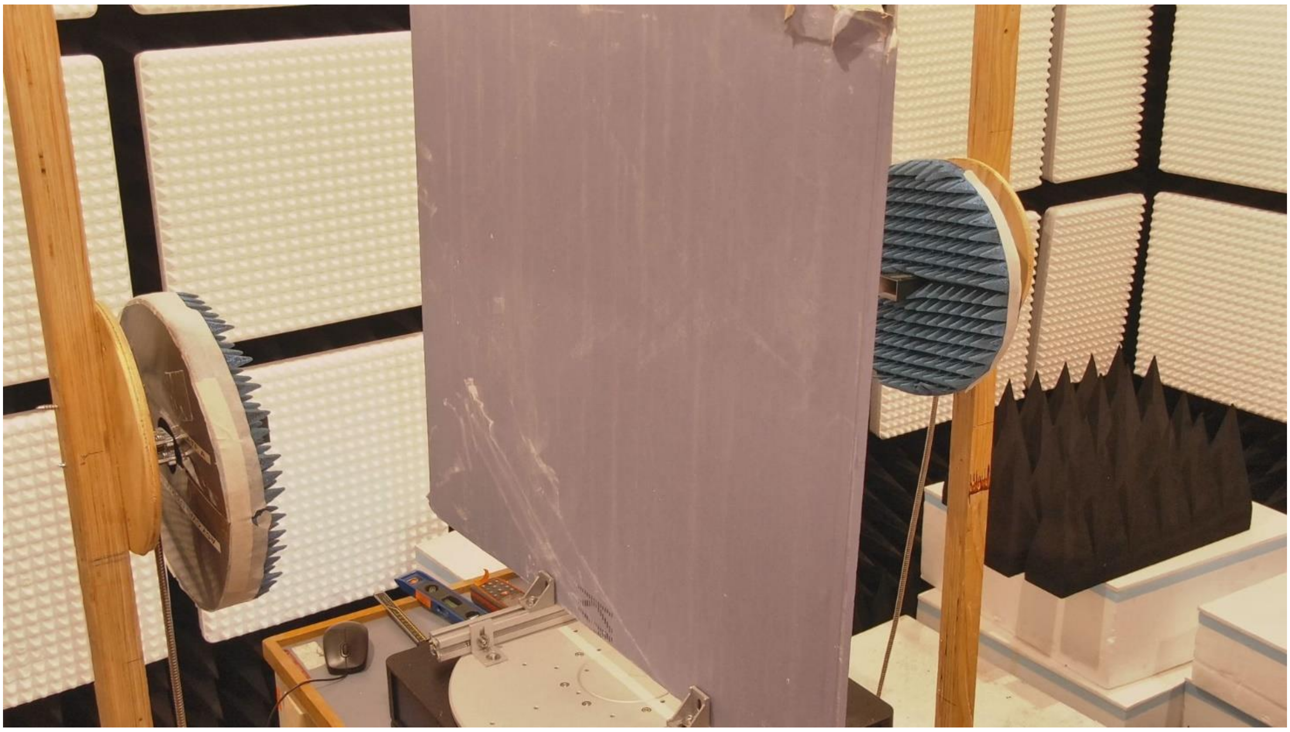

Acoustic troldtekt board21.66 mm

Acoustic rockfon board 19.48 mm

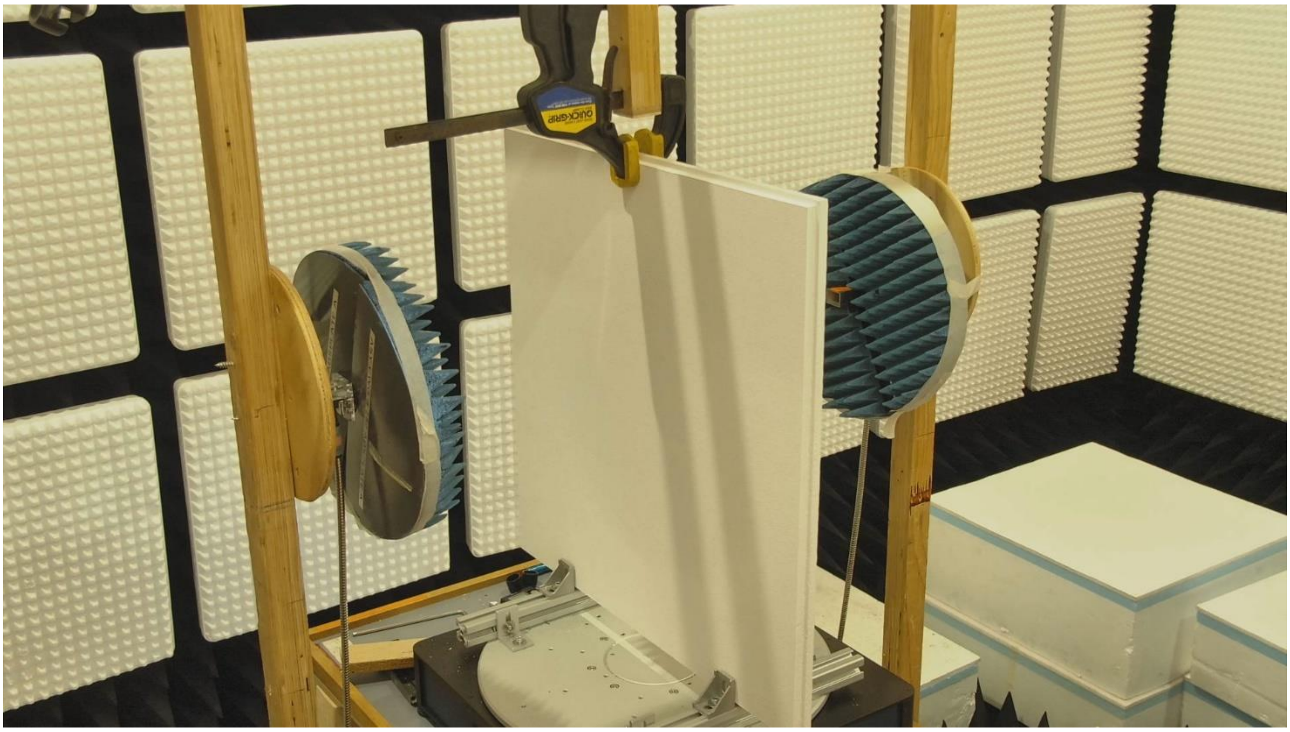

Outdoor tile 20.41 mm

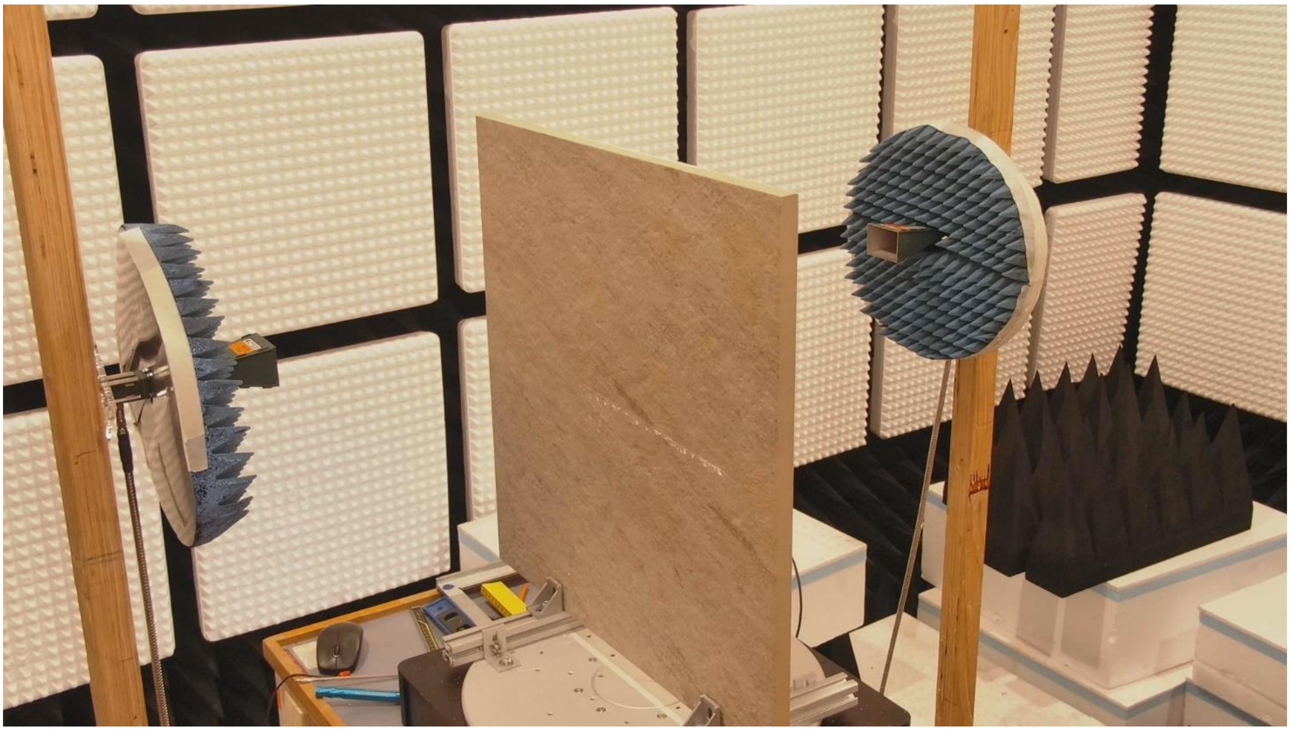

Facade cladding panel 9.56 mm

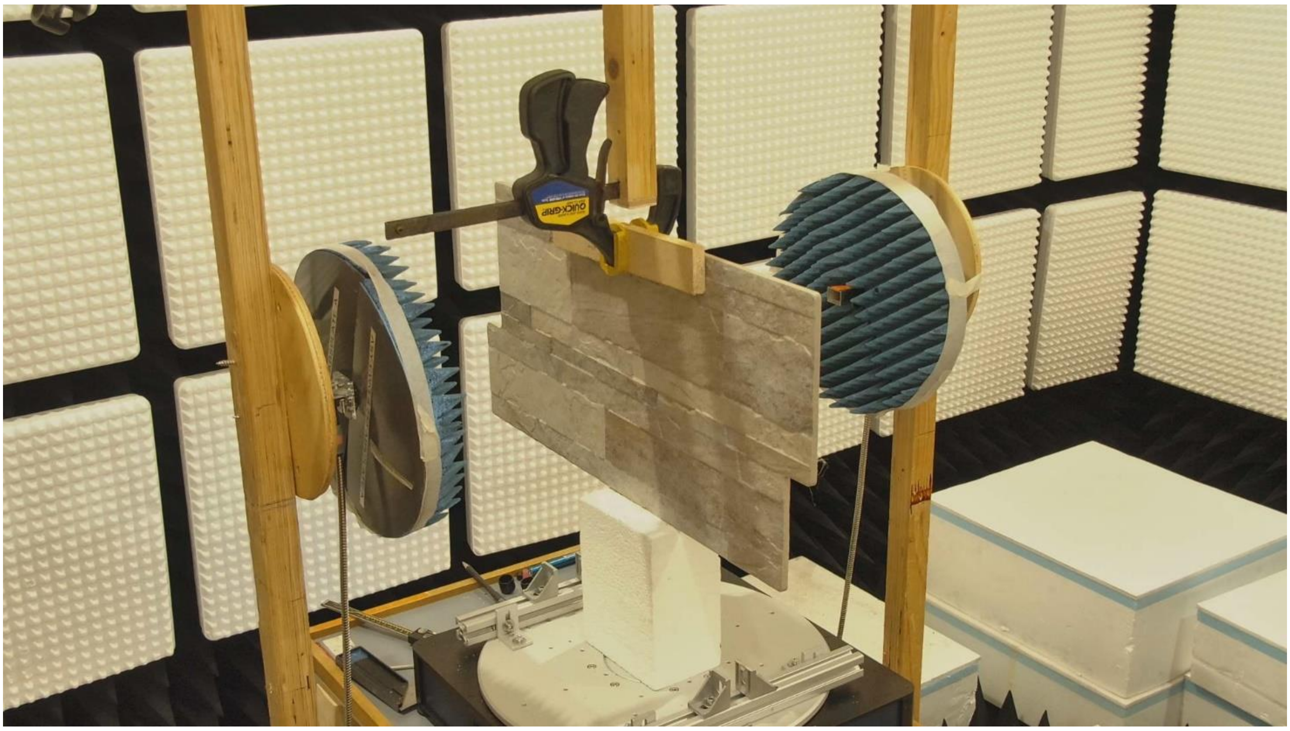

Outdoor concrete tile 50.5 mm

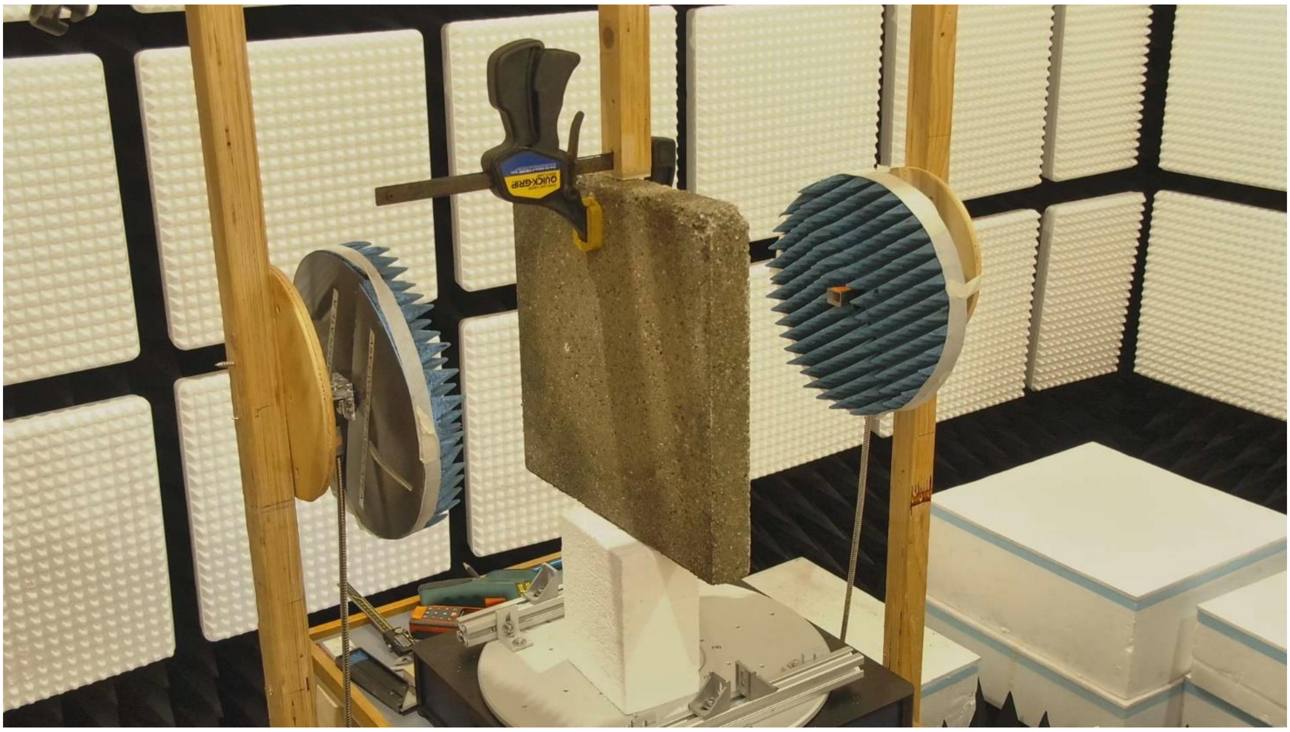

Appendix E

Uncertainty analysis of measurements

Material measurement

Uncertainty analysis of measurements

Test 1: Changing the distance in software, without changing the physical distance and unchanged calibration.

Meas Nr.	Time between the measurement	Distance between TX and the material	Precent
1	Start = 0	290	10 mm = 0,84%
2	1 min	300	50 mm in avg = 0.815%
3	1 min	350	100 mm in avg = 1.21%
4	1 min	400	200 mm in avg = 2.65%
5	1 min	450	
6	1 min	500	

Test 2: Changing software and physical distance to the same value, with unchanged calibration.

Meas Nr.	Time between the measurement	Precent (Change in software and physical position)	Precent (Change only in software)
1	Start = 0	50mm in avg = 3,48%	50mm = 0.867%
2	1min	100mm in avg = 6,33%	100mm = 0.138%
3	1min	150mm in avg = 6,59%	150mm = 0.119%

Test 3: Exact same measurement over time, 30 sec and 2 min delay between the measurement.

Meas Nr.	Time between the measurement	Distance between TX and the material	Precent (Change only in software)
1	0s	400	30 sec and 400mm = 0.412%
2	30s	400	4 min and 300mm = avg 0,618%
3	30s	400	6 min and 300mm = avg 0.408%
4	2min	300	8 min and 300mm = 0.73%
5	2min	300	
6	2min	300	
7	2min	300	

Test 4: Changing the cable position under the exact same measurement.

Nr. test	Change in TX	Change in RX	Present
1	0cm	0cm	0%
2	0cm	8cm	2.030%
3	0cm	8cm + 5cm	3,336%
4	5cm	Not changed	2,837%
5	5cm+10cm	Not changed	1,688%

Test 5: Changing the material position when the RX and TX poles position are static.

Nr. test	Position TX (cm)	Position RX (cm)	Present
1	0	0	0%
2	-2	+2	0.355%
3	-4	+4	3,592%
4	-6	+6	5,011%
5	+2	-2	5,126%
6	+4	-4	4,24%
7	+6	-6	2.785%